Ph.D. PROGRAM IN EARTH SCIENCES

XXXII CICLE

Integration of object-oriented modelling and geomorphometric methodologies for the analysis of landslide systems

SSD GEO/05

Ph.D. Student

Mario Valiante

Tutor

Professor Francesca Bozzano

Co-Tutors

Professor Marta Della Seta

Professor Domenico Guida (Department of Civil Engineering, University of Salerno)

Index

Extended Abstract

The main objective of my PhD research is to develop an object-oriented, hierarchical and multi-scale geomorphological approach to studying "landslide systems" meaning sets of landslides of different type evolving on the long-term with mutual interaction (sensu Guida et al. 1988, 1995; Coico et al. 2013; Valiante et al. 2016). The proposed approaches aim: 1) to improve the existing or new inventories, defining an object capable of storing both spatial and temporal relations between landslides in a single dataset, avoiding physical data fragmentation and logic inconsistency; 2) to build a robust conceptual model for the practical management of complex arrangements of landslides and their evolution.

This work also aims to contribute to the overall theme of landslide hazard assessment and mitigation, focusing on those cases where complex spatio-temporal arrangements of landslides interacts with engineering structures or infrastructures, for better understanding and quantify the interactions at various spatio-temporal scales between engineering works and natural processes.

The research has been conducted following three main strategies: 1) a "Top-Down approach" based on morphometric analyses on Digital Elevation Models (DEMs) to find whether a portion of landscape shows a set of "topographic signatures" ascribable to landslide systems; 2) a "Bottom-Up approach" based on the reconstruction of the landslide system through field activities starting from any of the landslides composing the system itself; 3) comparison of the above strategies using a training-target approach on selected case studies significant for different Italian landscapes.

The "Top-Down" approach is based on the application of morphometric techniques using Digital Elevation Models, such as Topographic Position Index (TPI) (Weiss 2001; Paron and Vargas 2007; De Reu et al. 2013), useful for the semi-quantitative delineation of main landforms, and Slope – Area Plots (Montgomery and Foufoula-Georgiou 1993; Booth et al. 2013; Tseng et al. 2015), exploited for the estimation of the erosional processes type acting on the slopes, and extended also to gravity-driven processes. Basically, the graphical plot of the topographic steepness as function of the drainage area can be subdivided in four main plot regions or curve segments, each one representing a dominant geomorphic process: I) hillslopes; II) hillslope-to-valley transition; III) debris flow dominated channels or landslides driven channels; IV) alluvial channels.

The "Bottom-Up" approach follows the GmIS_UniSA method proposed in Dramis et al. 2011. In the first steps data collected from field activities were stored referring to a symbol-based representation (SGN 1994; APAT 2007; ISPRA 2018) similarly to what has been done by many authors (Gustavsson et al. 2006; Devoto et al. 2012; Miccadei et al. 2012; Del Monte et al. 2016 among the others), in the next steps the original data is extended from the symbol-based to a full-coverage representation. The latter is then reclassified using the proposed object-oriented data model.

Such object-oriented data model is based on the assumption that any entity can be represented by exactly one object regardless of its complexity or inner structure (Egenhofer and Frank 1992). Complexity is then handled through the classification process: a real-world feature and its behaviour is described and encapsulated in a class definition, then any operation of simplification or generalization can be performed defining a set of sub-classes and super-classes. Any feature described by a class definition is an object (an instance of that specific class); simplifying, a class is

the description of a feature and its behaviour while an object is the feature itself (Atkinson et al. 1990; Chaudhri 1993; Kösters et al. 1997).

The described classification process results in a set of classes linked by parent-child relationship (generalized and specialized classes) and sibling relations (classes sharing a common super-class) in a hierarchical structure. Hierarchies are usually exploited to model, and therefore better handling complexity of natural systems; in this perspective a hierarchy is defined as a multi-level or layered system where each level can be decomposed in a number of interrelated subsystems until a non-decomposable elementary subsystem is defined (Simon 1962; Odum and Barrett 2005; Wu 2013). Depending on the objectives of a particular study or analysis, the hierarchical level closer to the study object is called focal level or level 0 which sets the starting point for decompositions (levels -x) or generalizations (levels +x) (Wu 1999).

Applying the previous concepts, the basic landslide inventory is built by means of usual techniques, such as field survey, remote sensing, desk studies, etc., then an object-oriented hierarchical model is applied resulting in a hierarchical classification of landslides. The focal level is set at the input inventory containing individual landslides as one object differentiated by type of movement. The proposed model assumes that a "functional interaction" (i.e. dynamic interaction) exists if the condition of spatial and temporal overlap between landslides is verified. This assumption can be evaluated through the integration of two topological models. The Dimensional Extended nine-Intersection Model (DE-9IM) (Egenhofer and Herring 1990a, b; Egenhofer and Franzosa 1991; Clementini et al. 1994) and the Region Connection Calculus (RCC8) (Randell et al. 1992; Cohn et al. 1997). Starting from the focal level, 2 levels of generalization are defined based on the topological relation between landslides: i) if two or more landslides of the same type have a 2-dimensional relation between their interior portion, they can be simplified in a landslide complex object having the same type of movement as the input features; ii) if two or more landslide complexes have a 2-dimensional relation between their interior portion or with the interior of another landslide which is not part of the input complex, they can be simplified in a landslide system object. A level of decomposition has been also implemented describing landslide components.

Once derived a landslide system, it is useful to define its Reference Hillslope, meaning the minimal portion of territory in which it is likely to evolve. To address this task Surface Networks can be a valid technique in order to objectively define the minimal portion of the topographic surface in which a gravitational process can develop and evolve. The extraction of Surface Networks from DEMs (Pfaltz 1976; Wolf 1991; Schneider 2003; Rana 2004) is based on the detection of the characteristic features of a surface called critical elements, such as critical points (local minima, local maxima and local saddles) and critical lines (ridgelines, connecting peak and passes, and courselines, connecting pits and saddles). This data structure has been exploited to decrease complexity of topography representing just its "mathematical skeleton" (Guilbert et al. 2016).

In order to test these methodologies, three italian case studies have been selected choosing sites with different geological settings and thus landsliding style. The choice of the study areas has been made also picking landslide recently reactivated with a great impact on anthropic activities. The selected case studies are:

- Corniolo - Poggio Baldi (FC) along the Bidente River valley;

- Roscigno (SA) on the south-western slopes of Mt. Pruno;
- North-eastern slope of the Rocca di Sciara relief in the valley of the Northern Imera river, close to Scillato village (PA).

The Corniolo – Poggio Baldi case study has been selected for the last reactivation of the Poggio Baldi landslide in March 2010. The movement developed as a rock-wedge slide evolving in a flow-like movement that produced the damming of the Bidente river and the formation of the Corniolo Lake, which is partially still present today. The main geological settings of the area are made of a sandstone-marly flysch with a dip-slope attitude.

The case of Roscigno refers the history of the abandoned "Old Roscigno" rural village. This ghost town has been transferred from about sixty years due to landsliding activity and is nowadays part of the Cilento UNESCO - Global Geopark. The village was built on the south-western slope of Mt. Pruno, mainly composed of terrigenous deposits such as calcarenitic-marly flysch, tectonically overlapping a clayey-marly flysch. The main movement affecting the slope is a deep-seated rock slope deformation, on top of which several shallow landslides developed, such as rotational slides and mud flows.

The Rocca di Sciara case study has been chosen for the last reactivation of the lower portion of the slope in April 2015. The event caused severe damages to the road network, also involving the Palermo – Catania highway leading to the failure of the Imera viaduct. The geological settings of the slope are made of a dip-slope bedding heterogenous sequence of limestone megabreccias and thick-bedded calcarenites, thin-bedded or laminated calcilutites and clayey flysch.

During these three years of research, several survey activities have been performed in order to reconstruct the geological and geomorphological setting of the case studies. All these activities were supported by the object-oriented perspective defined before, allowing objects definition and description directly on the field.

Both the "Top-Down" and the "Bottom-Up" strategies have been applied to the case studies. As for the first strategy, the contributing area reclassification shows mainly the hypothetical landslide-related channel as linear features, while the TPI reclassification highlights concave morphologies that can be related to landslides components, such as detachment areas, trenches, counterslopes, and so on. Both these methods can be useful techniques to assess potential landslides affected areas for a better planning of further activities such as field surveys, which are the starting point of the second strategy. Following the data collection, by direct surveys, desk studies or remote sensing, all the information has been rearranged within the object-oriented logic perspective; then, the hierarchical model allows to derive higher rank units, such as landslide complexes and landslide systems. Based on these derived objects, through the integration of Surface Networks it is possible to define the so-called "Reference Hillslope" for each landscape object.

Every landslide is characterized not only by its attributes but also by it spatial and temporal relations with the other movements. Coupling this object-oriented hierarchical approach with a temporal characterization of landslide features in the form of "events", semantically defined, it is possible to build an object-oriented and event-based database capable of storing both spatial and temporal relations between landslides.

The Top-Down approach showed some limitation in the recognition of deep-seated movements, while the Bottom-Up approach allowed the automatic reconstruction of the landslide hierarchies starting from the landslide inventory. A landslide system built with an accurate spatio-temporal inventorying of landslides can be a tool for the fast retrieval of useful information such as "how many events affected a slope and how they developed, their magnitude and frequency and how they interacted". All these data regarding the past and present activity of a slope are the assumption for understanding its most likely evolution, thus, to contribute to the formulation of reactivation scenarios. Moreover, the definition of the "reference hillslope" allow to objectively define the area/volume to be investigated starting from a reference object – a landslide, a landslide complex or a landslide system - , both for the planning of remediation and monitoring activities and as a starting point to search whether a landslide interacts with other geomorphic processes or anthropogenic activities.

1   Introduction

In the field of natural hazards, landslides are one of the most widespread and frequent occurrences, related both to natural and anthropic triggers, sometimes with catastrophic outcomes such as loss of lives (Evans et al. 2007; Cascini et al. 2008; Petley 2012; Barla and Paronuzzi 2013; Froude and Petley 2018). Landslides also often interfere with human activities, impacting on urban areas, various infrastructures such as roads, tunnels, bridges, pipelines and so on, and areas related to other socio-economic activities causing great economic losses (Alexander 1988; Fiorillo et al. 2001; Crosta et al. 2004; Evans and Bent 2004; Gattinoni et al. 2012; Genevois and Tecca 2013; Maiorano et al. 2014; Pankow et al. 2014; Schädler et al. 2015; Uzielli et al. 2015; Klose 2015; Bozzano et al. 2016; Smaavik and Heyerdahl 2016; Valiante et al. 2016; Bozzano et al. 2017; Esposito et al. 2017; Marinos et al. 2019 for example). In this framework, sometimes, structures or infrastructures are faced with complex arrangements of landslides rather than a single movement (Barredo et al. 2000; Borgatti et al. 2006; Corsini et al. 2006; Guida et al. 2006; Guerricchio et al. 2010; Di Martire et al. 2015; Schädler et al. 2015; Uzielli et al. 2015b; Bozzano et al. 2016; Lupiano et al. 2019). Such complexity can be related to different spatio-temporal arrangements of landslides: there can be a frequent occurrence of phenomena in a relatively small area (Haigh et al. 1993; Corbi et al. 1996; Crozier 2010a, b; Berti et al. 2013; Roback et al. 2018), or the spatial overlap of successive landslide events, like converging flow-like movements (Zuosheng et al. 1994; Cascini et al. 2008; Schädler et al. 2015), or relatively shallower phenomena developed over deep-seated movements (Guida et al. 1987; Guerricchio et al. 2000; Murillo-García et al. 2015), or partial mobilizations of previous landslides in nested structures (Lee et al. 2001), or various superimpositions of different landslide types (Stefanini 2004; Guida et al. 2006; Di Martire et al. 2015; Valiante et al. 2016) . Overlapping landslides derive from the temporal sequence of events and some authors already noticed that such cases need further attention and cannot be managed as a simple landslide (Corbi et al. 1999). Other authors also suggested the concept of path dependency for landslide susceptibility analysis, stating that pre-existing landslides could be a predisposing factor for future phenomena (Samia et al. 2017a, b). Besides spatial arrangements of landslides, even dealing with a single landslide implies to face its inner complexity, i.e. describe its components (Parise 1994, 2003; Fiorillo et al. 2001; Dai and Lee 2002; Niethammer et al. 2012; Dufresne et al. 2016; Morelli et al. 2018; Wang et al. 2018b; Catane et al. 2019). In this framework, when an active landslide considered in an engineering problem is part of a broader deformation/failure/flow context, define the reference area for remediation works or monitoring activities is quite a challenge, ideally it should be addressed taking into account the state of activity, hence frequency, of movements and their temporal evolution related to the temporal persistence of the geotechnical project object of the study.

Even in the cases where the object of the study is clear, being it a single landslide or a set of them, define the corresponding minimal portion of landscape to analyse is an open question. Sometimes geotechnical investigations or monitoring activities are planned and executed within the active landslide area or in its closer surroundings (Borgatti et al. 2006; Torreggiani 2009; Romeo et al. 2014; Abolmasov et al. 2015; Di Martire et al. 2015; Mazzanti et al. 2017), leaving out the geomorphological context in which the referenced phenomenon developed. Defining an objective "area of interest" starting from a well-known object may be an interesting task to address, in order to optimize monitoring activities and geotechnical investigations. The other way around, define first objective

landscape units as a basis for landslides analysis is not an easy task as well. Various methods have been proposed defining landscape partitions with different methodologies, such as grid-cells, terrain units, unique-condition units, slope units and topographic units (Carrara et al. 1991; Guzzetti et al. 1999 and references therein; Alvioli et al. 2016). All of them have been exploited for landslide susceptibility analyses (Carrara et al. 1991; Aleotti and Chowdhury 1999; Chung-Jo and Fabbri 1999; Van Westen et al. 2003; Yesilnacar and Topal 2005; Piacentini et al. 2012; Budimir et al. 2015; Luo and Liu 2018; Reichenbach et al. 2018). They are not suitable for site-specific scale studies, as they are usually computed at smaller scales and do not consider pre-existing landslides in their definition.

Existing inventories currently do not have the capability to store and retrieve such complexity in landslide arrangements, both because of the lack of a model describing spatio-temporal overlapping phenomena and because, most of the times, is not even possible to store or represent overlapping features within the same dataset as this is treated as a topological error (ESRI 2019). Despite this is extremely useful for various applications, such as administration boundaries or cadastral management, dealing with landslides, it is a crude limitation. Representing nested or overlapping landslides as a coverage of adjacent tiles produce a logic inconsistency between the topology of the data and the topology of the real-world features, as vertical relations between landslide events such as under-over, contained-contains, overlapping-overlapped, are not preserved causing a loss of information. Besides, current approaches in multi-temporal landslide inventories are usually based on the snapshot or "time-slices" model (Dragicévić 2004; Guzzetti 2006; Samia et al. 2017a), representing with different datasets the landslide inventory at a specific time or landslide events occurred in a specific time frame. Having multiple datasets for representing multitemporal information results in data fragmentation and a poorly management of temporal relations.

In order to describe spatial and temporal arrangements of landslides Guida et al. 1988 introduced the concept of landslides system as "a set of complex landslides (sensu Varnes 1978; Cruden and Varnes 1996) ascribable to a common initial deformation which, on long-term evolution, develops into differentiated morphotypes referring to type of movement, age and state of activity". The authors further differentiated the description of landslides associations based on movement types and state of activity (Guida et al. 1995) and since then, such terminology has been rarely used for the description of landsliding phenomena in southern Italy (Guida et al. 2006; Coico 2010; Sinistra Sele River Basin Authority 2012; Coico et al. 2013; Valiante et al. 2016).

Starting from the overall topic of the definition of the relations between complex arrangements of landslides and engineering works, this research aims to: i) define a conceptual model, based on the concept of "landslide system", for the description of associations of landslides and their spatial and temporal relations; ii) implement such a model in a database structure capable of storing both spatial and temporal information in a single dataset, avoiding physical fragmentation and logic inconsintency of the data, allowing to quickly retrieve information about the number of interacting phenomena, their temporal occurrence, hence the slope evolution, their spatial relations and so on; iii) define an objective methodology to bound the minimal area to be attentioned for a landslide or a set of landslides.

The model has been developed defining an original object-oriented and hierarchical classification for landslides. In this hierarchy, landslides are preliminarly defined at the focal level and two levels of aggregation based on topological relations describe various association of landslides. After, just

one level of decomposition containing landslide components was defined, leaving a second one (landslide element) for further geospatial, topological and mereo-logical researches.

The object-oriented data model has been chosen as optimal knowledge reasoning and representation of the geospatial domain of interest, because of its intrinsic hierarchical structure, its flexibility in the classification procedures, adapting to any natural system, and the capability to define procedures (called methods or functions) to dynamically access and manipulate classes attributes reducing the volume of information needed to be actually stored (Egenhofer and Frank 1987; Worboys et al. 1990; Worboys 1994; Kösters et al. 1996). This model is not a new landslide classification technique as it relies on existing classifications for movement types (Varnes 1978; Cruden and Varnes 1996; Hungr et al. 2014), but it is intended for the description of landslide associations, their spatial and temporal relations and as a tool to build, update and manage landslide inventories.

2 Theoretical background

2.1 Object-oriented data modelling

In the field of geosciences, words as "object-oriented" or "object-based" usually refer to the well-known technique of the Object-Based Image Analysis (OBIA). This practice is based on the classification of raster datasets mainly by clustering pixels sharing common properties defining vector polygons called "objects", which can be further decomposed or aggregated following user-defined rules (Hay and Castilla 2008; Blaschke et al. 2014; Louw and van Niekerk 2019). This segmentation procedure can be applied on any raster dataset for several purposes such as on Digital Elevation Models (DEM) and their derivatives (slope, curvature, hydrology, etc…) for landforms recognition (Drăguţ and Blaschke 2006; Eisank et al. 2011; Guida et al. 2012; Barzani and Salleh 2016), as well as on multispectral or panchromatic remote sensing imagery for land-use/cover analysis (Zhou et al. 2009; Li et al. 2014; Wang et al. 2018a). Efforts have been made also in the automatic recognition of landslides using OBIA both on DEMs and various remote sensing products (Fernández et al. 2008; Van Den Eeckhaut et al. 2012; Feizizadeh and Blaschke 2013; Moosavi et al. 2014; Mezaal and Pradhan 2018). The common foundation of all the OBIA techniques is that every image (digital domain) depict real-word features (concept domain), thus every "image object" derived through OBIA should correspond to a "geographic (geomorphological) object" (Castilla and Hay 2008; Eisank et al. 2011). However, all these concepts are borrowed from the original object-oriented paradigm, OBIA is just one of its applications.

2.1.1 The object-oriented paradigm

Object-orientation concepts were developed in the '60s as structures for programming languages in order to overcome existing limitations. Then-existing simulation languages, based on procedural standards as a set of instructions, were not sufficient to model real-world systems (Holmevik 1994; Kindler and Krivy 2011). The need to develop a programming language containing both a system description and the functions describing its processes, led to the invention of Simula, considered the first full-fledged object-oriented programming language (Dahl and Nygaard 1968; Dahl 2002). Most of the languages used nowadays for scientific applications are object-oriented, the most relevant are C++, Java, Python and partially R and MATLAB. According to Lewis and Loftus (2015) and Phillips (2018), the key concepts or main features of any object-oriented language are:

- Abstraction: features can be described through a classification, i.e. any feature is modelled with a class definition containing both its description and variables (attributes) and the procedures or functions available for that class (methods). Any instance (practical example) of that specific class is called object. Relations between classes are modelled through generalization, association and aggregation;
- Encapsulation: variables and functions definition inside a class allow final users to manipulate objects through methods without interfering with the original properties of the class itself (data hiding);
- Inheritance: classes can contain sub-classes which share their super-class attributes and methods;
- Polymorphism: different object types have their own different implementation of the same function or method.

2.1.2 Object-oriented databases

With the spreading of object-oriented programming languages, users started to think whether Database Management Systems (DBMS) could also benefit of the object-oriented paradigm features. The well-established Relational model (Codd 1970) (RDBMS) proved some limitations such as lack of complex data types, data structures limited to the table format, atomic values, etc. (Chaudhri 1993; Ghongade and Pursani 2014; Aziz et al. 2018).

According to The Object-Oriented Database System Manifesto (Atkinson et al. 1990), a DBMS to be defined as such, must ensure at least:

- Support for complex objects: tuples, lists, arrays, multimedia data types, etc., as well a set of operators to handle them;
- Object identity: any object exists regarding of its values, meaning that any values alteration (updates) do not compromise object persistence. This can be extremely useful for referencing and assignment operations;
- Encapsulation: as in the original concept, both the data describing a model and the procedures available for that model are stored within the database;
- Classification: any object is described by a set of attributes and can be manipulated with a set of functions both declared by a class definition;
- Class hierarchies: subclass definitions allow to share attributes and methods among classes related by parent-child relation;
- Overriding: this is a derivation of the polymorphism concept. Different classes can have the same names for attributes or methods, but the underlying behaviour is different;
- Extensibility: users can add their custom classes, data types and functions;
- Persistence: obviously, as required for any DBMS, data must survive the execution of the process defining them to be reused in another process;
- Secondary storage management: the DBMS should be able to manage any kind of support for the storage of data;
- Concurrency: data should be accessible by different users at the same time;
- Recovery: data integrity should be ensured in any case of system failure;
- Ad Hoc Query Facility: data should be queryable.

Even if Object-Oriented Database Management Systems (OODBMS) have been developed and existed in the last 20 years, they struggled to be a valid competitor for RDBMS. This is due mainly to the lack of standards, in fact RDBMS can rely on a strong mathematical basis and on a unified Structured Query Language (SQL) while OOBDMS strongly depends on the language they are conceived (Aziz et al. 2018). However, different DBMS, though being notoriously based on the Relational model, started to implement several features of the Object-Oriented model in the last years. Such hybrids have been defined Object-Relational Database Management Systems (ORDBMS) ant two renowned examples are the open-source PostgreSQL and the commercial Oracle DB (Oracle® 2019; The PostgreSQL GDG 2019).
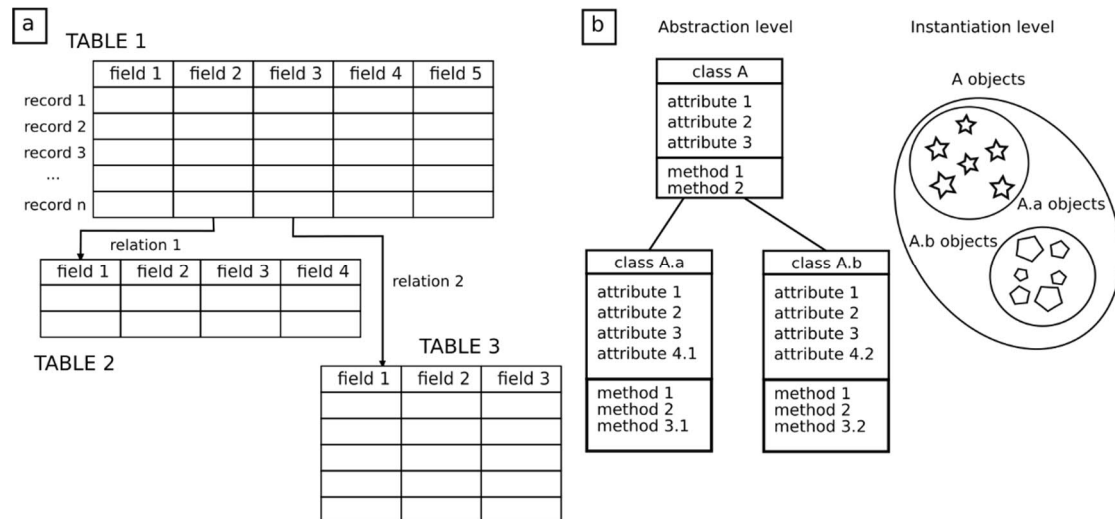
Figure 1 – The relational model (a) compared to the object-oriented model (b)

2.1.3   Object-oriented modelling for geospatial data

OODBMS have been widely acknowledged as the optimal structure for the storage and manipulation of geographical information (Löwner 2013). Egenhofer and Frank (1987) firstly proposed an object-oriented model for the manipulation of spatial information based on the abstraction concepts of classification, generalization and aggregation, introducing a hierarchical structure with single or multiple inheritance of attributes and methods. Following their pioneering work, a series of concepts and structures have been proposed. To better model interactions among the defined classes, Worboys et al. (1990) introduced functional relationships between object as links describing their mutual connections. Later they characterize geo-objects having a four-dimensional structure (Worboys 1994):

- Spatial dimension, which defines geometrical and topological properties;
- Temporal dimension, where their persistence in time and evolution is stored;
- Graphical dimension, storing properties regarding the graphical representation;
- Textual-numerical dimension, storing attributes and data.

Upon these bases, several data structures have been proposed both for general-purposes spatial databases (Egenhofer and Frank 1992; Kösters et al. 1996; Fonseca and Egenhofer 1999; Borges et al. 2001; Khaddaj et al. 2005) and specialised data, such as census/administrative units (Worboys et al. 1990), topographic information (Shahrabi and Kainz 1993), archaeology (Tschan 1999; Holt 2007) and city planning (Gröger et al. 2004). Moreover, different specialized applications have been developed based on object-oriented models (Câmara et al. 1996; Kiran Kumar et al. 1996; Kösters et al. 1997; Posada and Sol 2000; Holt 2007; Chen et al. 2012).

Abstraction mechanisms to describe a system are based on the assumption that any entity can be represented by exactly one object regardless of its complexity or inner structure using classification (Dittrich 1986). Complexity is modelled through generalization, association and aggregation (Egenhofer and Frank 1992). Generalization groups several classes of objects with common operations into a more general super-class, and it is described by the relations is-a or can-be-a, the inverse process is specialization; association relates two or more independent objects which can have an identity as a group, it is described by the relations member-of or a-set-of; aggregation relates an

6

entity with its components and is described by the relations part-of or consists-of, the inverse process is decomposition (Figure 2).
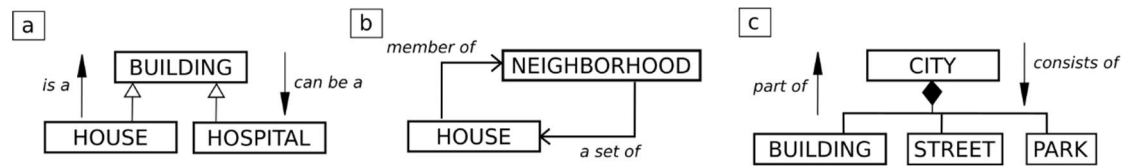

Figure 2 – Generalization (a), association (b) and aggregation (c). (modified from Hegenhofer & Frank, 1992)

2.1.4   Hierarchy

As described before, object-oriented methods strongly rely on relationships among classes. These relations can be such as generalization-specialization, aggregation-decomposition or association: all these connections define a hierarchical structure.

In a hierarchical structure, classes and sub-classes are related by parent-child relationship, while classes sharing a common super-class are called siblings (Tsichritzis and Lochovsky 1976; Singh et al. 1997; Glover et al. 2002; Malinowski and Zimányi 2004). A hierarchy is defined as a multi-layered system, where each level can be decomposed until a non-decomposable level is defined (Simon 1962; Odum and Barrett 2005; Wu 2013). While the object-oriented classification defines specific relationships among classes, hierarchical levels are a relative structure and depend on the purpose to which they are applied. Based on the objective of an analysis, the centre of the hierarchy (Focal level) can be any object of interest, and its parents define levels of generalization or aggregation (levels +x), while its children define levels of specialization or decomposition (levels -x) (Wu 1999, 2013) (Figure 3).
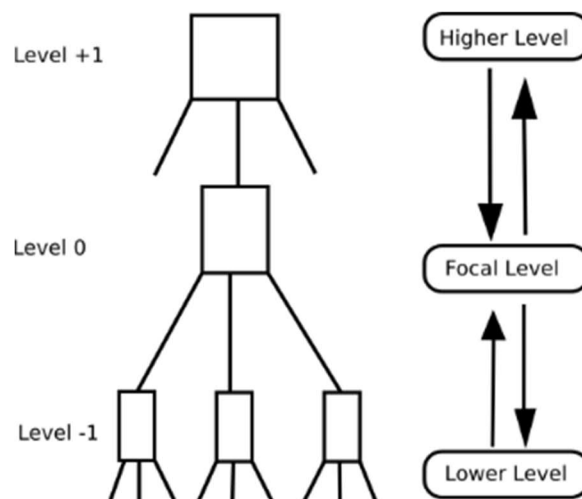
Figure 3 - Hierarchical structure (modified from Wu, 2013)

2.2   Spatio-temporal data analysis

Typical queries and operations on geographical objects often are based on their spatial properties and temporal attributes. A major benefit of spatial databases over general-purpose databases is indeed the integration of common functions capable of reading and manipulating the basic spatial characteristic of an object in order to retrieve more complex spatial relationships. Such capabilities are the foundation of all the modern Geographic Information Systems (GIS) (Heywood et al. 2006).

Spatial relationships can be classified in three main categories (Egenhofer and Herring 1990a):

- Geometric relationships: anything that can be measured within a referenced system, such as distances, directions and angles, areas, volumes, etc.
- Spatial order relationships: regarding the objects ordering in a referenced space. These properties are usually dualistic and common examples are in front – behind or above – beneath;
- Topological relationships: describing the relative arrangements of objects in space. These properties are usually invariant under common transformations or distortions such as translation, scaling, rotating, stretching, etc.

Temporal queries require the modelling and storage of temporal information. Time could be expressed as a point or as an interval where time points represent exact moments and time intervals represent any time span. However, both these two definitions can be generalized in time intervals, as time points are a relative concept and depend on the time scale in which they are referred (Allen 1983; Nebel and Bürckert 1995; Van Beek and Manchak 1996). Relations among time intervals are defined in Allen 1983, describing their relative position in the time dimension (Figure 4). Temporal Geographic Information Systems (T-GIS) are defined as GIS capable of storing and manipulating temporal information in order to perform spatio-temporal queries (Yuan 2008).

Predicates	Pictorial example
X before Y	x x x
Y after X	y y y
X meets Y	x x x x
Y met-by X	y y y y
X overlap Y	x x x x
Y overlapped-by X	y y y y
X during Y	x x x
Y includes X	y y y y y y
X starts Y	x x x
Y started-by X	y y y y y y
X finishes Y	x x x
Y finished-by X	y y y y y y
X equals Y	x x x x y y y y

Figure 4 - Allen's temporal predicates (modified from Nebel & Bürckert, 1995)

2.2.1 Topological models

To describe spatial relations between objects, two topological models for spatial reasoning have been exploited in this work: the Dimensionally Extended nine-Intersection Model (DE-9IM) (Egenhofer and Herring 1990a, b; Egenhofer and Franzosa 1991; Clementini et al. 1994) and the Region Connection Calculus (RCC) (Randell et al. 1992; Cohn et al. 1997). The DE-9IM is a topological model used to describe the spatial relations of two geometries (points, lines, polygons) in two dimensions. The basic assumption for this model is that every object in the R^2 space has an interior ($I(a) = a^o$), a boundary ($B(a) = \partial a$) and an exterior ($E(a) = a^e$) and the spatial relation of two geometries is evaluated in the form of a 3x3 intersection matrix with the form:

$$DE9IM(a,b) = \begin{bmatrix} \dim(a^o \cap b^o) & \dim(a^o \cap \partial b) & \dim(a^o \cap b^e) \\ \dim(\partial a \cap b^o) & \dim(\partial a \cap \partial b) & \dim(\partial a \cap b^e) \\ \dim(a^e \cap b^o) & \dim(a^e \cap \partial b) & \dim(a^e \cap b^e) \end{bmatrix}$$

where dim is the maximum number of dimensions of the intersection of the interior, boundary, and exterior of geometries a and b (dim(point) = 0, dim(line) = 1, dim(polygon) = 2). These values can be expressed as boolean values where FALSE means non-intersection and TRUE any other value. The resulting matrix can be also expressed as a 9 characters alphanumeric string. RCC describes regions by their possible relations to each other. RCC8 consists of 8 basic relations that are possible between two regions. Integrating the two models, RCC8 relation can be converted in 12 DE-9IM matrices and thus in 12 alphanumeric strings which can bel implemented in a database dictionary (Figure 5).

RCC8   DE-9IM
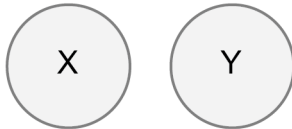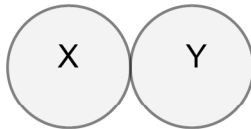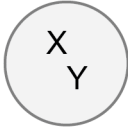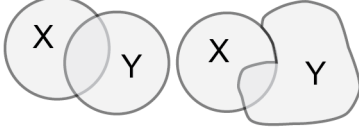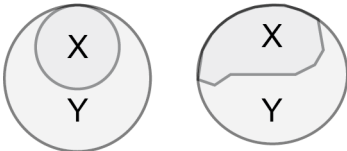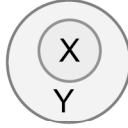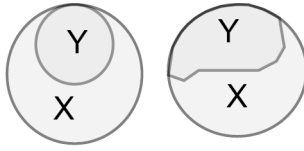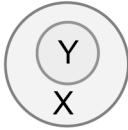
RCC8	DE-9IM matrix	String
X DC Y disconnected	$\begin{bmatrix} F & F & 2 \\ F & F & 1 \\ 2 & 1 & 2 \end{bmatrix}$	FF2FF1212
X EC Y externally connected	$\begin{bmatrix} F & F & 2 \\ F & T & 1 \\ 2 & 1 & 2 \end{bmatrix}$	FF2F01212 FF2F11212
X EQ Y equals	$\begin{bmatrix} 2 & F & F \\ F & 1 & F \\ F & F & 2 \end{bmatrix}$	2FFF1FFF2
X PO Y partially overlapping	$\begin{bmatrix} 2 & 1 & 2 \\ 1 & T & 1 \\ 2 & 1 & 2 \end{bmatrix}$	212101212 212111212
X TPP Y tangential proper part	$\begin{bmatrix} 2 & 1 & 2 \\ F & T & 1 \\ F & F & 2 \end{bmatrix}$	212F01FF2 212F11FF2
X NTPP Y non-tangential proper part	$\begin{bmatrix} 2 & 1 & 2 \\ F & F & 1 \\ F & F & 2 \end{bmatrix}$	212FF1FF2
X TPPi Y inverse tangential proper part	$\begin{bmatrix} 2 & F & F \\ 1 & T & F \\ 2 & 1 & 2 \end{bmatrix}$	2FF10F212 2FF11F212
X NTPPi Y inverse non-tangential proper part	$\begin{bmatrix} 2 & F & F \\ 1 & F & F \\ 2 & 1 & 2 \end{bmatrix}$	2FF1FF212

Figure 5 - RCC8 topological model and its conversion in DE9IM matrices

2.2.2 Temporal models

Time can be handled in different ways in GIS, thus in databases. Two recurrent models are the snapshot model and the event-based model. In a snapshot model, each dataset represent the state of a system in a precise time frame, it could be considered as a photography of a system's state in a specific instant (Peuquet and Duan 1995; Dragicévić 2004; Gutierrez et al. 2007). In event-based approaches, objects within a dataset are characterized with temporal attributes describing their time persistence (Peuquet and Duan 1995; Worboys and Hornsby 2004). Referring to landslides, an event can be described as a set of landslides mobilized by the same trigger (Napolitano et al. 2018) or by domino-effect (Martino 2017). The main difference between these two models is that in the snapshot model the temporal characterization is assigned to the whole dataset, while in the event-based approach, objects within the dataset have their own temporal characterization. Using an event-based approach reduce data fragmentation, allowing to store all the information within one dataset and, at the same time, reduce data redundancy which reflect a reduction in data volume.

Figure 6 - Snapshot model (a), vs event-based model (b)

3 Object-oriented model for landslides

The object-oriented model developed in this research relies on terminologies and concepts previously introduced for the study of peculiar spatial arrangements of landslide phenomena. Guida et al. 1988 introduced the concept of "la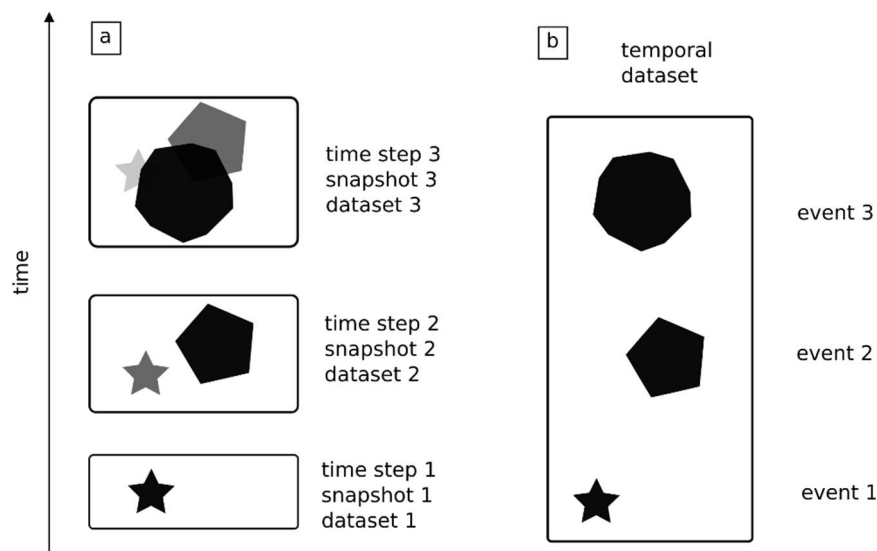ndslide system" as "a set of complex landslides (- a slope movement that involves a combination of one or more of the principal type of movements - sensu Varnes 1978; Cruden and Varnes 1996) ascribable to a common initial deformation which, on long-term evolution, develops into differentiated morphotypes referring to type of movement, age and state of activity". Later on, they defined a more detailed classification for interconnected landslides based on the comparison of their type, age and state of activity (Guida et al. 1995):

- Landslide association – having same type of movement, same age and same state of activity;
- Landslide group – having same type of movement, same age and different state of activity;
- Landslide family – having same type of movement, different age and different state of activity;
- Landslide system – having different type of movement, different age and different state of activity.

Following the hierarchical and multi-scalar model for geomorphological mapping described in Dramis et al. 2011, the previous classification has been simplified. The focal level (level 0) of the hierarchy is composed by the landslides themselves while two levels of generalization describe sets of landslides: i) landslide complexes result from the aggregation of landslide with the same type of movement spatially connected (level +1); ii) landslide systems are defined as a set of landslides of any type spatially connected (level +2). A level of decomposition stores landslide components (level -1). In this work the defined hierarchical and multi-scale classification has been structured in an object-oriented model suitable for database design and rules for the aggregation of landslides based on topological relations have been defined. An event-based approach has been also implemented in order to store and manipulate the temporal characterization of landslides.

3.1 Landslide classes (Focal level)

In this level landslides are classified referring to the updated classification of Hungr et al. 2014 (Figure 7). Classes are defined primarily considering the main type of movement, then the involved material. The original 32 types (48, if movements involving soils and rock-ice are distinguished) proposed by the authors are grouped into 21 landslide classes. This merging operation has the only purpose to simplify the aggregation procedure for the next level of generalization (§ 3.2) and does not intend to generalize the original classification, in fact, every class here defined as two movement type attributes, in which types are picked from the original 48 types discussed in Hungr et al. 2014 (§ 4.2.2). The 21 classes that have been identified are:

1. Rock fall class – class containing rock falls;
2. Soil fall class – includes granular materials falls, such as boulder falls, debris falls and silt falls;
3. Rock topple class – includes topple phenomena involving rock materials, such as rock block topples and rock flexural topples;
4. Soil topple class – topple movements in granular soils like gravel topples, sand topples and silt topples;

5. Rock rotational slide class – contains rock slides with a main rotational movement component;
6. Rock planar slide class – contains rock slides on a planar surface;
7. Rock wedge slide class – rock slides on a wedge-like surface;
8. Rock compound slide class – contains rock compound slides;
9. Rock irregular slide class – containing rock irregular slides;
10. Soil rotational slide class – includes clay rotational slides and silt rotational slides;
11. Soil planar slide class – contains clay planar slides, silt planar slides, gravel slides, sand slides and debris slides;
12. Soil compound slides class – class containing clay compound slides and silt compound slides;
13. Rock slope spread class – contains rock slope spreads;
14. Granular soil spread class – includes sand liquefaction spreads and silt liquefaction spreads;
15. Cohesive soil spread class – class containing sensitive clay spreads;
16. Rock avalanche class – class containing rock avalanches;
17. Soil dry flow class – includes sand dry flows, silt dry flows and debris dry flows;
18. Granular soil wet flow class – contains sand flowslides, silt flowslides, debris flowslides, debris flows, debris floods and debris avalanches;
19. Cohesive soil wet flow class – includes sensitive clay flowslides, mud flows, earthflows and peat flows;
20. Deep-seated slope deformation class – contains mountain slope deformations and rock slope deformations;
21. Shallow slope deformations class – includes soil creep processes and solifluctions.

Currently, all these classes share the same set of basic attributes, which are described in the next chapter where the database design is discussed. Methods (functions) developed so far are also shared among these classes and mainly deal with spatial and temporal properties of the objects:

- Events – retrieve the recorded events involving the referenced landslide;
- First-event – retrieve the first recorded event involving the referenced landslide;
- Last-event – retrieve the last recorded event involving the referenced landslide;
- Siblings-complex – retrieve all the landslides forming the landslide complex in which the referenced landslide is contained, spatial and temporal relations are specified;
- Siblings-system – retrieve all the landslides forming the landslide system in which the referenced landslide is contained, spatial and temporal relations are specified;
- Parent-complex – retrieve the landslide complex in which the reference landslide is contained;
- Parent-system – retrieve the landslide system in which the reference landslide is contained;
- Components – retrieve the referenced landslide components.

Type of movement	Rock	Soil
Fall	1. *Rock/ice* fall[a]	2. *Boulder/debris/silt* fall[a]
Topple	3. Rock block topple[a]	5. *Gravel/sand/silt* topple[a]
	4. Rock flexural topple	
Slide	6. Rock rotational slide	11. *Clay/silt* rotational slide
	7. Rock planar slide[a]	12. *Clay/silt* planar slide
	8. Rock wedge slide[a]	13. *Gravel/sand/debris* slide[a]
	9. Rock compound slide	14. *Clay/silt* compound slide
	10. Rock irregular slide[a]	
Spread	15. Rock slope spread	16. *Sand/silt* liquefaction spread[a]
		17. Sensitive clay spread[a]
Flow	18. *Rock/ice* avalanche[a]	19. *Sand/silt/debris* dry flow
		20. *Sand/silt/debris* flowslide[a]
		21. Sensitive clay flowslide[a]
		22. Debris flow[a]
		23. Mud flow[a]
		24. Debris flood
		25. Debris avalanche[a]
		26. Earthflow
		27. Peat flow
Slope deformation	28. Mountain slope deformation	30. Soil slope deformation
	29. Rock slope deformation	31. Soil creep
		32. Solifluction

Figure 7 - The revised Varnes classification for landslides (from Hung *et al.*, 2014)

3.2 Landslide complex classes (level +1)

The definition of the landslide complex classes relies on the concept of functional interaction between objects (Worboys et al. 1990). To form a landslide complex object, referring to the DE-9IM topological model, a functional interaction is defined as a 2-dimensional topological relation between objects members of the same landslide class (§ 3.1). Based on the RCC8 model, two or more landslide objects are eligible for the aggregation in a landslide complex object if their topological relation is partially overlapping, tangential proper part, inverse tangential proper part, non-tangential proper part or inverse non-tangential proper part. The equals relation, even satisfying the functional interaction requirements is unrealistic (Figure 8). Landslide objects that do not share functional interaction with other landslide objects, are reported as "isolated landslides" and do not reach the aggregation phase (Figure 9a).

Having 21 landslide classes, the same amount of landslide complex classes is derived:

1. Rock fall complex class;
2. Soil fall complex class;
3. Rock topple complex class;
4. Soil topple complex class;
5. Rock rotational slide complex class;
6. Rock planar slide complex class;
7. Rock wedge slide complex class;

13

8. Rock compound slide complex class;
9. Rock irregular slide complex class;
10. Soil rotational slide complex class;
11. Soil planar slide complex class;
12. Soil compound slides complex class;
13. Rock slope spread complex class;
14. Granular soil spread complex class;
15. Cohesive soil spread complex class;
16. Rock avalanche complex class;
17. Soil dry flow complex class;
18. Granular soil wet flow complex class;
19. Cohesive soil wet flow complex class;
20. Deep-seated slope deformation complex class;
21. Shallow slope deformations complex class.

As for the landslide classes, currently, all these classes share the same set of attributes and methods. Attributes will be discussed in the database design chapter (§ 4.2.2), while the defined methods are:

- Events – retrieve the recorded events involving landslides contained in the reference complex;
- First-event – retrieve the first recorded event for the reference complex;
- Last-event – retrieve the last recorded event for the reference complex;
- Siblings – retrieve all the complexes forming the landslides system in which the reference complex is contained;
- Parent – retrieve the landslide system in which the complex is contained;
- Movement types – retrieve all the movement types contained in the reference complex;
- Landslides – retrieve all the recorded landslides forming the reference complex.
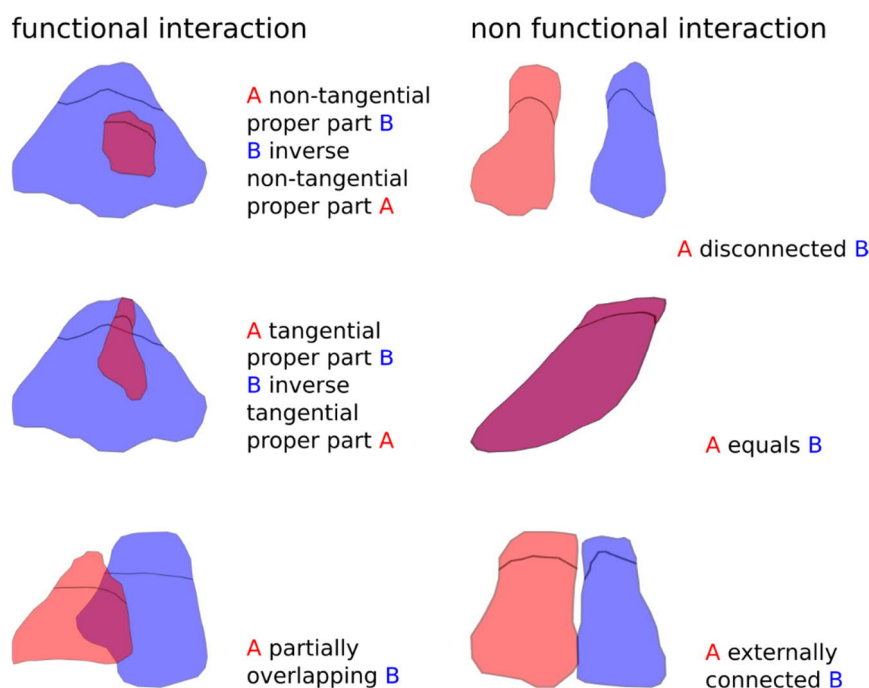
Figure 8 – Functional interaction topologies

3.3   Landslide system class (level +2)

The landslide system class is built upon the aggregation of the previous declared classes. In this case the condition of functional interaction is defined as a 2-dimensional topological relation between two or more landslide complex objects or landslide objects of any type. In this case, landslides that do not form a complex can be aggregated in a system directly if they have a functional interaction with complexes or other landslides of different type. The topological relations that satisfy the functional interaction condition are the same as for the landslide complex classes. Landslide complex objects that do not share a functional interaction with other objects, as for landslide objects, are reported as "isolated landslide complex" (Figure 9b).

Methods available so far for this class are:

- Events – retrieve the recorded events involving the landslides contained in the selected system;
- First-event – retrieve the first recorded event for the selected system;
- Last-event – retrieve the last recorded event for the selected system;
- Childs-complex – retrieve the landslide complexes contained in the selected system;
- Childs-landslides – retrieve the landslides contained in the selected system;
- Movement types – retrieve all the movement types contained in the selected system.
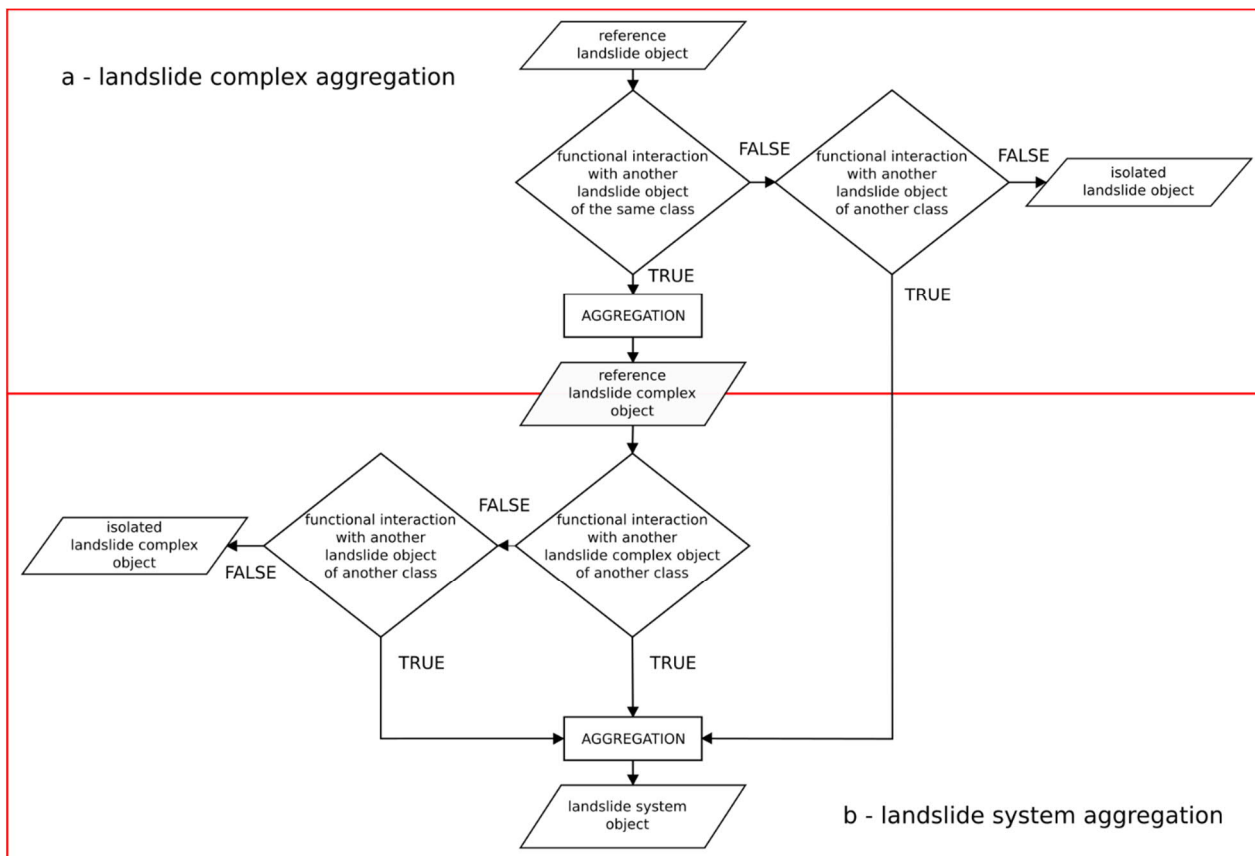
Figure 9 - Logical model for the aggregation of landslide complex objects and landslide systems objects

3.4   Landslide component classes (level -1)

Landslide components are defined in these classes. At this level, major areal features are considered, such as detachment areas, bodies, debris etc. Minor areal features or linear and point features could

be considered for a further level of detail (level -2) but are not included in this work. Moreover, the implementation has been limited at the actual classes needed for the training sites.

Referring for example to the rock rotational slide class, the sub-classes defined are:

- RRS detachment area class – containing detachment areas;
- RRS body class – containing rock rotational slides accumulation areas.

3.5   Temporal characterization and vertical relations

Every landslide object has attached temporal attributes for the time of occurrence which define an event. The relationship between landslides and events is many-to-one, meaning that one landslide object corresponds to a single event while one event can contain multiple landslide objects. Time of occurrence can be expressed as an exact value, when the date of occurrence is known, or as a range, when the exact time of occurrence is unknown, but a time interval can be deduced. For landslides contained in the same time interval a relative chronology can be implemented, based on field observations, remote sensing data analysis or any other mean.

Temporal characterization of landslides is crucial for the correct management of vertical relationships. In this framework, vertical relationship means both spatial sorting of the type under – over and temporal sorting of the type older - younger. As for the law of superimposition, older objects lie under younger objects while younger objects lie over older objects. In particular cases where an older object is entirely mobilized by a deeper, younger object (tangential proper part or non-tangential proper part topological relations), the older object, even being physically over the younger object, loose its "status" of landslide object and became part of the new landslide object debris. Within the temporal dataset it will be displayed under the younger object, being older. In the case of several overlapping phenomena within the same event, an overlap index is introduced as secondary sorting parameter.

For better space-temporal data handling, basic topological relations have been integrated with temporal relationships. Based on the 8 relationships of the RCC model and Allen's paradigms, referring to the object "A" and the object "B", their topological relationship may vary whether A is younger than B or vice-versa (Figure 10):

- *A Partially Overlap B*
    - *A before B* $\rightarrow$ *A overlapped by B* $\wedge$ *B overlaps A*
    - *A after B* $\rightarrow$ *A overlaps B* $\wedge$ *B overlapped by A*
- *A Tangential Proper Part B* $\vee$ *A NonTangential Proper Part B*
    - *A before B* $\rightarrow$ *A covered by B* $\wedge$ *B covers A*
    - *A after B* $\rightarrow$ *A superimposed on B* $\wedge$ *B contains A*
- *A inverse Tangential Proper Part B* $\vee$ *A inverse NonTangential Proper Part B*
    - *A before B* $\rightarrow$ *A contains B* $\wedge$ *B superimposed on A*
    - *A after B* $\rightarrow$ *A covers B* $\wedge$ *B covered by A*

The Equals relationship, as mentioned before, is not considered, while the Disconnected and the Externally Connected relationships are not affected by the temporal statement as their vertical sorting is invariant.

A *Partially Overlap* B
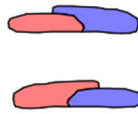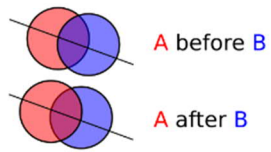
A before B — A *overlapped by* B and B *overlaps* A

A after B — A *overlaps* B and B *overlapped by* A

A *Tangential Proper Part* B or A *non-Tangential Proper Part* B
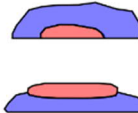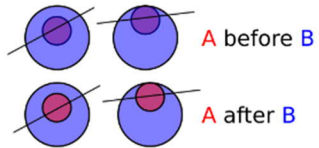
A before B — A *covered by* B and B *covers* A

A after B — A *superimposed on* B and B *contains* A

A *inverse Tangential Proper Part* B or A *inverse non-Tangential Proper Part* B
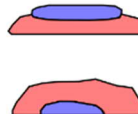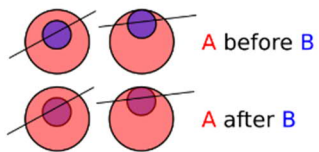
A before B — A *contains* B and B *superimposed on* A

A after B — A *covers* B and B *covered by* A

Figure 10 - Integration of topological and temporal relations

4   Methods

In order to test the proposed object-oriented hierarchical model, two main parallel strategies and a final comparative one have been developed and applied on three training sites in Italy.

In the Top-Down approach, morphometric analyses have been applied to investigate if complex arrangements of landslides, such as landslide systems, have a peculiar "topographic signature". To this end, Slope-Area plots and Topographic Position Index have been used, the first for the topographic classification of slope processes, the latter for the definition of morphometric features ascribable to landslide processes. For all the raster elaborations, the open-source software Grass GIS©7.8.0 (current version) has been used, both for data storage and manipulation. For the computation of Topographic Position Index, a custom plugin written in python has been implemented inside Grass GIS©, the code can be found in the appendix.

At the same time, the Bottom-Up approach has been applied for the direct recognition of landslides, both from field activities and remote sensing data analysis. After landslide inventorying, the object-oriented hierarchical model has been applied and landslides hierarchies have been derived. Finally, results from the previous approaches have been compared to test the strength of the Top-Down approach for landslides identification.

4.1   Top-Down approach

4.1.1   Topographic Position Index

Topographic Position Index (TPI) has been defined as the integer difference between a point elevation (z_0) and the mean elevation of its surrounding neighbourhood ($\bar{z}$) (Weiss 2001).

$$TPI = int((z_0 - \bar{z}) + 0,5)$$

So defined, TPI provides information about the relative position of a point in the landscape. Positive values mean that the elevation of the point is higher than the surrounding mean elevation, so the point is in a prominent-convex position, while negative values result from points having an elevation lower than that of their surroundings, so the point is in a depressed-concave position. Values near 0 represent points with an elevation about the same of the mean elevation of its neighbours, this is possible on flat areas or straight slopes (Figure 11).
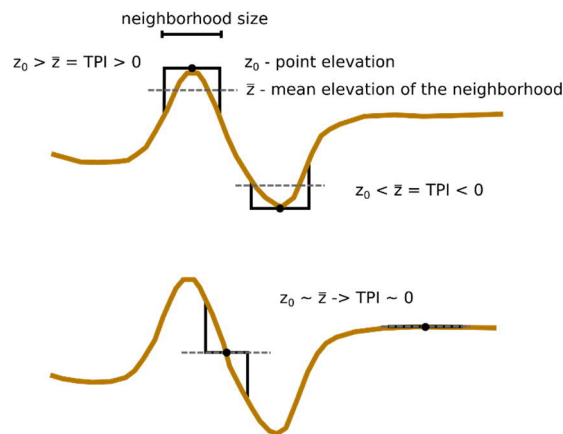
Figure 11 - Topographic Position Index values (modified from Weiss, 2001)

On Digital Elevation Models (DEM) the algorithm compares the elevation of each cell with the mean elevation of the neighbourhood in which, usually, the reference cell is the central point. The neighbourhood needs to be defined in terms of shape and dimension. The most common neighbourhood geometries have been compared: circular, square and annulus (Jenness 2006; Tagil and Jenness 2008; De Reu et al. 2013). The annulus neighbourhood has a wider range of values but excludes data contained in the inner radius, while the square geometry has a short range of values. In this perspective, the circular neighbourhood has been selected as optimal both for completeness and resolution (Figure 12).
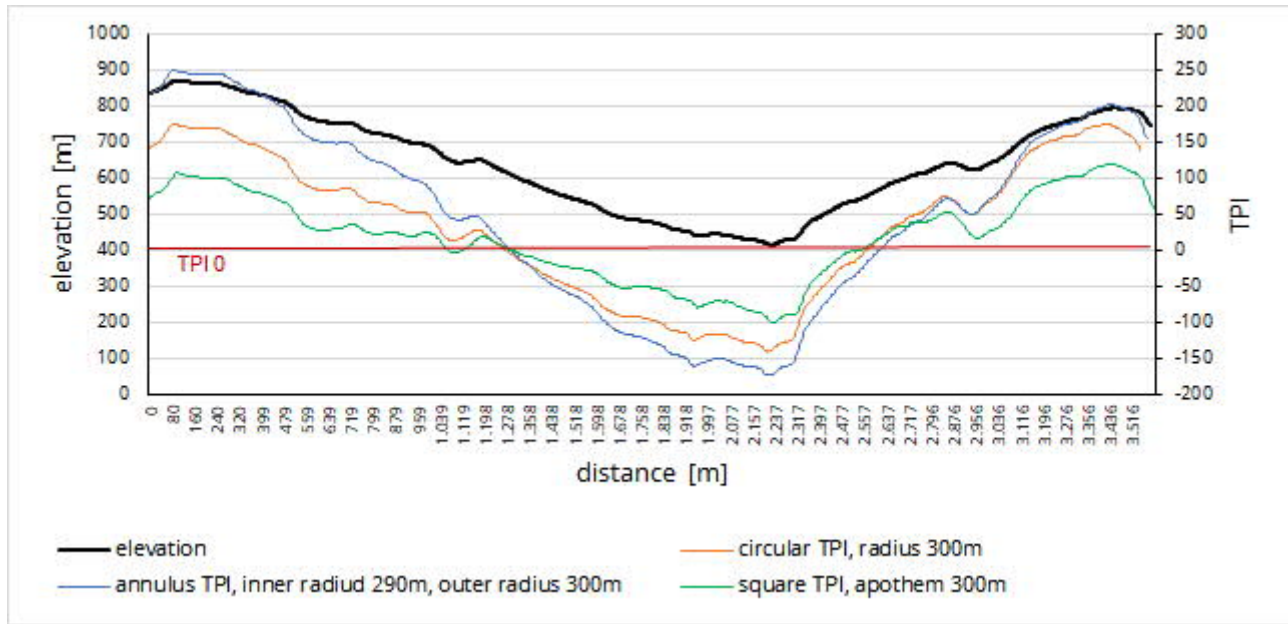
Figure 12 - Comparison of the resulting TPI values from different neighbourhood shapes, test on one of the case studies (§ 5.2)

Once defined the neighbourhood geometry, the radius needs to be defined. Usually this step is an iterative procedure as the radius is set once the output meets the purpose of a particular study (Tagil & Jenness, 2008). To address the subjectivity in the choice of the radius, the analysis has been carried out on the aggregation of several outputs computed with an increasing value of radius following an exponential sequence of 2^n cells, from 2^0 to 2^{10}, corresponding to a range of 5 m to 5120 m using a 5 m – resolution DEM. The various levels of TPI have been also standardized using the formula proposed in Weiss, 2001:

$$TPI_{std} = int\left(\left(\left(\frac{TPI - mean}{standard\ deviation}\right) * 100\right) + 0,5\right)$$

In this relation, mean and standard deviation parameters are derived from each raster dataset at every step. The result of this operation consists of two stacks of eleven raster datasets each, the first containing the effective TPI data and the last containing the standardized TPI data for every radius. Lastly, both the stacks have been aggregated by calculating mean and standard deviation (Figure 13). For the effective TPI values, datasets computed with larger neighbourhood have a major impact on the result because of their large values, while, for the standardized datasets, values are much more comparable as they are reduced at the same distribution size. In a morphometric perspective, this means that the mean of the effective values is more representative of the small-scale morphology, while the mean of the standardized values emphasizes local features (Figure 14). The

19

raster datasets containing the mean values of both TPI and standardized TPI have been then reclassified using the 6 slope position scheme also suggested in Weiss, 2001, useful for basic landscape classification (De Reu et al. 2013; Kriticos et al. 2015; Gruber et al. 2017) (Figure 15).

standardization

2^0 = 1 cell = 5 meters ⟶	tpi_0001c ⟶	std_tpi_0001c
2^1 = 2 cells = 10 meters ⟶	tpi_0002c ⟶	std_tpi_0002c
2^2 = 4 cells = 20 meters ⟶	tpi_0004c ⟶	std_tpi_0004c
2^3 = 8 cells = 40 meters ⟶	tpi_0008c ⟶	std_tpi_0008c
2^4 = 16 cells = 80 meters ⟶	tpi_0016c ⟶	std_tpi_0016c
2^5 = 32 cells = 160 meters ⟶	tpi_0032c ⟶	std_tpi_0032c
2^6 = 64 cells = 320 meters ⟶	tpi_0064c ⟶	std_tpi_0064c
2^7 = 128 cells = 640 meters ⟶	tpi_0128c ⟶	std_tpi_0128c
2^8 = 256 cells = 1280 meters ⟶	tpi_0256c ⟶	std_tpi_0256c
2^9 = 512 cells = 2560 meters ⟶	tpi_0512c ⟶	std_tpi_0512c
2^{10} = 1024 cells = 5120 meters ⟶	tpi_1024c ⟶	std_tpi_1024c

tpi_mean   std_tpi_mean
tpi_dev   std_tpi_dev

Figure 13 - TPI datasets used for this study
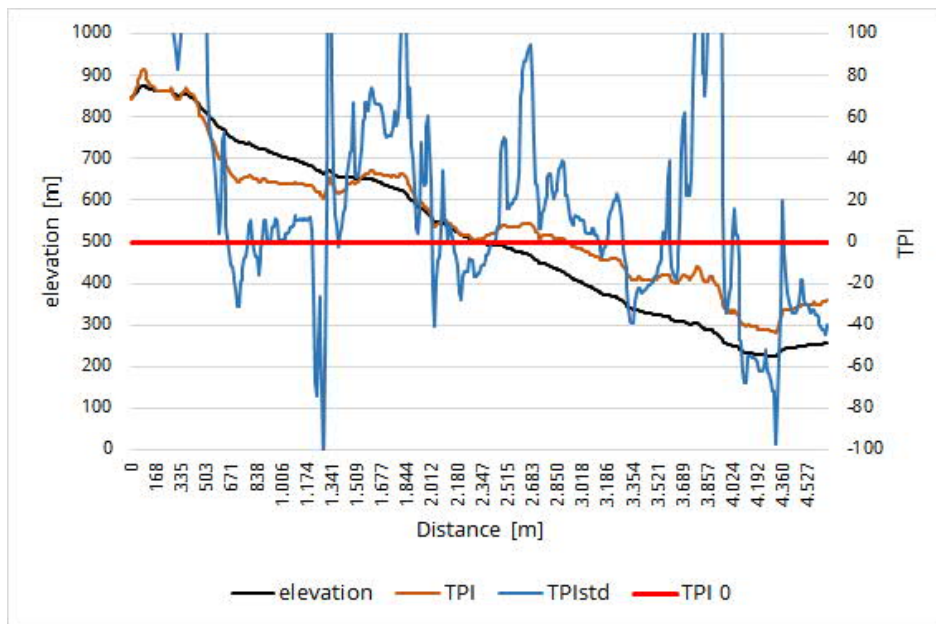
Figure 14 - Comparison of the TPI values derived from the mean of the effective datasets and the mean of the standardized datasets, peaks of the TPIstd function are cut for readability; example profile from one of the case studies (§ 5.2)

TPI > std   ■ red   ridge

0,5 std < TPI <= std   ■ orange upper slope

-0,5 std < TPI <= 0,5 std; slope > 5°   □ yellow middle slope

-0,5 std < TPI <= 0,5 std; slope <= 5°   ■ green flat slope

-std < TPI <= -0,5 std   □ cyan   lower slope

TPI <= -std   ■ blue   valley
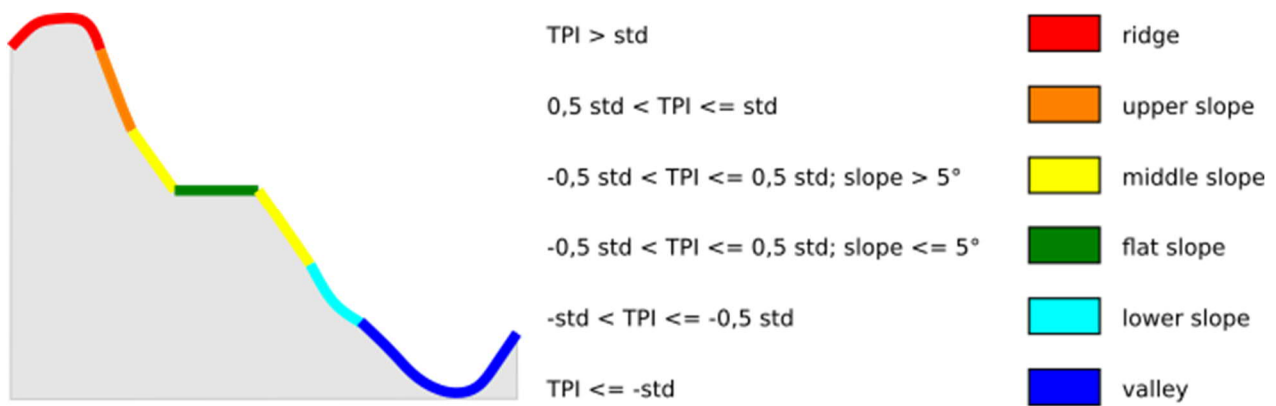
Figure 15 - Slope positions

4.1.2   Slope-Area plots

Slope – Area Plots (Montgomery and Foufoula-Georgiou 1993; Booth et al. 2013; Tseng et al. 2015) have been exploited for the estimation of the erosional process types acting on the slopes, including also landslide phenomena. The purpose of this analysis is to detect the hypothetical landslide-related channels as a preliminary tool for landslides detection.

Basically, the graphical plot of the topographic steepness as function of the drainage area can be subdivided in four main regions or segments, each one representing a dominant geomorphic process: I) hillslopes; II) hillslope-to-valley transition; III) debris flow dominated channels or landslides driven channels; IV) alluvial channels (Figure 16a).

Slope and contributing area values have been plotted for each case study and domain thresholds have been defined analysing the slope derivative values (Vergari et al. 2019). Threshold for the I – II boundary has been set at the first zero value of the slope derivative, corresponding to the maximum value of the Slope – Area function; threshold between II and III domains has been set at the next zero of the derivative function which reflects an interruption in the steady decreasing trend of the II domain; the last threshold is marked by the last zero of the derivative values corresponding to the transition from fluctuating values to a steady decreasing trend in the slope function (Figure 16b).
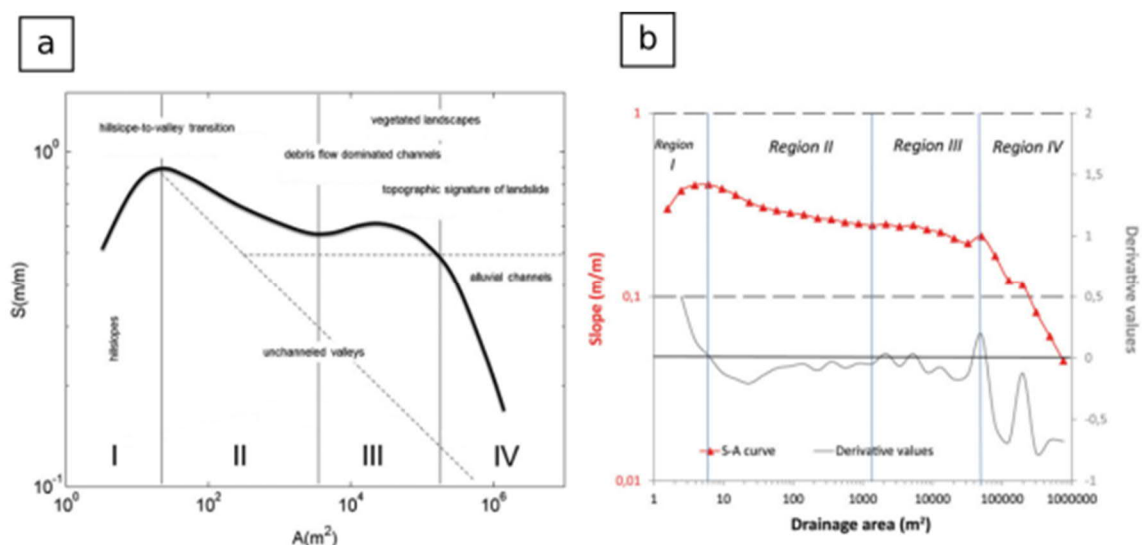
Figure 16 - Slope-area plots and thresholds definition (from Tseng et al., 2015; Vergari et al., 2019)

21

4.1.3   TPI and S-A plots integration

For the recognition of landslide-related features an original comparison of TPI and slope values has been made as a new approach. Values from the mean TPI dataset and the mean standardized TPI dataset have been also plotted against the contributing area, defining a "TPI function" and a "Standardized TPI function". Using thresholds derived from the S-A function, a range of values can be delimited on the Standardized TPI function corresponding to region III of the S-A plot defining a range of values that allow the reclassification of the mean standardized TPI raster into a set of morphometric features probably related to landslides. In the same way, a "fluvial domain" can be defined on the TPI function, corresponding to the IV region of the S-A plot. This new "fluvial region" obtained reclassifying the mean TPI raster has been used to filter features in the "landslides domain" obtained with the Standardized TPI function (Figure 17). The standardized TPI function has been chosen for landslide features identification as its values emphasize local morphological variations, while the effective TPI function is more suitable for the definition of the fluvial domain as its values reflect small-scale morphologies such as major valleys (Figure 18).

The range of standardized TPI values segmented with this approach is entirely composed of negative values. As negative TPI values correspond to concave morphologies, this analysis returns only concave features probably related to landsliding processes and not the entire landslide, convex portions of a landslide, such as bulgings and debris accumulations are not detected.
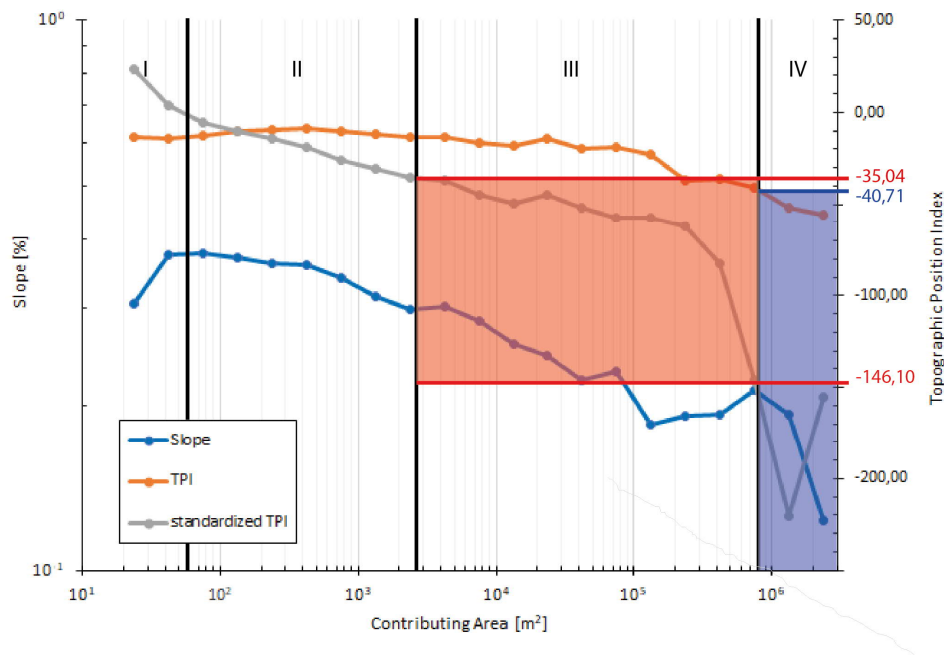
Figure 17 – Example Slope Area Plots and TPI integration derived from one of the case studies (§ 5.3.3)
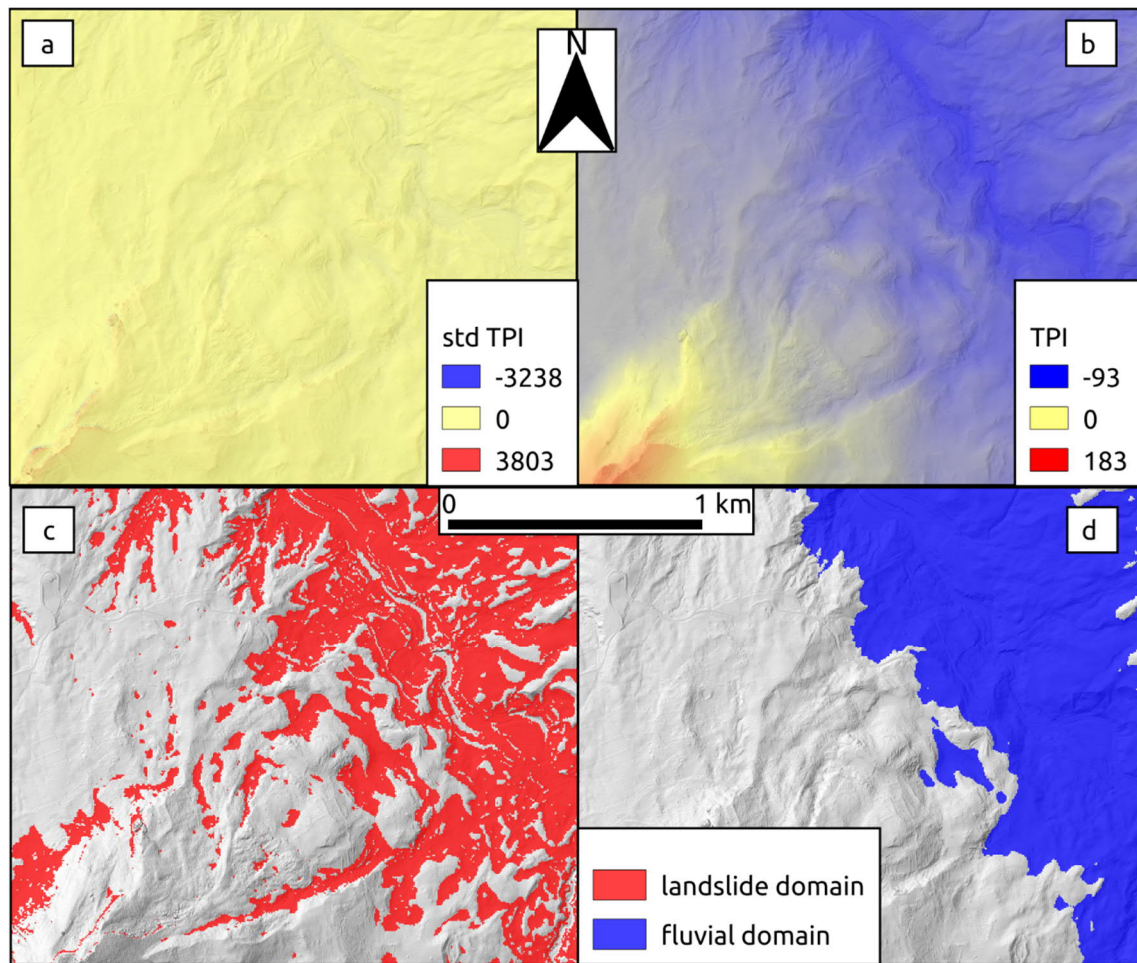
Figure 18 - a - c) mean values of the standardized TPI, continuous and reclassified using threshold shown in the previous figure; b - d) mean valued of the TPI values, continuous and reclassified; example from a case study (§ 5.3)

4.2 Bottom-Up approach

4.2.1 Landslides inventory and landslide maps

The basic landslides inventory has been built by means of field survey, remote sensing data analysis, such as aerial photographs and collecting data from previous existing inventories. Following the procedure proposed by Dramis et al. 2011 for general geomorphological mapping, inventoried features have been first stored with a symbol based approach (SGN 1994; APAT 2007; Gustavsson et al. 2008; Gustavsson and Kolstrup 2009; ISPRA 2018). Then, data have been processed in a GIS environment, converting symbols in proper landslide objects, producing a full coverage landslide map (Dramis et al. 2011; Guida et al. 2015) (Figure 20). In this full-coverage representation, the overlapping portions between landslides are preserved and not cut as usual, as they are crucial for the aggregation procedures (Figure 19). After these operations, data have been imported in the database designed following the proposed object-oriented model (§ 3).
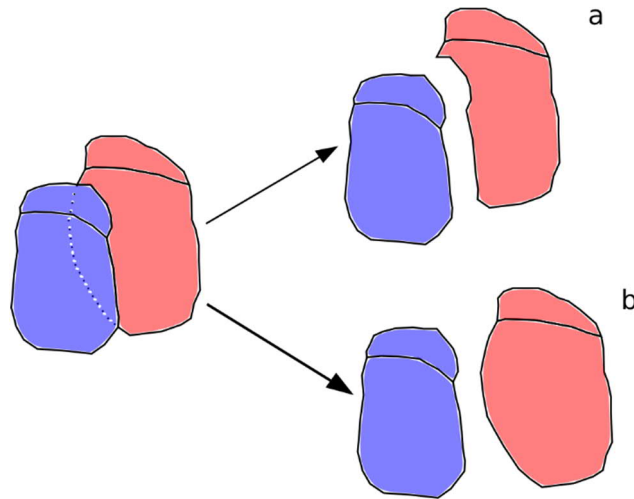
Figure 19 - representing overlapping features a) as adjacent tiles cutting the overlapping portion, b) maintaining the overlapping portion ensuring correct topological relations
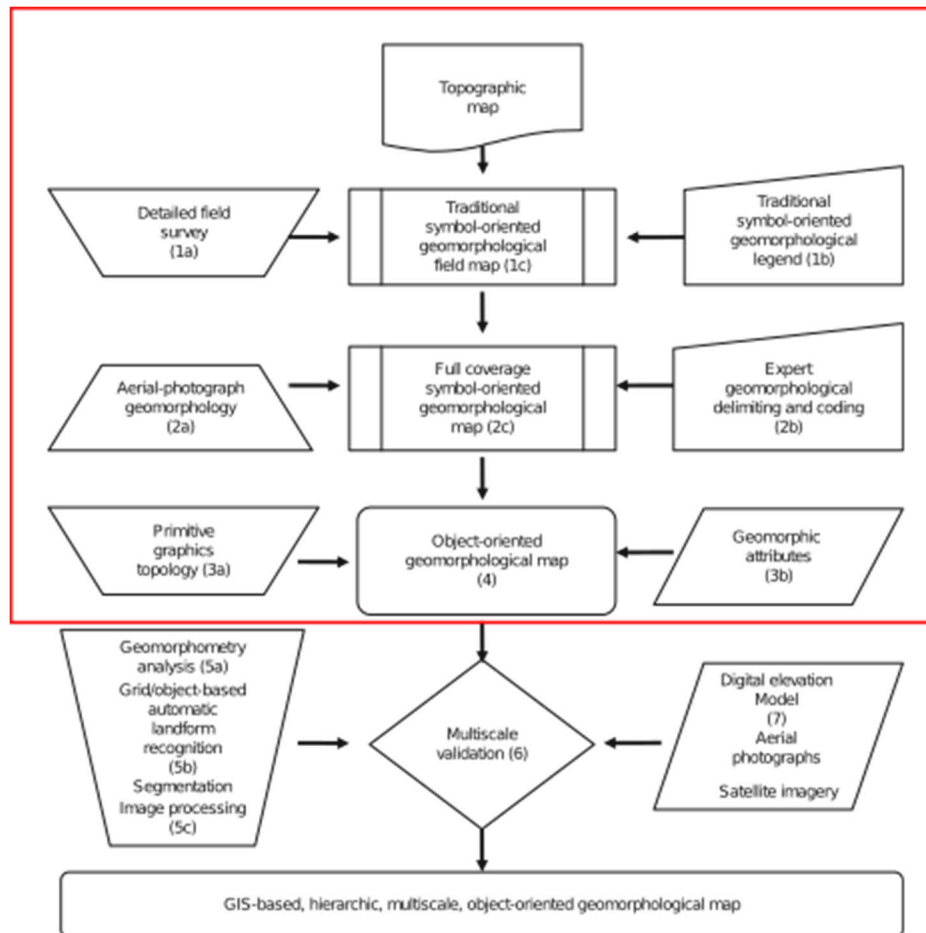
Figure 20 - GmIS-UniSA mapping model, the red square highlights the operations performed in the framework of this research (from Dramis *et al.*, 2011)

4.2.2   Database design

The database used for this work is PostgreSQL© 11.0 with PostGIS© 2.5 extension (current versions). Database maintenance and manipulation is achieved using PgAdimn4 and the pgcli command line tool, while QGIS 3.4 LTR© is used for data query and visualization.

PostgreSQL© is an object-relational database management system (ORDBMS) and is not fully object-oriented, but a set of object-oriented features is already available:

- Inheritance – generalization and specialization are fully supported;
- Support for complex objects and extensibility – custom data types and functions can be declared;
- Overriding – the same function can have different behaviours based on the input arguments.

Some other features are not natively implemented, but can be emulated with a few workarounds:

- Encapsulation and classification – these features can be emulated with custom data types for the attributes, and custom functions for methods;
- Aggregation – automatic aggregation based on class membership can be reproduced using PostgreSQL views and/or materialized views along with PostGIS aggregate functions like ST_Union or ST_Collect.

Lastly, object identity is not available as it is a concept strictly related to the object-oriented paradigm and as such, it is a feature only available in fully object-oriented languages and there is no way to implement such feature in a RDBMS. As for now, objects are stored as table records.

Based on the model described in § 1, the database has been structured into three main blocks: a dictionary block, a data block and a visualization block.

In the dictionary block, tables containing reference terminology are included. The main purpose of this data is to prevent errors during the process of data entry, therefore, to maintain data integrity. These tables are accessed through foreign key by the tables contained in the data block and by some of the dictionary tables themselves. The terminology contained in this block is about landslides (Hungr et al. 2014) and spatio-temporal topology semantics (Allen 1983; Egenhofer and Herring 1990b; Randell et al. 1992). The defined tables are:

- Landslides material types, containing reference information about landslides material;
- Landslides movement types, containing reference information about landslides movement type;
- Landslides types, containing reference terminology about landslide types, this table also refer to the material and movement type tables;
- Topological predicates, containing predicates for the RCC8 topological model and their corresponding matrixes for the DE9IM topological model;
- Temporal predicates, containing Allen's predicates for temporal relationships;
- Spatio-temporal predicates, containing spatio-temporal predicated defined in § 3.5, this table also refer to the RCC8 and temporal table.

The data block is structured to contain the instances of the object-oriented model. Here, a table is defined for every class declared in the model (§ 1), meaning that the final result will be having 21 tables for landslide objects, 21 tables for landslide complex objects and one table for landslide systems. As for now, landslide tables are not further specialized as they share the same set of attributes:

- Landslide id, string type ('LNS_nnn') manual, contains the landslides id, this id is shared with reactivations of the same landslide;
- Event id, integer type mandatory, contains the event id for that landslide, these ids must be sequential, their ordering is the same of the temporal sequence of the events;
- Landslide event id, string type ('LNS_nnn_nnn') mandatory, this is the landslide unique id and derives from the combination of landslide id and event id and id used to distinguish between different reactivations of the same landslide, this is also the primary key of the table;
- Overlap index, integer type mandatory, contains the overlap index for landslides of the same event, default value is 0;
- Movement type 1, string type mandatory, contains the main type of movement of the landslide, refers to the movement types dictionary table;
- Movement type 2, string type optional, contains the secondary type of movement of the landslide, refers to the movement types dictionary table;
- Insert time, date type automatic, this field contains the time of data entry;
- Date, date optional, this field contain the date when the landslide occurred;
- Date range start, date type optional, this field contains the starting date for the range of time in which the landslide occurred,
- Date range end, date type optional, this field contains the ending date for the range of time in which the landslide occurred.
- Geometry, geometry type mandatory, contains the geometry of the landslide.

Even though date, date range start and date range end are all optional fields, at least one of them is required for the correct temporal characterization of landslides. These fields are generic date types (YYYY-MM-DD), but if the only information available is a month or a year, they can be expressed as YYYY-MM-01 for months and YYYY-01-01 for years.

Landslide complex tables are materialized views derived from the aggregation of the landslide tables following the procedure described in § 3.2. These objects have not an exact temporal characterization as they can contain different landslides occurred at several times, but their vertical sorting is achieved computing the "mean event" from the aggregated landslides event ids, so that the most active complexes are ensured to be on top. Attributes for these tables are:

- Complex id, string type ('CPX_nnn') automatic, this is the landslide complex unique id and the primary key of the table;
- Mean event id, float type mandatory, this is the mean event id computed from the aggregation of the landslide tables;
- Geometry, geometry type automatic, contains the geometry of the landslide complex derived from the aggregation of the landslide geometries.

The landslide systems table, as for the previous tables, is a materialized view built upon the aggregation of the previous data. Attribute available for this table are:

- System id, string type ('SYS_nnn') automatic, this is the landslide system unique id and the primary key of the table,
- Geometry, geometry type automatic, contains the geometry of the system derived from the aggregation of the complexes and landslides geometries.

As for landslide complexes, systems have not an exact temporal characterization. Moreover, considering how they are built, for landslide systems vertical sorting is invariant as they do not overlap.

It is worth noting that attributes in this tables are essentials, meaning that the only data that is physically stored is about information that cannot be retrieved in any other way, for everything else, methods (functions) are used instead.

Landslide component table derive from the generalization of two main component groups, as far for the ones needed in this research:

- Detachments
- Accumulations

These two categories branch themselves into the basic landslide components classes, as discussed in § 3.4. Attributes defined for these classes are:

- Landslides id, string type mandatory, contains the landslide unique id where the component belongs, referenced with the relative landslide table;
- Component id, string type ('XXX_nnn') automatic, contains the component id, it's the primary key of the table;
- Geometry, geometry type mandatory, contains the geometry of the component.

In the visualization block, objects from the data block are re-arranged for the correct visualization. The vertical sorting is applied using the temporal characterization of landslides. This process only applies to components, landslides and complexes as systems, as for their definition, do not overlap, thus do not need vertical sorting (Figure 21).

All the SQL code for the reproduction of this database structure is available in the appendix.
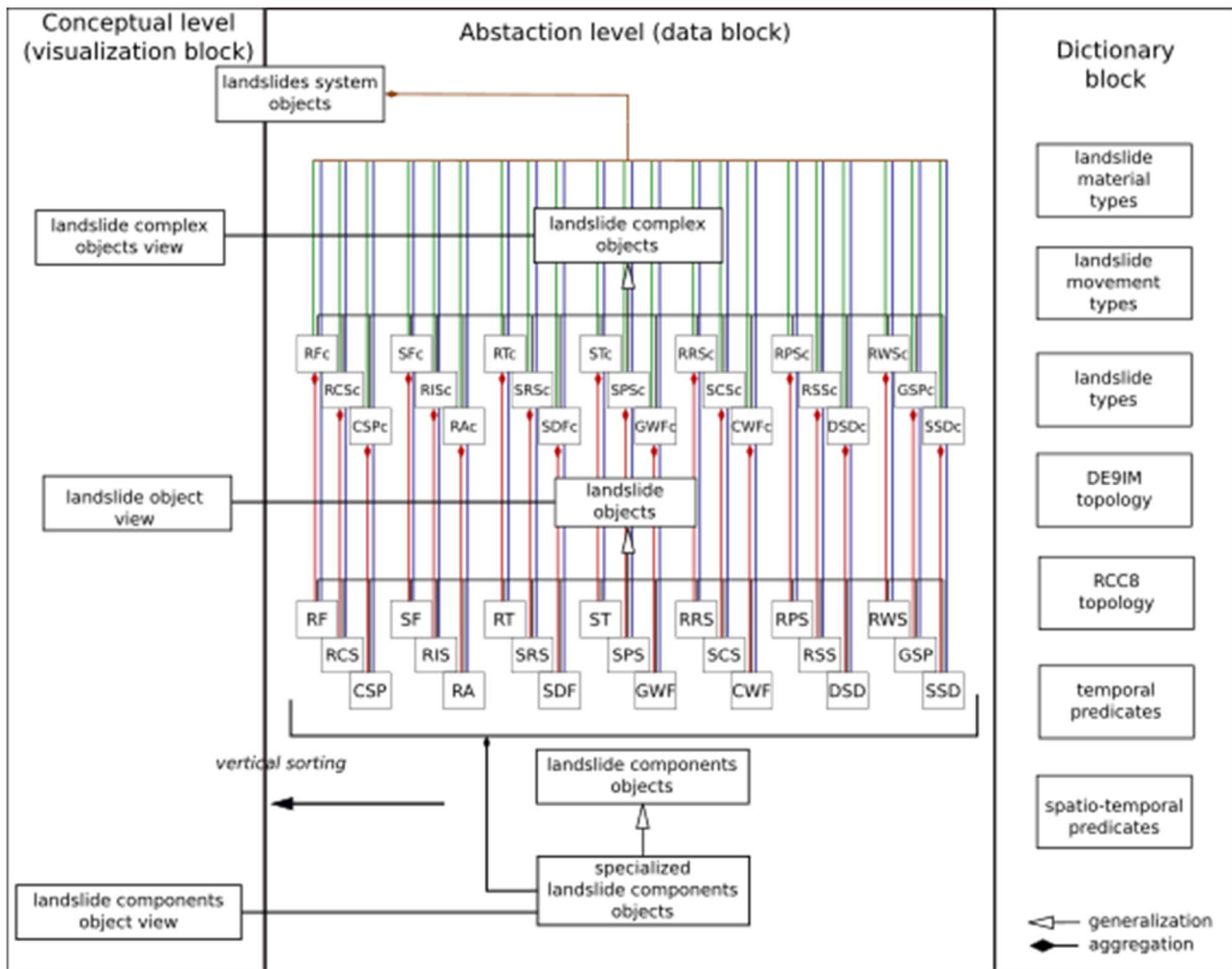
Figure 21 - Database design for the proposed object-oriented model, acronyms for landslide tables and landslide complex tables refer to the classes defined in § 1

4.2.3   Reference hillslope

Once defined a landslide object or any other super-object, its interior could be described as the portion of landscape in which any observer is certain that that specific phenomenon (or several) is occurred or is occurring. On the other hand, its exterior should be the portion of landscape in which any observer is equally certain that the same phenomenon is not occurred or is not occurring. However, the latter statement could be not so true in the closer proximity of a landslide boundary, this area could be described as the portion of landscape in which there is no occurrence at the observation time but at the same time has the highest likelihood to be involved in a future reactivation. In this regard, referring to the egg-yolk model (Clementini 2004; Bittner and Stell 2008; De Felice et al. 2011), a landslide, or its generalizations, can be defined as a landform, or a complex or a system considering super-objects, with broad boundaries, with a core region and a vague or uncertain boundary (Cohn et al. 1997; Guilbert et al. 2016; Guilbert and Moulin 2017) (Figure 22).
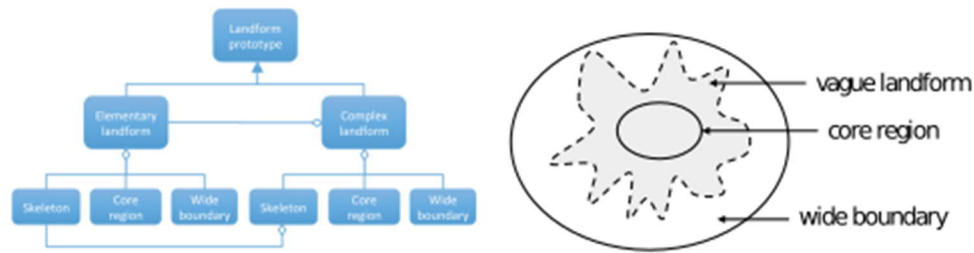
Figure 22 - Landform ontology and Egg-yolk model (from Guilbert *et al.*, 2016)

In this perspective, the reference hillslope is here defined as the portion of landscape containing both the core region and the broad boundary of a reference object (a landslide, a complex or a system), or the area in which it lies and is likely to evolve. The concept of reference hillslope is similar to that of slope unit, a landscape partition bordered by drainage and divide lines used as zonation for landslide susceptibility assessment (Carrara et al. 1991; Guzzetti et al. 1999; Alvioli et al. 2016, 2018). The main difference between slope units and reference hillslopes is that the first are computed from DEMs using hydrological properties of the topographic surface and are unaffected from pre-existing landslides, while the latter are defined starting from pre-existing landslide objects, or super-objects, and its vertices and edges are derived from the DEM using Surface Networks.

Surface Networks are built upon the extraction of the mathematical skeleton of a generic surface (Pfaltz 1976; Rana 2004; Guilbert et al. 2016; Wolf 2017). This skeleton consists of nodes, which are the critical points of the topographic surface (local maxima or peaks, local minima or pits and local saddles or passes), and edges connecting passes to peaks (ridgelines) and passes to pits (courselines), also called critical lines (Figure 23). This data structure has been exploited for surfaces characterization in various fields such as computer graphics (Sahner et al. 2008), geography (Hu et al. 2014), materials engineering, electronics and medicine (Senin et al. 2013), other than topography (Schneider 2003; Bremer et al. 2004; Rana 2004; Blanc et al. 2011; Clarke and Romero 2017; Rocca et al. 2017).

The set of critical points and critical lines defines "slope regions" and the set of slope regions in which a landslide object, or any other super-object, is entirely contained form the reference hillslope of that specific object.
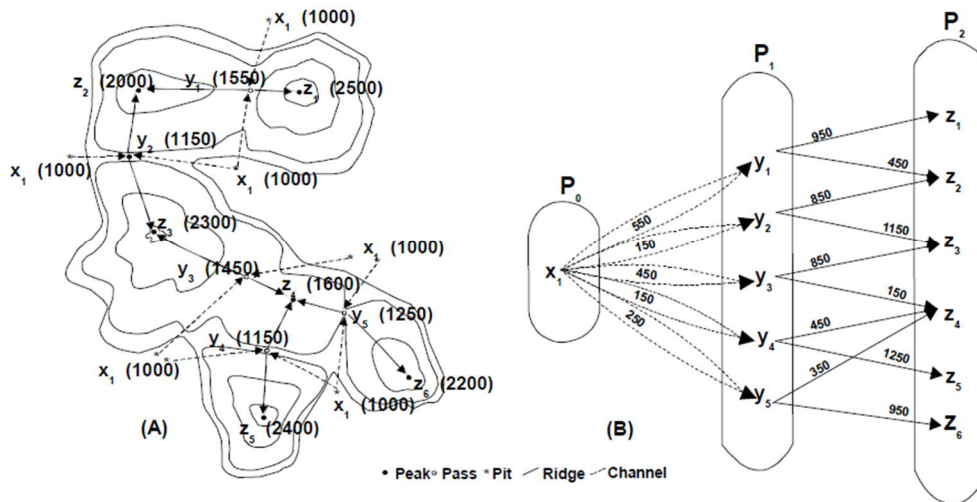
Figure 23 - Surface Network (from Rana 2000)

The so-defined terrain unit can be considered the basic landscape portion to be investigated when studying a landslide or the starting point to search whether that specific phenomena interacts with other landslides or not. If any other landslide with functional interaction falls within the reference hillslope, then the set of landslides ascend to the hierarchical rank of landslide complex or landslide system, depending on the landslide types, and the reference hillslope can be recomputed on the new set.

4.3   Top-Down and Bottom-Up comparison

Results from both the previous approaches have been compared. The Top-Down approach returns the candidate landslide features derived from morphometric analyses on DEMs, while the Bottom-Up approach returns landslide inventories and landslide hierarchies from direct or remote surveys. The datasets have been compared using confusion matrices (Powers 2007), where data from the Top-Down approach are the predicted values and data from the Bottom-Up approach are the actual values. Confusion matrices compare sample data with the results of a prediction, computing prediction errors: type I errors are false positive (FP) values, which are positive in the prediction but are actually false; type II errors are false negative (FN), which are negative in the prediction but are actually true. Correct predictions are true positive (TP) and true negative (TN) (Figure 24).

Figure 24 - Confusion matrix, green represents exacts predictions, red represents errors (modified form Powers, 2007)

Based on the relationship between these values, various relations are derived:

- Recall (True Positive Rate, TPR), the percentage of correctly predicted true values over the total of true actual values;
- False positive rate (FPR), the percentage of wrong positive predictions over the total of false actual values;
- Precision (Positive Predicted Values, PPV), the percentage of correctly predicted true values over the total of predicted positive values;
- Accuracy (ACC), the percentage of correctly predicted values, both positive and negative, over the whole dataset.

$$TPR = \frac{TP}{TP + FN} \quad ; \quad FPR = \frac{FP}{TN + FP} \quad ; \quad PPV = \frac{TP}{TP + FP} \quad ; \quad ACC = \frac{TP + TN}{TP + FP + FN + TN}$$

Since the Top-Down approach returns just concave features probably related to landslides and do not detect whole landslides, Precision values (Positive predicted values, PPV) and false positive rates (FPR) have been chosen over the Recall (True positive rate, TPR) and the accuracy in order to assess prediction performance.

Data from the previous approaches have been converted to a binary logic format, 1-0 = True-False, and analysed using the confusion matrix. The four datasets used for the analysis are:

- Actual values: 1 = landslide, 0 = non landslide, derived from the landslides inventory;
- Predicted values: 1 = landslide concave feature, 0 = other features, derived from the reclassification of standardized TPI values;
- Filter: 1 = fluvial domain, 0 = non fluvial domains, derived from the reclassification of the actual TPI values;
- Predicted values filtered: 1 = landslide concave feature, 0 = other features, derived from the reclassification of standardized TPI values removing values contained in the fluvial domain.

All these datasets have been clipped to the reference hillslope computed for the various landslide systems for an optimized comparison.

5 Case studies

5.1 Corniolo – Poggio Baldi

This site is located in northern Italy, in the Emilia-Romagna region, along the upper portion of the Bidente river in the Santa Sofia municipality. This case study has been chosen after the last reactivation of the Poggio-Baldi landslide, which caused the damming of the Bidente river and the interruption of a main provincial road, other than the destruction of a few private buildings (Figure 25).
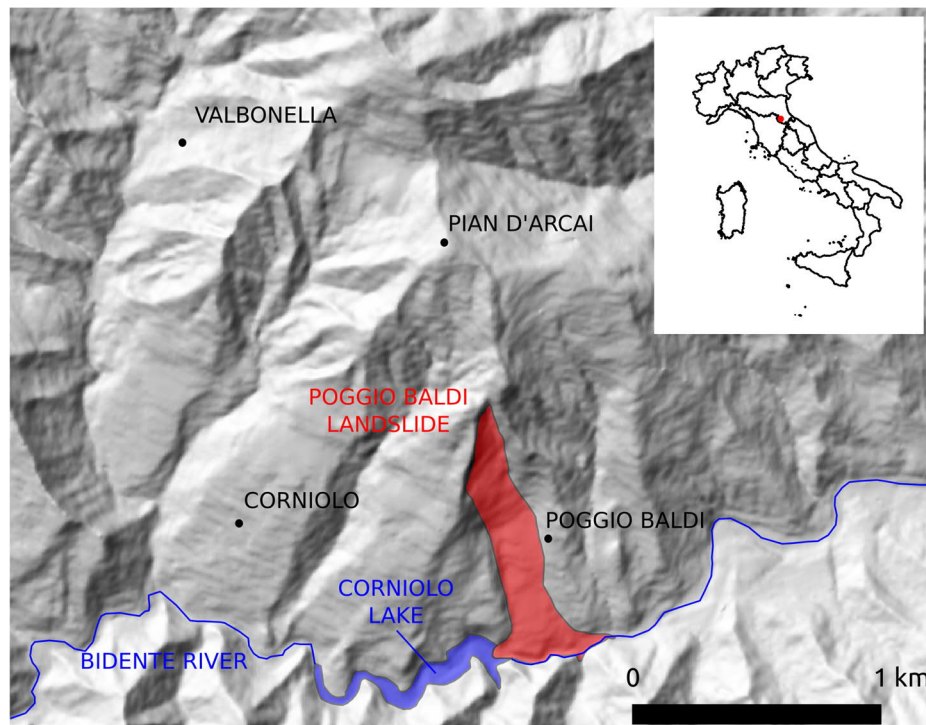
Figure 25 - Corniolo - Poggio Baldi case study location

5.1.1 Geological and geomorphological settings

The study area is part of the Forlivese Apennine and the outcropping terrains mainly belong to the Marnoso-Arenacea Romagnola Fm. (Martelli 2002). In this area, this formation is subdivided in several members based on the ratio between the arenaceous and pelitic content (A/P ratio), the representative member of the study area is the Corniolo member, which is made of sandstones interbedded with claystones, rarely carbonaceous, with an A/P ratio between ½ and 1/3, usually beds present a tabular structure (Ricci Lucchi 1981; Martelli 2002). The investigated area belongs to an imbricate fan thrust chain portion (Boyer and Elliott 1982) and the hillslope object of this study lies on the S. Benedetto in Alpe thrust, which overlaps the Ridracoli tectonic unit over the Isola unit (Martelli 2002) (Figure 26). The main bed attitude is south-western dipping, perpendicular to the main thrust line, with various dip angles (Figure 27).
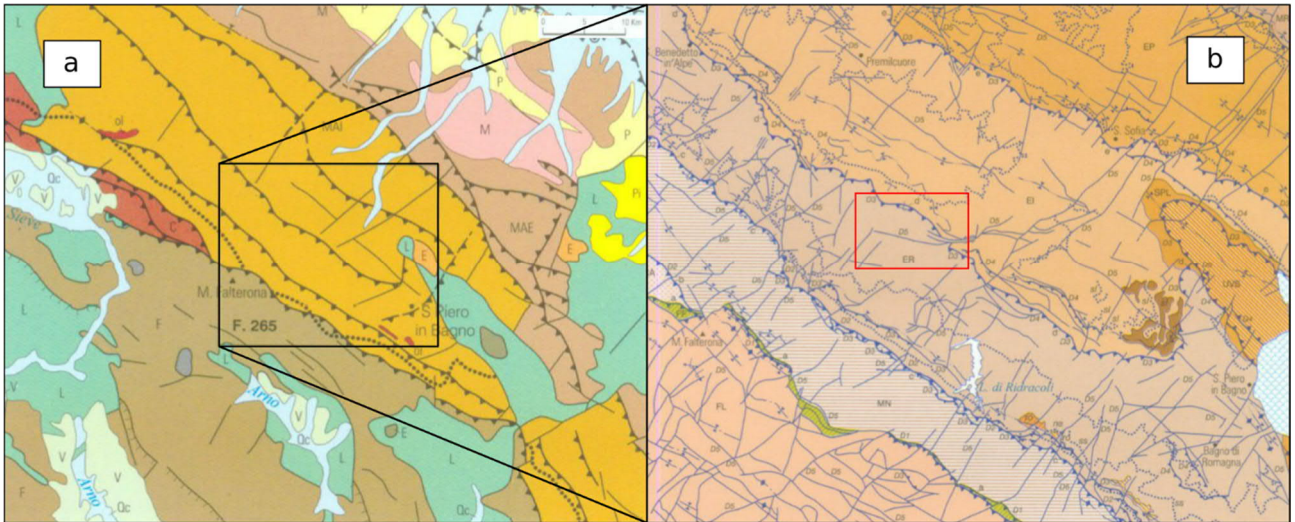
Figure 26 - a) regional geological settings: V - lacustrine deposits; P - marine deposits; P1 – Pliocene continental deposits; M – evaporites; MAE – upper Marnoso-Arenacea Fm.; MAI – lower Marnoso-Arenacea Fm.; C – Caste Guerrino Unit; F – Falterona Unit; L – Liguride Units; b) local geological settings: FL – Mt. Falco Unit; MN – Mt. Nero Unit; ER – Ridracoli Unit; EI – Isola Unit; EP – Pianetto unit; the red box highlights the study area
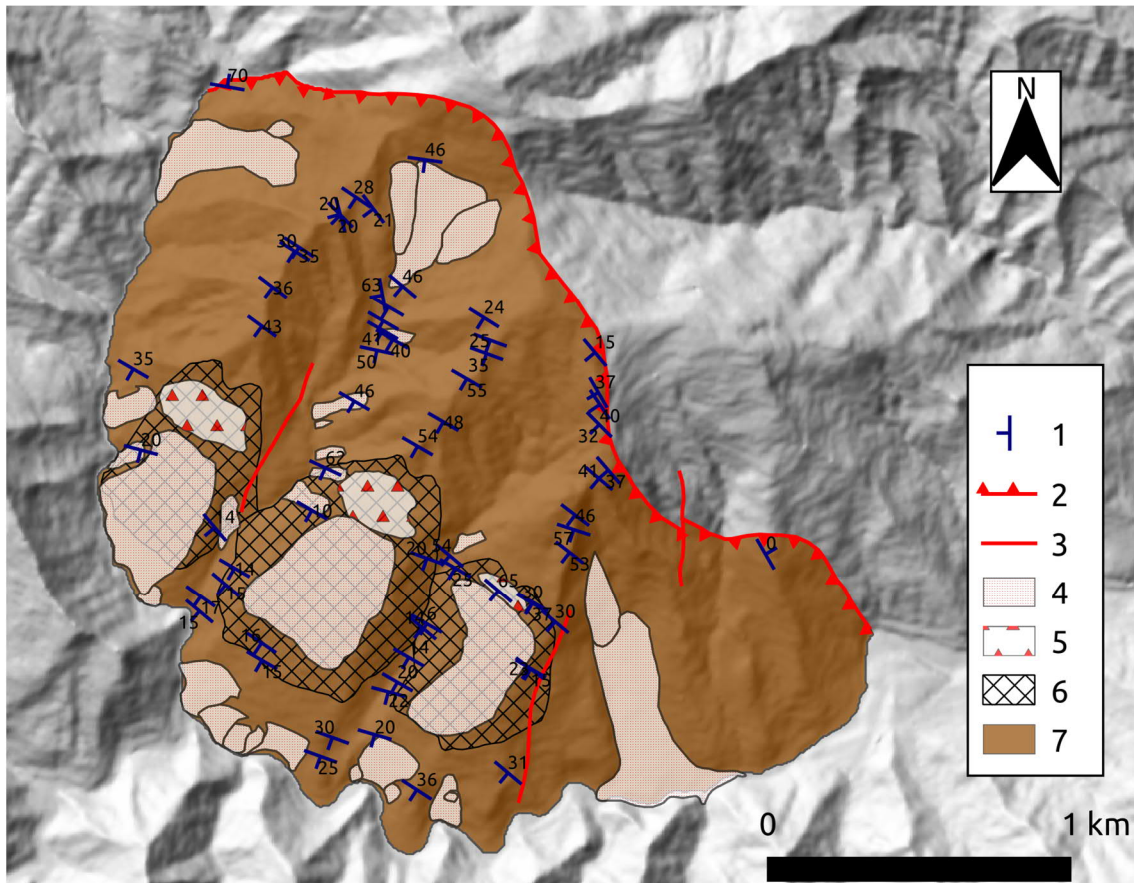
Figure 27 - Geological map of the Corniolo area: 1) bedding with dip angles; 2) thrust fault; 3) undefined fault; 4) landslide debris; 5) colluvium; 6) wasted rock mass; 7) Marnoso Arenacea Fm. – Corniolo member (modified after Di Luzio 2019)

The actual morphologies of the Corniolo hillslopes strongly depends on the litho-structural settings of the area. The selective erosion of flysch deposits allowed the development of landforms such as structurally controlled stepped slopes or ribbon-like slopes. In some areas, on cataclinal slopes

landforms such as flatirons developed. Moreover, these geological settings favoured the development of several landsliding phenomena, such as planar slides or wedge slides.

5.1.2   The Poggio Baldi landslides

The last reactivation of the Poggio Baldi landslide dates back to March 19, 2010 as a consequence of increased pore water pressure caused by rapid snow melting (Mazzanti et al. 2017). Volume of the landslide body has been estimated to about 4 million m^3. The landslide caused the damming of the Bidente river with the consequent formation of the Corniolo lake, which is still present (Figure 33b). The landslide also caused the interruption of the main provincial road and the destruction of a few private buildings, luckily without casualties.

The initial movement has been classified as a rock-wedge slide evolved in debris flowslide. A previous reactivation of the movement dates back to February 28, 1914, when the collapse happened as a granular flow. Moreover, the main scarp and probably the river inflection is already visible on the historical maps of the Forlì province (1888) (Figure 28).
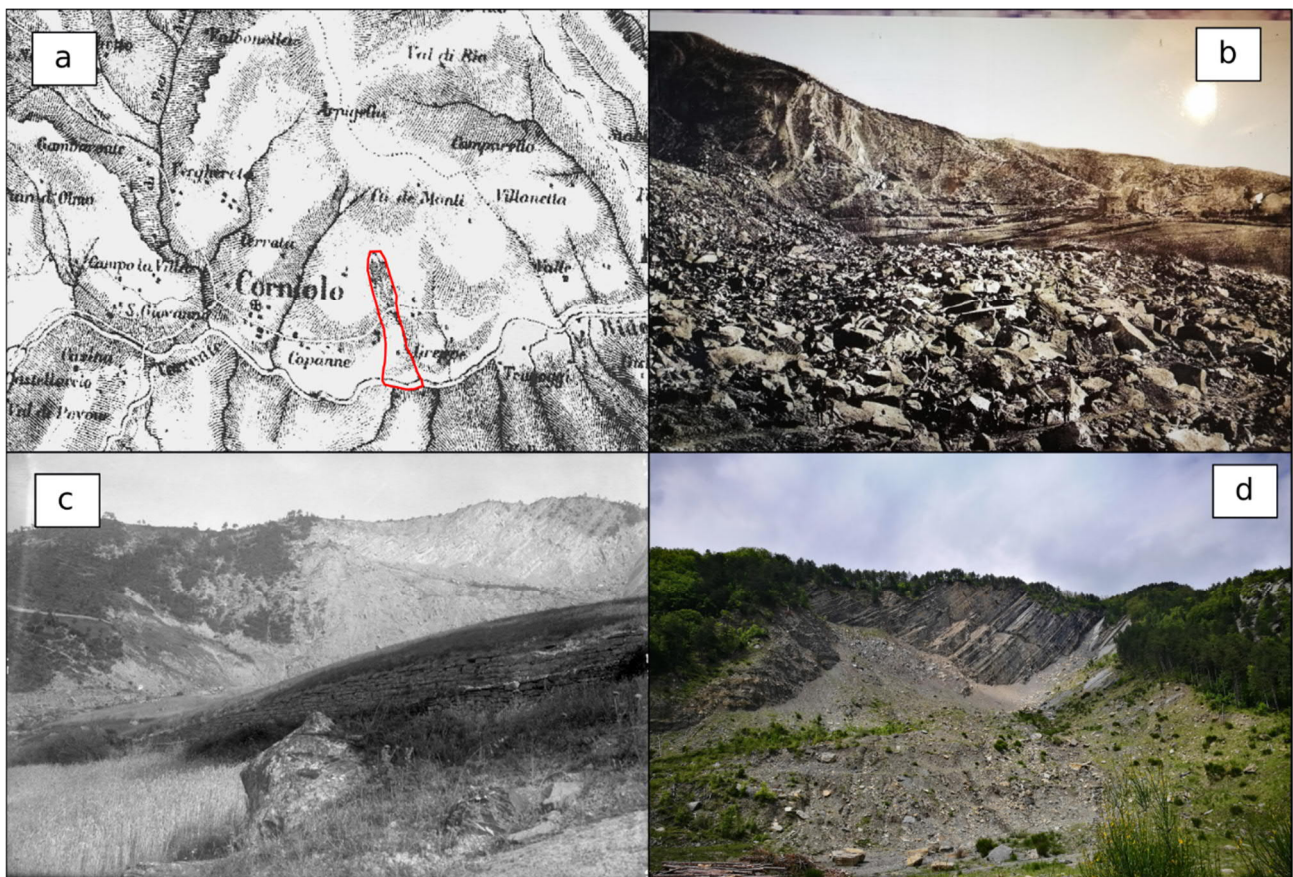
Figure 28 – The Poggio Baldi landslide: a) excerpt from the historical map of the Forlì province, the approximate location of the 2010 landslide is highlighted; b) after the rock avalanche event of 1914; c) the slope in 1924 (from Emilia Romagna region and Forlì province archives); d) the scar area today (photo taken in May, 2019)

5.1.3   Top-Down Approach

The Digital Elevation Model used for this case study has been acquired from the Emilia-Romagna regional databases, cell resolution is 5 meters and it is derived from aerial photogrammetric survey.

Starting from the area affected by the 2010 reactivation of the Poggio Baldi landslide, the analyses have been extended at the whole southern and western slopes of the Pian D'Arcai relief, as, besides

Poggio Baldi, other local villages, such as Corniolo and Verghereto, are affected by gravity-driven instabilities (Torreggiani 2009), thus, further operations have been focused to search whether all of these phenomena have some kind of relation rather than focusing just on the last occurrence from 2010.

The analysis of the Topographic Position Index shows the slope domains of the Pian d'Arcai relief southern and western slopes, ranging from the main ridges of the top relief to the Bidente valley. Effective values of the TPI highlight main physiographic features, such as the top of Pian D'Arcai relief and the surrounding heights and the main Bidente river valley and its tributaries. Along the slopes, values of the slope position change linearly from upper slope, to middle slope and lower slope without particular accidents. Values of the standardized TPI, instead, show features at a detailed scale and better highlight flat slopes. Ridges and channels are much more detailed, showing also secondary features, not recognizable with the effective TPI values. Secondary ridges branch almost to the valleys, while channels better reflect the natural sinuosity. An interesting feature is how areas classified as "lower slope" extend along the slopes, almost to the ridges in certain areas, such as at the Poggio Baldi site (Figure 29).
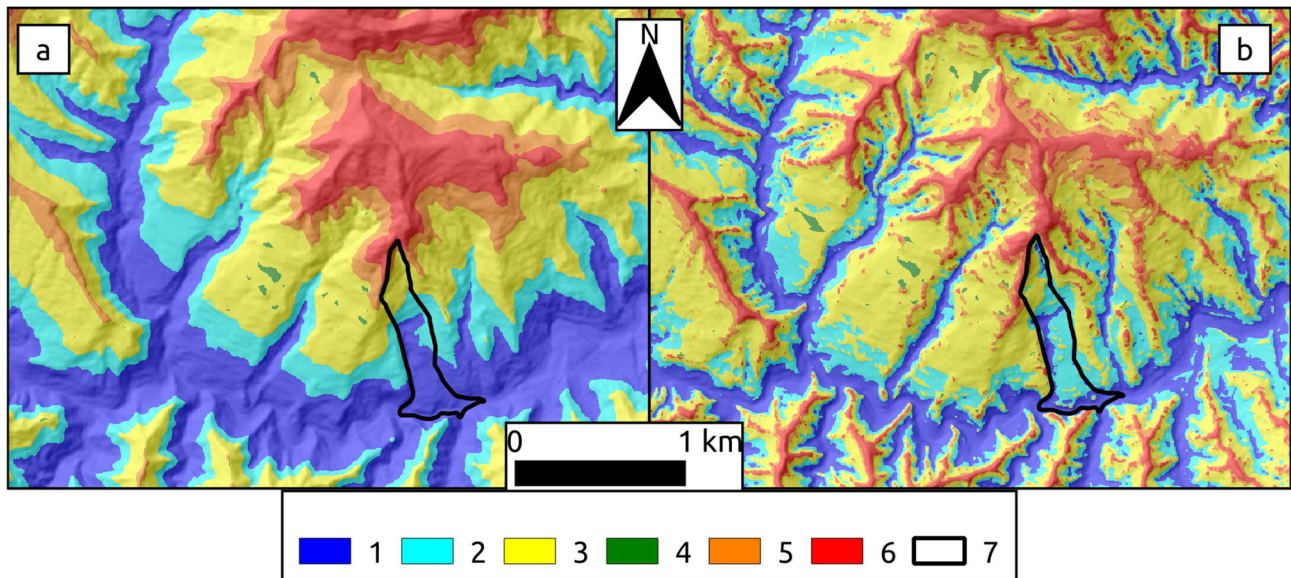
Figure 29 – TPI maps reclassified in slope positions: a) effective values, b) standardized values. 1) valley; 2) lower slope; 3) middle slope; 4) flat slope; 5) upper slope; 6) ridge; 7) 2010 landslide event

From the analysis of the Slope-Area function, thresholds for the contributing area have been derived which define slope processes domains (Figure 30). In this case the III domain has not been defined thresholding zero values in the derivative function, which do not reach the zero but instead starts to fluctuate between a constant value, depicting a non-linear decreasing trend in the Slope-Area function:

- I-II – Hillslope to channel transition: 133 m^2;
- II-III – Channels to landslide dominated channels: 13.225 m^2;
- III-IV – Landslide dominated channels to alluvial channels: 4.216.965 m^2.
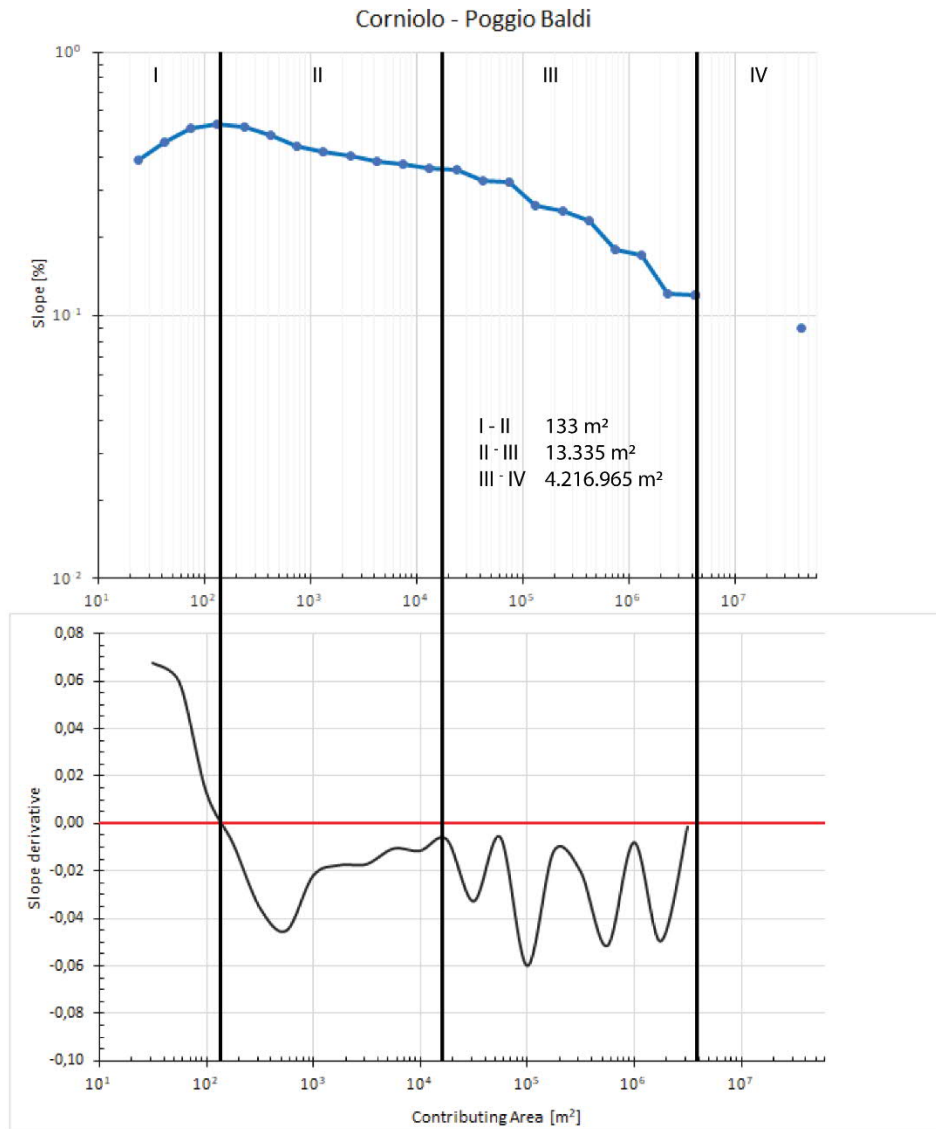
Figure 30 – Slope-Area plot for the Corniolo area

The graphical plots of both TPI and standardized TPI against the contributing area have been also thresholded using the previous derived values for the slope as described in § 4.1.3. In detail, the III region of the Slope-Area plot corresponds to a standardized TPI range from -44,55 to -135,27, while the IV region corresponds to the TPI values less than -69,46 (Figure 31). These ranges have been used to derive candidate landslide related features, reclassifying the mean values of the standardized TPI, and of the fluvial domain, reclassifying the mean values of the actual TPI (Figure 32).
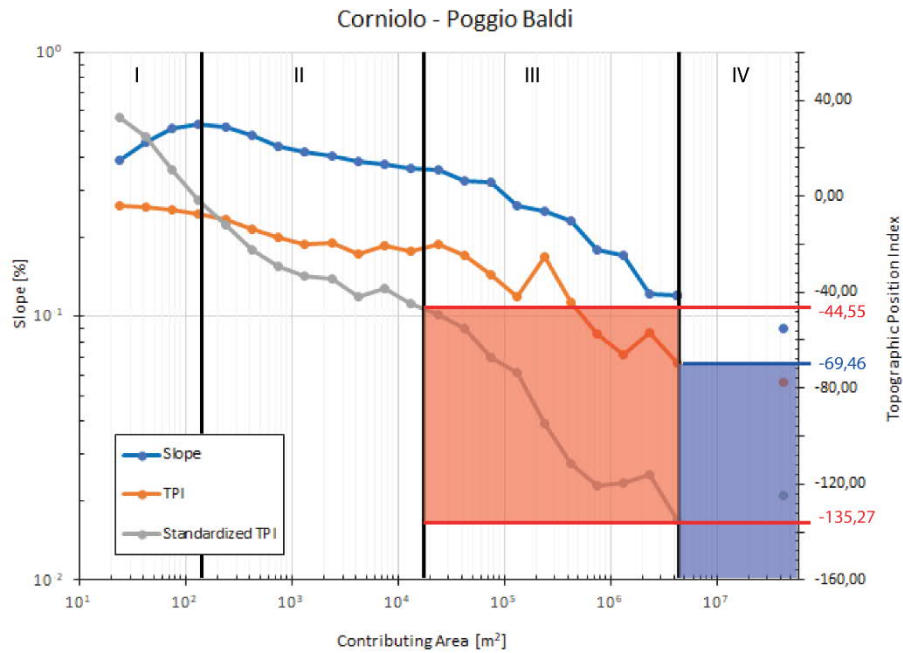
Figure 31 – TPI values in the Slope-Area plot
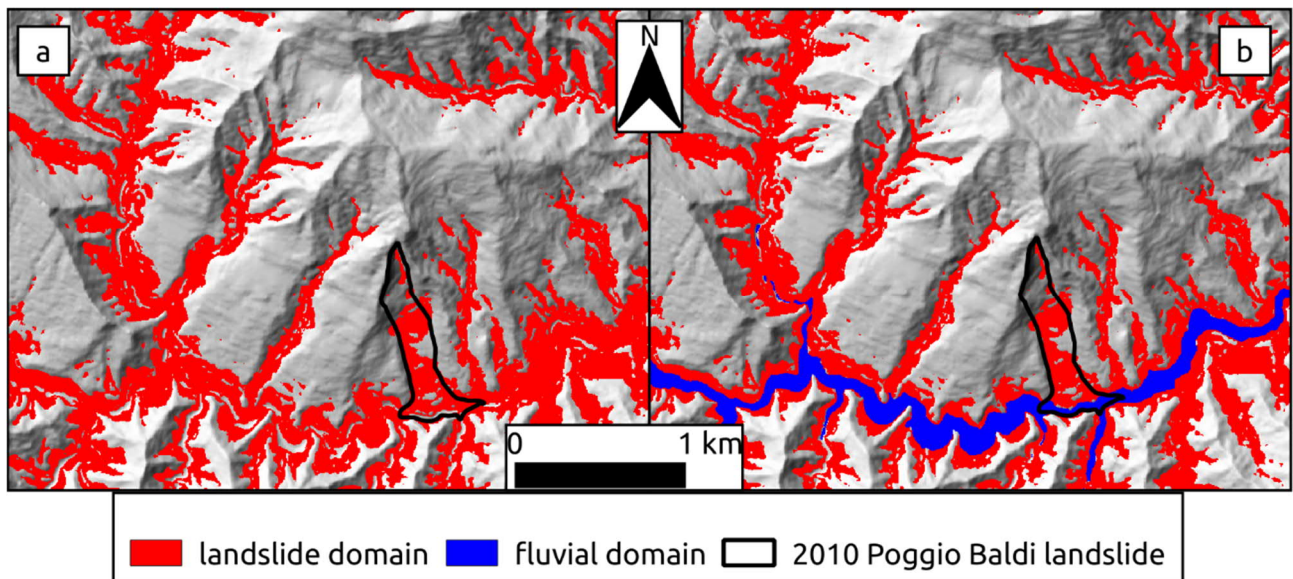
Figure 32 - Landslide domain from the reclassification of the standardized TPI dataset, a) non-filtered values, B) filtered values

5.1.4 Bottom-Up approach

The landslide inventory has been built mainly by direct field surveys (May 2017, May and July 2018, May 2019). Inventoried landslides have been stored using the object-oriented model discussed in chapter 1. At the focal level of the hierarchy, individual landslides are represented.

At the Poggio Baldi site, the recognized sequence of events is stored, starting from the old rock-wedge slide supposedly already happened in the late 1800, and the granular flow event of the February 28, 1914, then follows the last event of the March 19, 2010 and the consequent rock falls at the head of the wedge slide, still active and monitored today (Mazzanti et al. 2017) (Figure 33a). Besides these larger phenomena, a few others have been inventoried at the foot slope, which

remobilized their debris. As a spatio-temporal overlap of different types of landslides, these phenomena can be aggregated in the Poggio Baldi landslide system.

Extending the analysis to the slopes surrounding the Corniolo village, three large dormant rock compound slides have been inventoried, their detachment areas are still evident along the slopes in the form of flatirons (Figure 33c). Such landforms, even being not of gravitational morphogenesis, may have been enlarged or preserved by the landslide slipping. Above these rock compound slides developed a series of minor rock planar slides or rock wedge slides. Their combination allows the aggregation to the landslide system level.

On the foot slopes, along the Bidente riverbed, several rock planar slides have been inventoried; most of them, as for their spatial relations, can be aggregated into two landslide complexes. North of the Corniolo village, just beneath the main ridge of the Pian d'Arcai relief, a rock rotational slide complex has been inventoried (Figure 33d). The last notable object along the slopes surrounding the Corniolo village, is the Valbonella rock planar slide – debris flowslide (Figure 34).

Figure 33 - a) The Poggio Baldi wedge-slide detachment area, rock falls detaching from the cliff are visible; b) the Corniolo lake at the toe of the same landslide; c) outcropping bed surface with buckling structures; d) hummocky structures due to rotational sliding
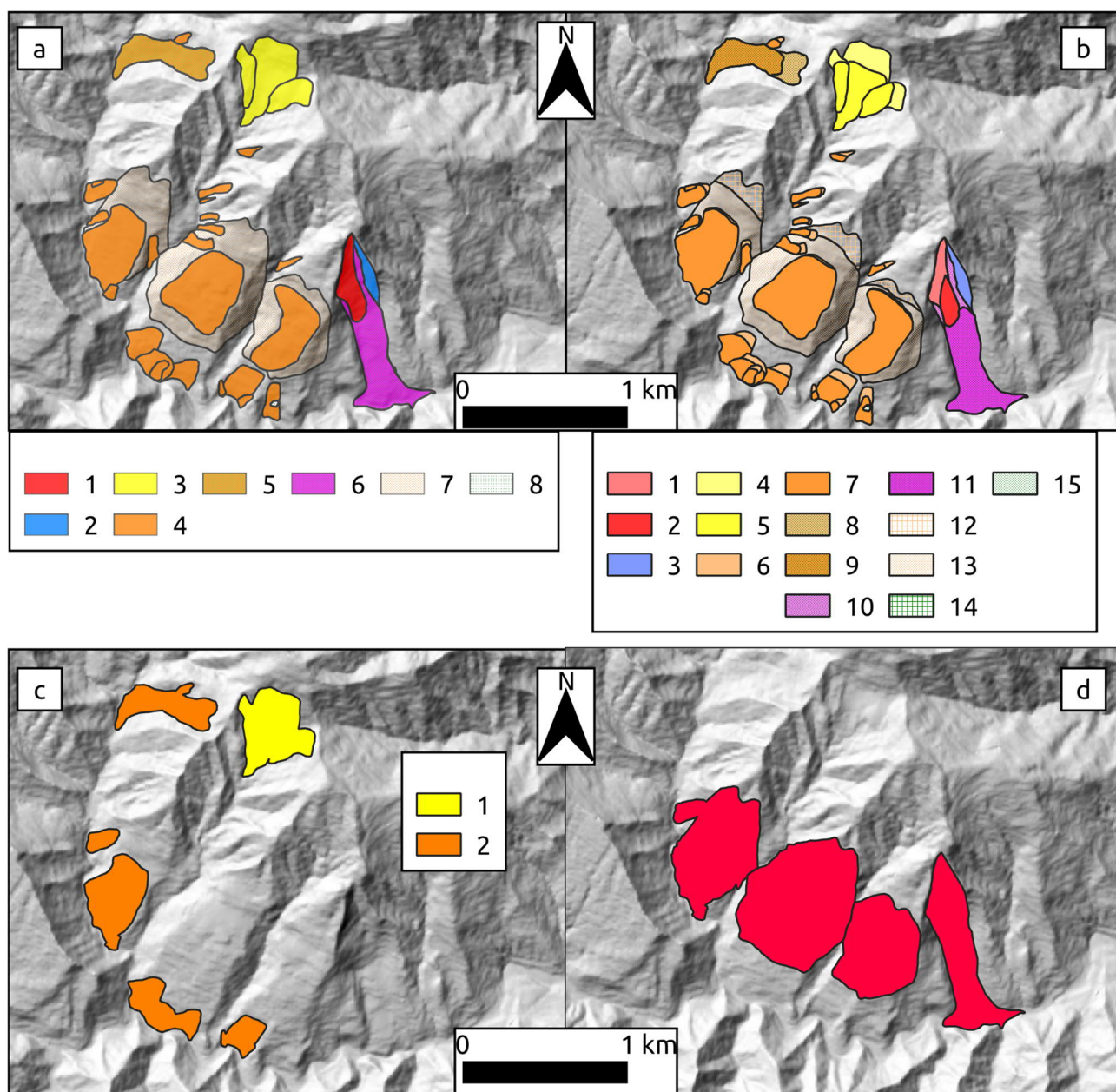
Figure 34 – Landslide maps for the Corniolo case study: a) landslide map (focal level), 1) rock fall, 2) rock avalanche, 3) rock rotational slide, 4) rock planar slide, 5) rock planar slide – debris flowslide, 6) rock wedge slide – debris flowslide, 7) rock compound slide, 8) debris slide; b) landslide components (level -1), 1) rock fall detachment area, 2) rock fall debris, 3) rock avalanche detachment area, 4) rock rotational slide detachment area, 5) rock rotational slide body, 6) rock planar slide detachment area, 7) rock planar slide body, 8) rock planar slide – debris flowslide detachment area, 9) rock planar slide – debris flowslide body, 10) rock wedge slide – debris flowslide detachment area, 11) rock wedge slide – debris flowslide body, 12) rock compound slide detachment area, 13) rock compound slide body, 14) debris slide source area, 15) debris flowslide debris; c) landslide complexes (level +1), 1) rock rotational slide complex, 2) rock planar slide complex; d) landslide systems (level +2)

All the inventoried landslides have been temporally characterized in order to reconstruct the event sequence. All the collected evidences allowed to recognize at least eight time intervals or events: i) the oldest recorded phenomena are the rock compound slides, their age is currently unknown and their time positioning has been derived through their spatial relations with other movements (Figure 35a); ii) on top of the rock compound slides, three rock planar slides developed, the starting time of these movement is unknown too but they are considered still active today (Torreggiani 2009) (Figure 35b); iii) in this time interval, all the movements occurred roughly before the 1900 are placed,

such as the first instance of the Poggio Baldi landslide, inferred from the historical maps (Figure 35c); iv) in this time period landslides younger than iii are placed, their features are still clearly visible along the slopes (Figure 35d); v) this is the 1914, February 28 event occurred at Poggio Baldi (Figure 35e); vi) here, the last reactivation of the Poggio Baldi landslide is contained, dated 2010, March 19 (Figure 35f); vii) this interval contain all the movements occurred after the Poggio Baldi landslide, such as the rock fall on it detachment area (Figure 35g); viii) the recent movements are stored here, such as landslides occurred in 2017, date of the first field survey (Figure 35h).
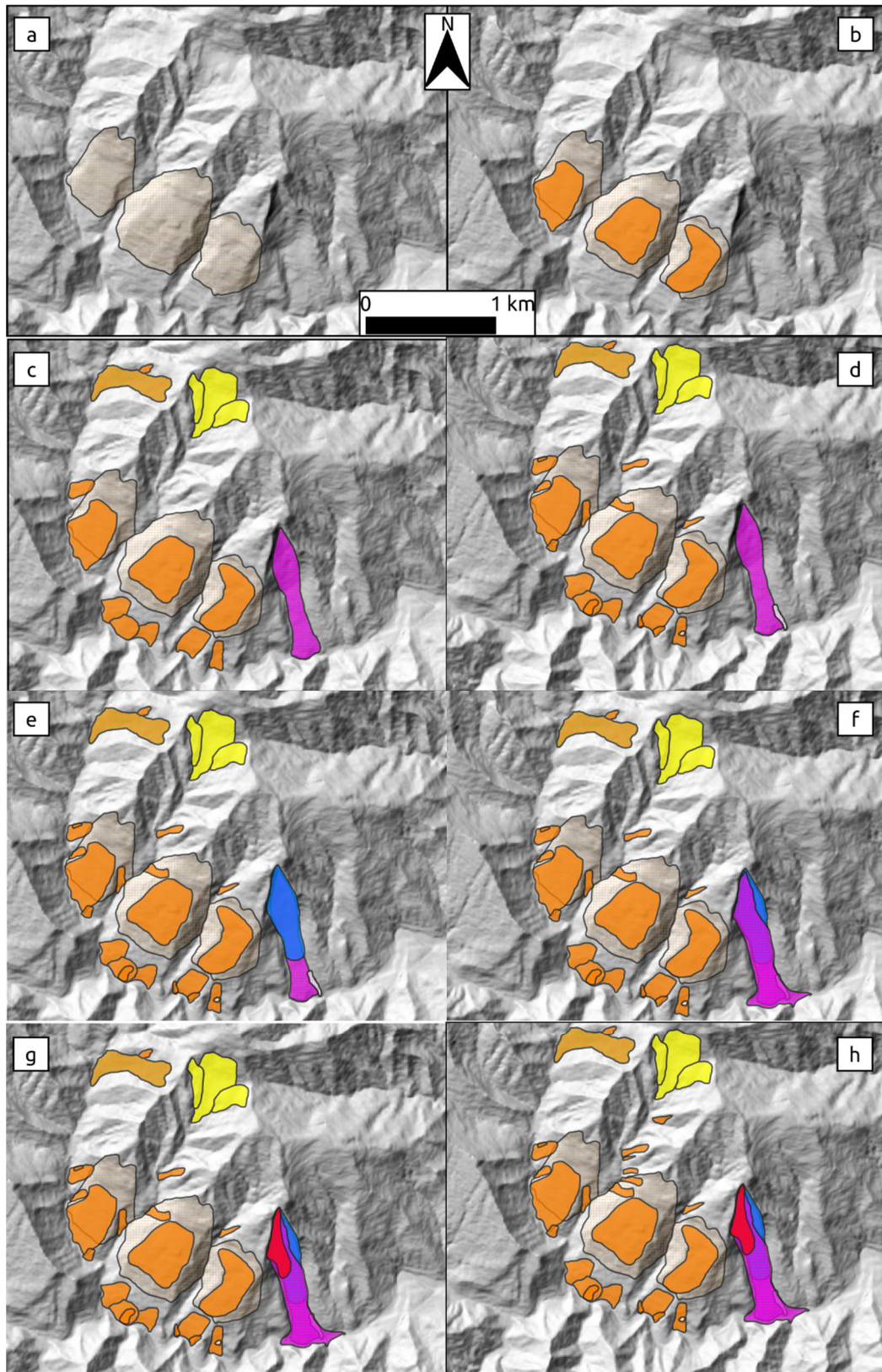
Figure 35 - Landslide event succession, refer to the text for the steps and to Figure 34 for the legend

The reference hillslope has been also computed for the Poggio Baldi landslide system, starting from the surface network derived from the DEM (Figure 36, Figure 37). The total area bounded by the reference hillslope it's about 0,54 km², about the double of the size of the entire landslide system. Inside the reference hillslope there is no other movement sharing a functional interaction with the

objects composing the landslide system, thus the aggregation procedure that led to its definition is confirmed. However, there is a portion of a rock compound slide within the identified area, but it is disjoint from our reference system. This state could be considered a transitory phase from two disjoint system to the formation of a larger landslide system, because, sharing portion of the reference hillslope means a higher probability of interaction in future reactivations of both the objects.
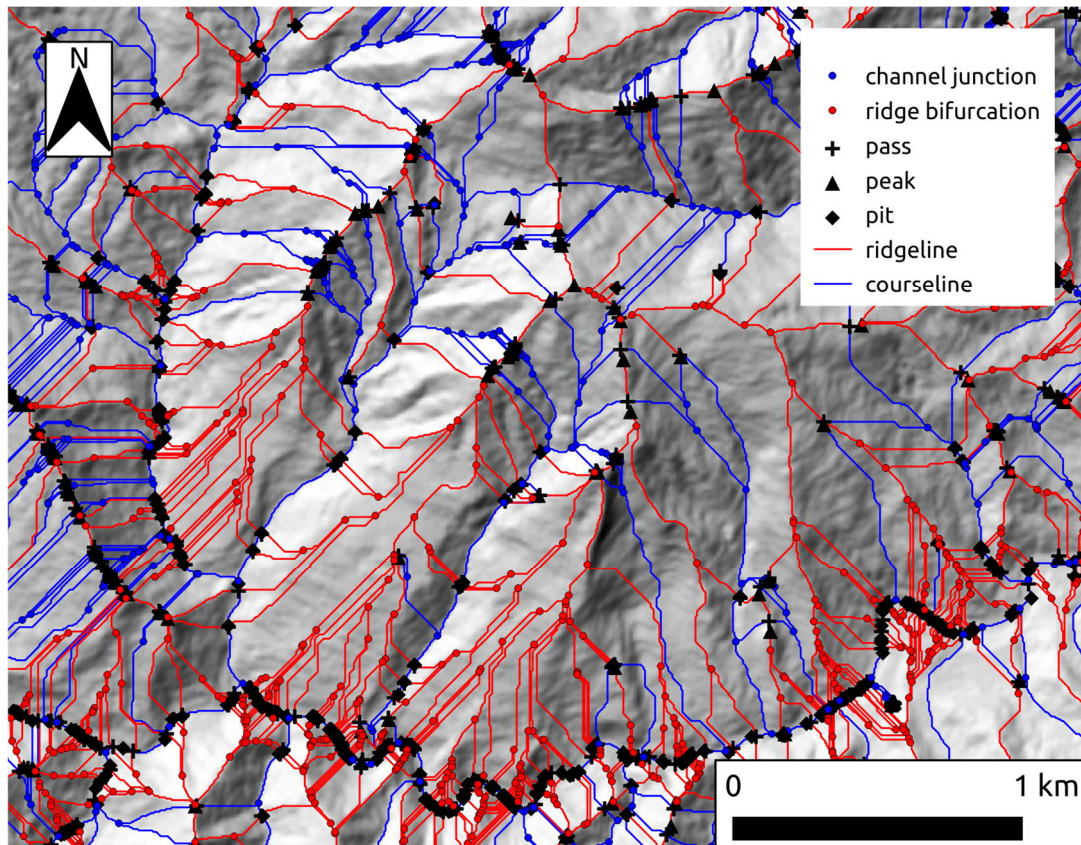
Figure 36 - Surface network for the Corniolo area
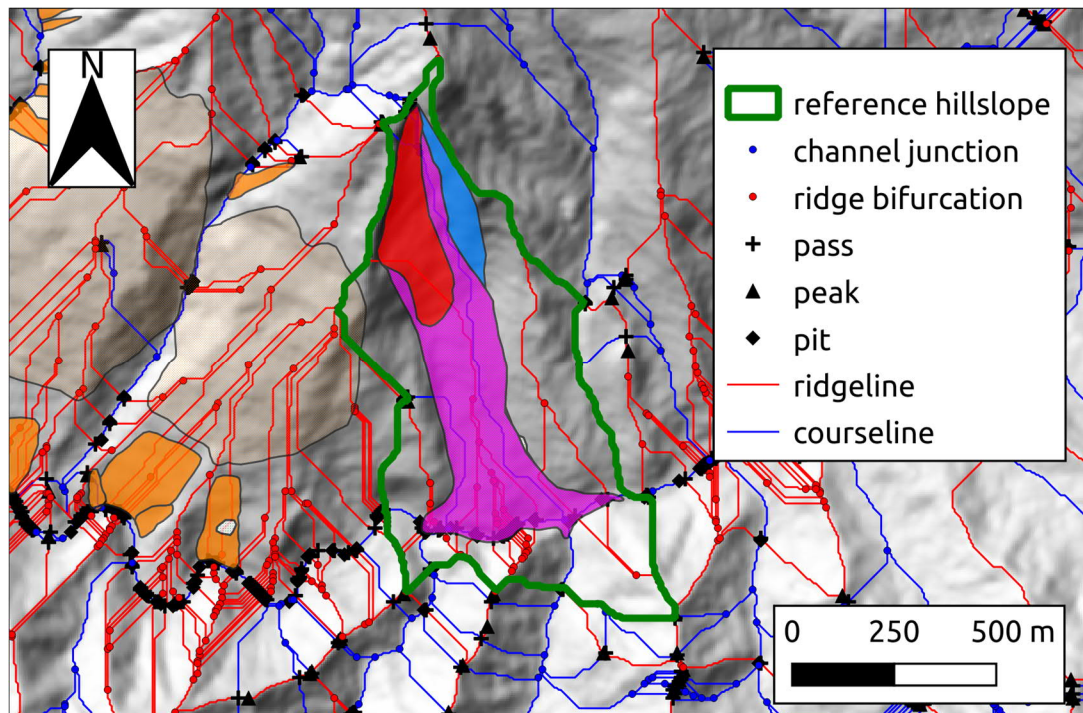
Figure 37 - Reference hillslope for the Poggio Baldi landslide system

5.1.5 Approaches comparison

Datasets from both the approaches have been categorized in a binary classification and then compared using the confusion matrix (Figure 38). Comparing morphometric features with the landslide inventory, the following values results computing the confusion matrix:

- Non-filtered values:
  - False Positive Rate = 12,2%
  - True Positive Rate = 24,5%
  - Accuracy = 69,2%
  - Precision = 45,5%
- Filtered values:
  - False Positive Rate = 10,6%
  - True Positive Rate = 22,1%
  - Accuracy = 69,6%
  - Precision = 46,4%
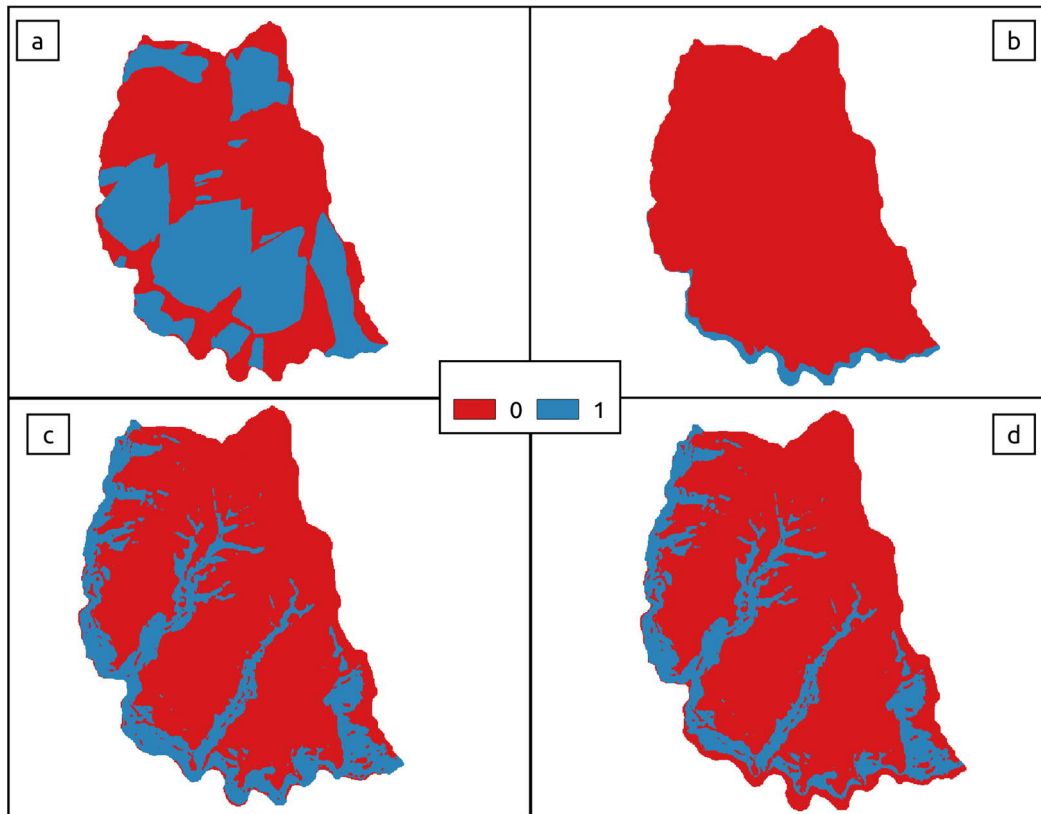
Figure 38 – Input datasets for the confusion matrix: a) actual values, 0 = no landslide, 1 = landslide; b) filter, 0 = non-fluvial domains, 1 = fluvial domain; c, d) predicted values before and after the filtering operation, 0 = other domains, 1 = landslide domain

5.2 Mt. Pruno – Roscigno

The Mt. Pruno relief is located in southern Italy in the Salerno province; it is the highest relief of the Roscigno municipality. The relevance of this case study is mainly due to the connection between landslides and cultural heritage, in fact two historical settlements are here threatened by landslides: The Old Roscigno ghost town and the ancient Enotrian settlement on the flat top of Mt. Pruno, now archaeological site. Since 2010, this site is also part of the Cilento geopark (Aloia and Guida 2012) (Figure 39).
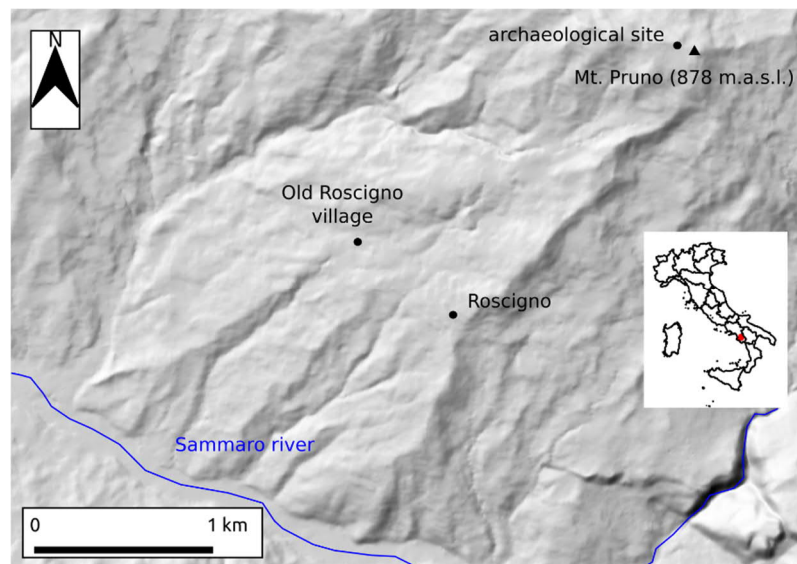
Figure 39 – Location of the study area

5.2.1 Geological and geomorphological settings

The Cilento area is part of the central-southern Apennine chain. In this portion of the chain, the main geological setting is the result of a complex overlapping of an alternation of basins and carbonate platforms during the Apennine orogeny. In detail, from west to east, it is possible to recognize the tyrrhenian basin, the apenninic platform, the lagonegrese-molisano basin and the Apulian platform (Mostardini and Merlini 1986; Vitale et al. 2010, 2011, 2013).

Terrains outcropping in the study area belong to the Tyrrhenian basin successions. These deposits were differentiated into three main domains, thus tectonic units: liguride domain (Nord-Calabrese tectonic unit), sicilide domain (Sicilide tectonic unit) and para-sicilide domain (Castelnuovo Cilento tectonic unit) (Cammarosano et al. 2004). All these terrains are also called Internal Units and are mainly composed of silico-clastic materials, with occasional carbonatic components, in turbiditic sequences. Starting from the Burdigalian, these units overlap each other during the apenninic orogeny (Cammarosano et al. 2004).

The area of Mt. Pruno is in the northern Cilento, where the Internal Units widely crop out. The main structure of the relief is made by the tectonic overlap of the para-sicilide unit over the sicilide unit. This terrigenous domain is bordered by the Alburno chain in the north and by the Mt. Motola – Mt. Chianello reliefs in the south, both of these structures belong to the Apennine platform carbonatic domain.

The recognized formations in this area are: i) "Argille Varicolori Superiori" Fm. (upper Oligocene – lower Miocene), greyish to blue-greenish or reddish clays and claystones with chaotic structure, belonging to the sicilide tectonic unit, the upper limit is tectonic with ii) "Torrente Trenico" Marls and Calcarenites Fm. (Chattian – Burdigalian), marly-calcareous and marly arenaceous turbidites, this formation belong to the para-sicilide tectonic unit (Figure 41).

A recent review on the geology of the Campania region, merged the sicilide domain with the para-sicilide domain into a new para-sicilide domain. This cause the "Argille Varicolori Superiori" Fm. to be merged into the new Parasicilide Tectonic Unit and the "Torrente Trenico" Marls and Calcarenites Fm. to be part of "Monte Sant'Arcangelo" Fm. (Vitale and Ciarcia 2018).
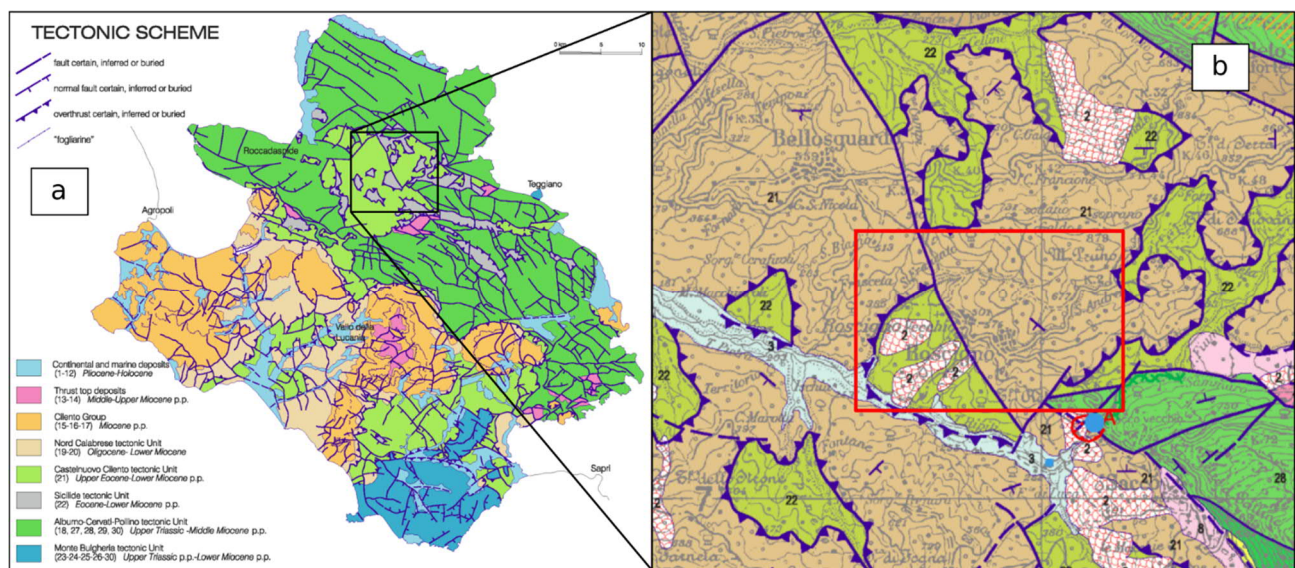
Figure 40 - a) regional geological settings of the Cilento area; b) local geological settings, the red box highlights the study area
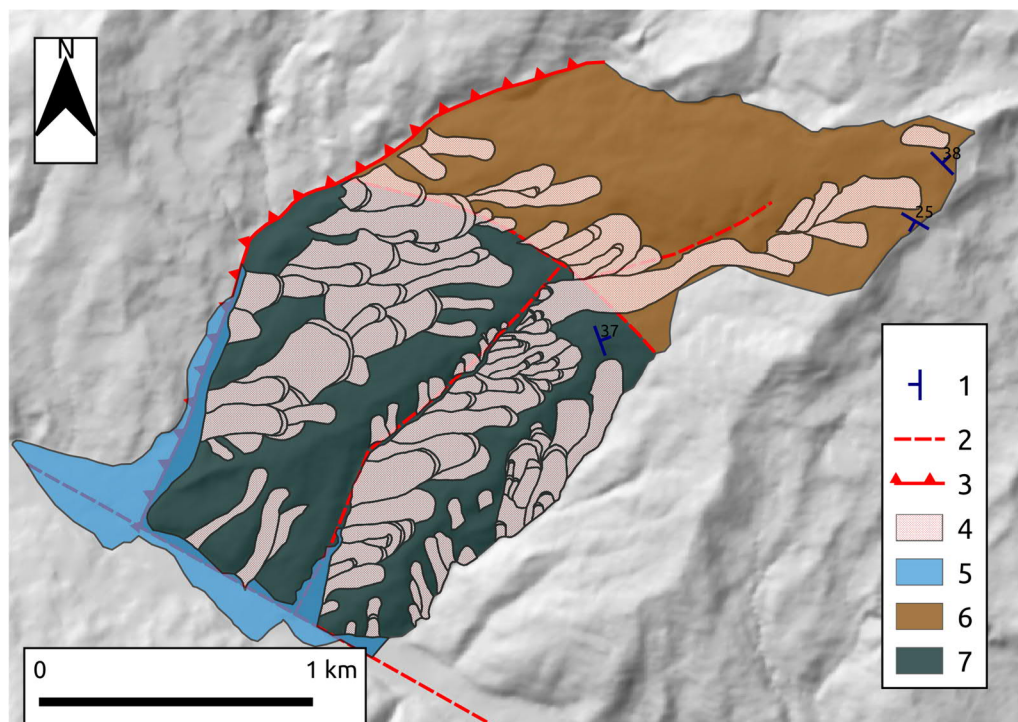
Figure 41 - Geological map of the study area, 1) bedding with dip angles, 2) inferred fault, 3) thrust fault, 4) landslide debris, 5) alluvial deposits, 6) Monte Sant'Arcangelo Fm., 7) Argille Varicolori Fm. (modified after Guida et al., 2007)

The Roscigno municipality is part of the Ripiti creek basin, right tributary of the Calore Salernitano river, which is a left tributary of the Sele river, the second largest river in the Campania region. The Ripiti creek has experienced several incision phases, as reflected by several erosional surfaces at different elevation along the slopes (de Riso and Santo 1997). This gradual deepening is testified also by several hanging fluvial channels along the carbonatic slopes bordering the Ripiti creek basin. An example are the paleo-channels of the Sammaro river on the western slopes of the Mt. Motola (de Riso and Santo 1997; Putignano and Schiattarella 2008; Aloia and Guida 2012). This evolution led to the progressive outcropping of the Internal Units and both their terrigenous composition and the high tectonization of the rock masses, favoured the establishment of complex landslide phenomena.

5.2.2   The Old Roscigno town

Mt. Pruno is a great example of interaction between anthropic activities and landslide processes. The Old Roscigno village is a ghost town on the south-western slope of Mt. Pruno. The village has been involved in landslide processes at least from the second half of the XIX century, in fact the first law stating the urge to relocate the village dates back to 1908 and fundings for a reconstruction project were allocated in 1913 (Italian law n. 445/1908; Royal Decree n. 453/1913). The village was definitely abandoned in 1964 (Catenacci 1996).

First clues of gravity-induced deformation on this slope can be traced back to the III-IV century B.C., when an Enotrian settlement was located on the flat top of Mt. Pruno. It is assumed that instabilities involving the top of Mt. Pruno are among the causes that lead to the abandonment of the village (Calcaterra et al. 2014).

Figure 42 - a, b, c) The Old Roscigno Village: surroundings of the main square, the church, the public fountain and a private house, all of them with visible deformations induced by the instabilities; d) the archaeological site of Mt. Pruno (modified from Greco 2016)

5.2.3   Top-Down approach

The topographic dataset used for this case study is derived from the interpolation of the only data available with a good resolution, such as the elevation contours available in the topographic database of the Campania region at 1:5.000 scale. The dataset is derived from the 2004-2005 aerial photogrammetric survey and the raster elevation model has been interpolated with a 5m resolution, using the nearest neighbourhood method of ArcMap.

Effective values of the TPI show the slopes reclassified in slope positions, highlighting the mountainous ridge of Mt. Pruno and the Sammaro river valley. The analysis of the standardized values of TPI gives much more detail on the local morphology. Along the slopes there are a lot of dandling features classified as lower slopes along with flat slopes, this alternation of concave and flat morphologies along the slopes could be related to landsliding processes (Figure 43).
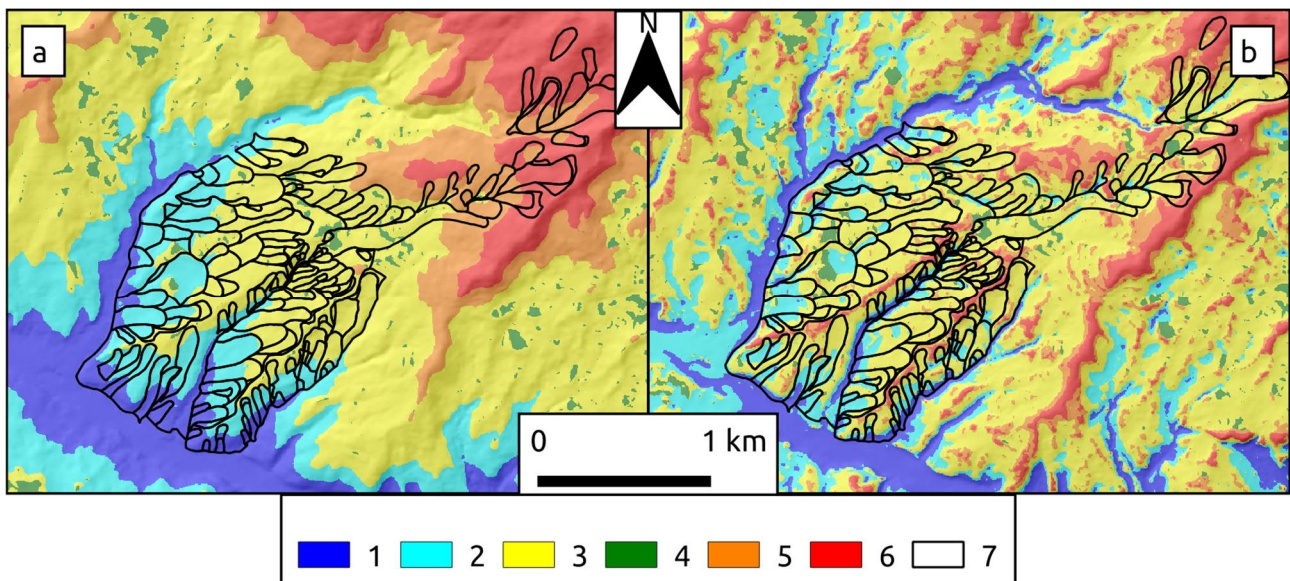
Figure 43 - TPI maps reclassified in slope positions: a) effective values, b) standardized values. 1) valley; 2) lower slope; 3) middle slope; 4) flat slope; 5) upper slope; 6) ridge; 7) landslides

From the analysis of the Slope-Area function, thresholds for the contributing area have been derived which define slope processes domains (Figure 44):

- I-II – Hillslope to channel transition: 178 m^2;
- II-III – Channels to landslide dominated channels: 4.217 m^2;
- III-IV – Landslide dominated channels to alluvial channels: 2.371.374 m^2.
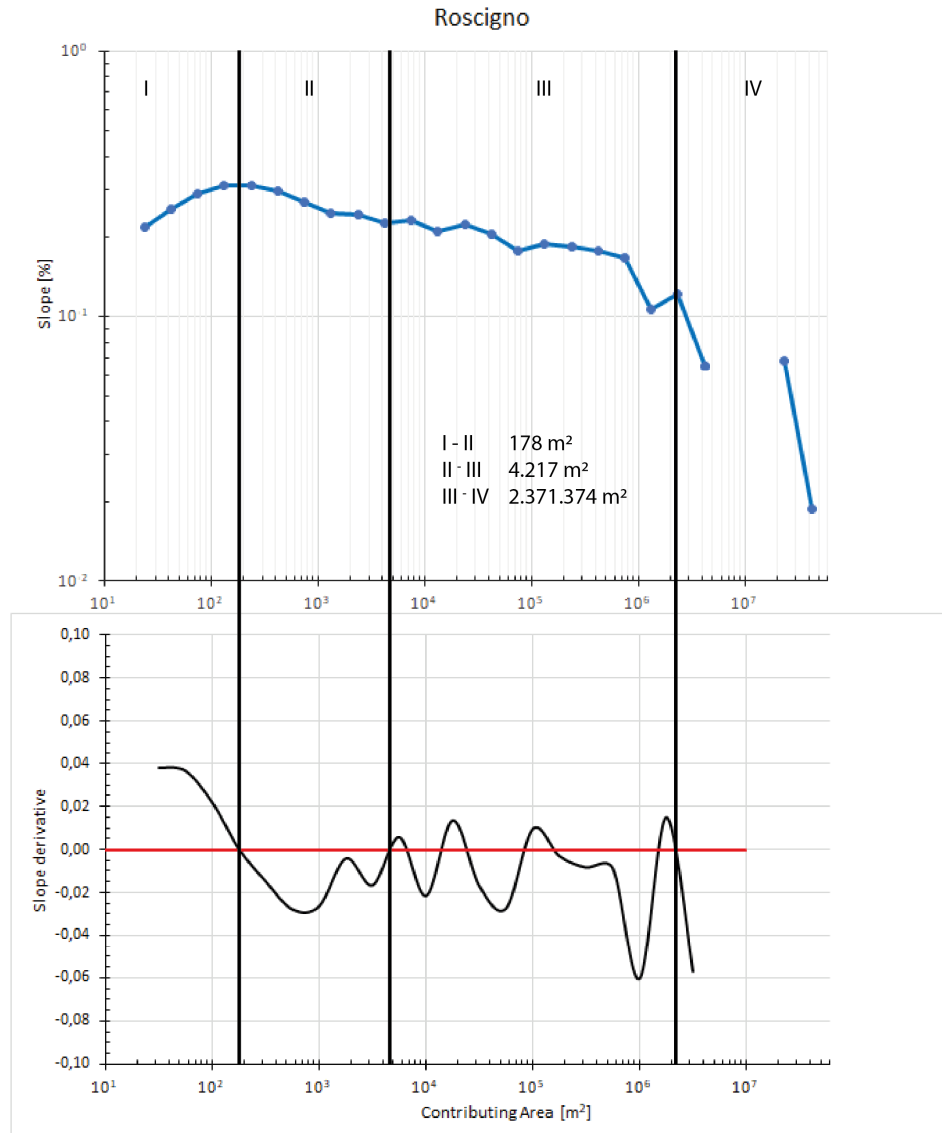
Figure 44 - Slope-Area plot for the Roscigno area

The graphical plots of both TPI and standardized TPI against the contributing area have been also thresholded using the previous derived values for the slope. In detail, the III region of the Slope-Area plot correspond to a standardized TPI range from -28,24 to -135,36, while the IV region correspond to the TPI values less than -37,00 (Figure 45). These ranges have been used to derive candidate landslide related features, reclassifying the mean values of the standardized TPI, and the fluvial domain, reclassifying the mean values of the actual TPI.
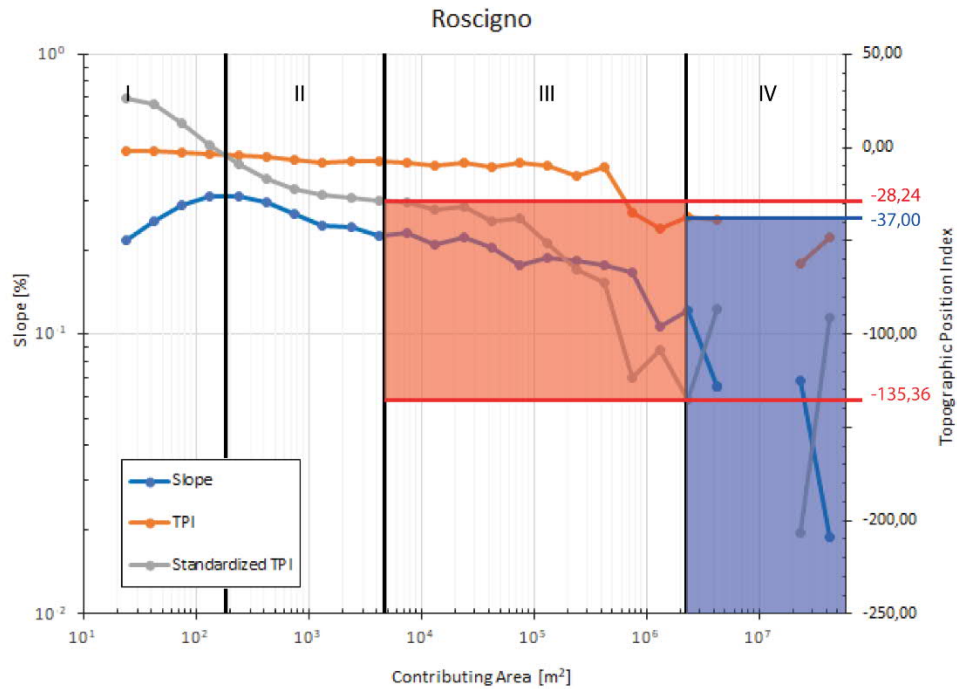
Figure 45 - TPI values in the Slope-Area plot
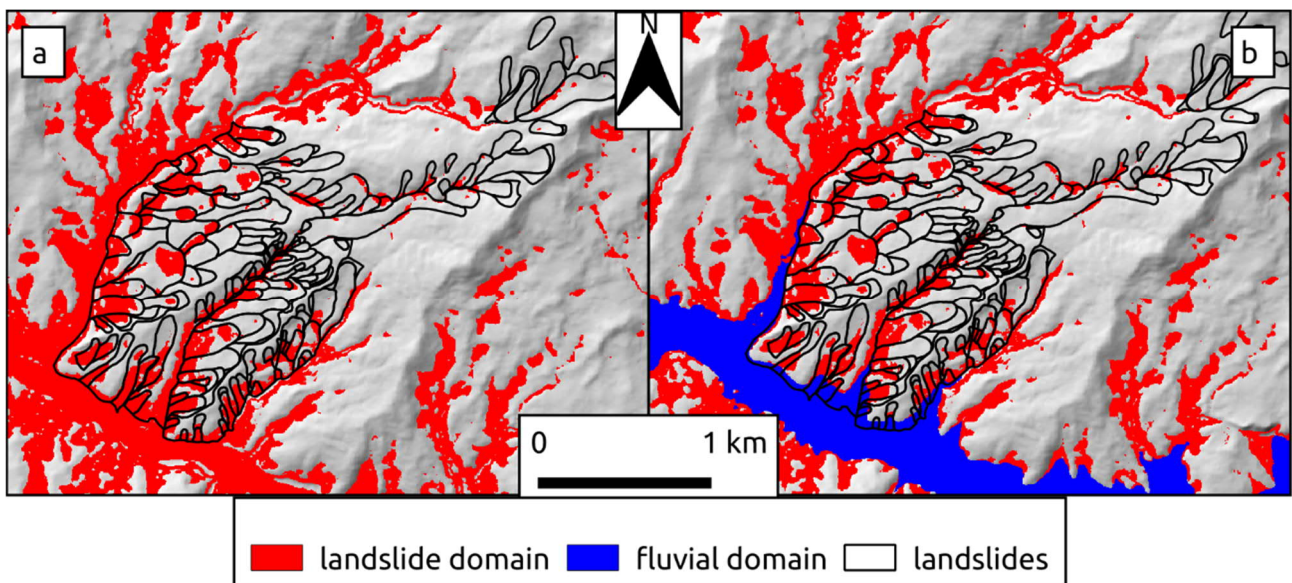
Figure 46 - Landslide domain form the reclassification of the standardized TPI dataset, a) non-filtered values, B) filtered values

5.2.4 Bottom-Up approach

The landslide inventory has been derived from previous data collection (PAI – River Basin Authority Plan for Hydrogeological Risk) integrated with field survey (July 2017 during PhD activities and January – June 2015, July 2016 before PhD activities).

The main feature affecting the slope is the rock slope deformation that caused the abandonment of the Old Roscigno village. Its components, such as the main trench, are still visible in the area of the village, where several buildings are tilted (Figure 47c, d). On top of the deep-seated movement, shallower phenomena developed, like rotational slides or flow-like movements, most of which can

be aggregated in landslide complexes. From the top of Mt. Pruno, also a few rotational slides - earth flows reach the upper portion of the rock slope deformation (Figure 48, Figure 47b).

All these movements, as for their spatial relations, can be aggregated in the Old Roscigno landslide system. Its reference hillslope has been computed aggregating surface network regions containing the system, resulting an area of about 2,7 km².

Figure 47 - a) deformed road at the entrance of the Old Roscigno village; b) counterslope and reworked landslide debris within a clay rotational slide; c -d) buildings deformed within the main trench of the deep-seated slope deformation
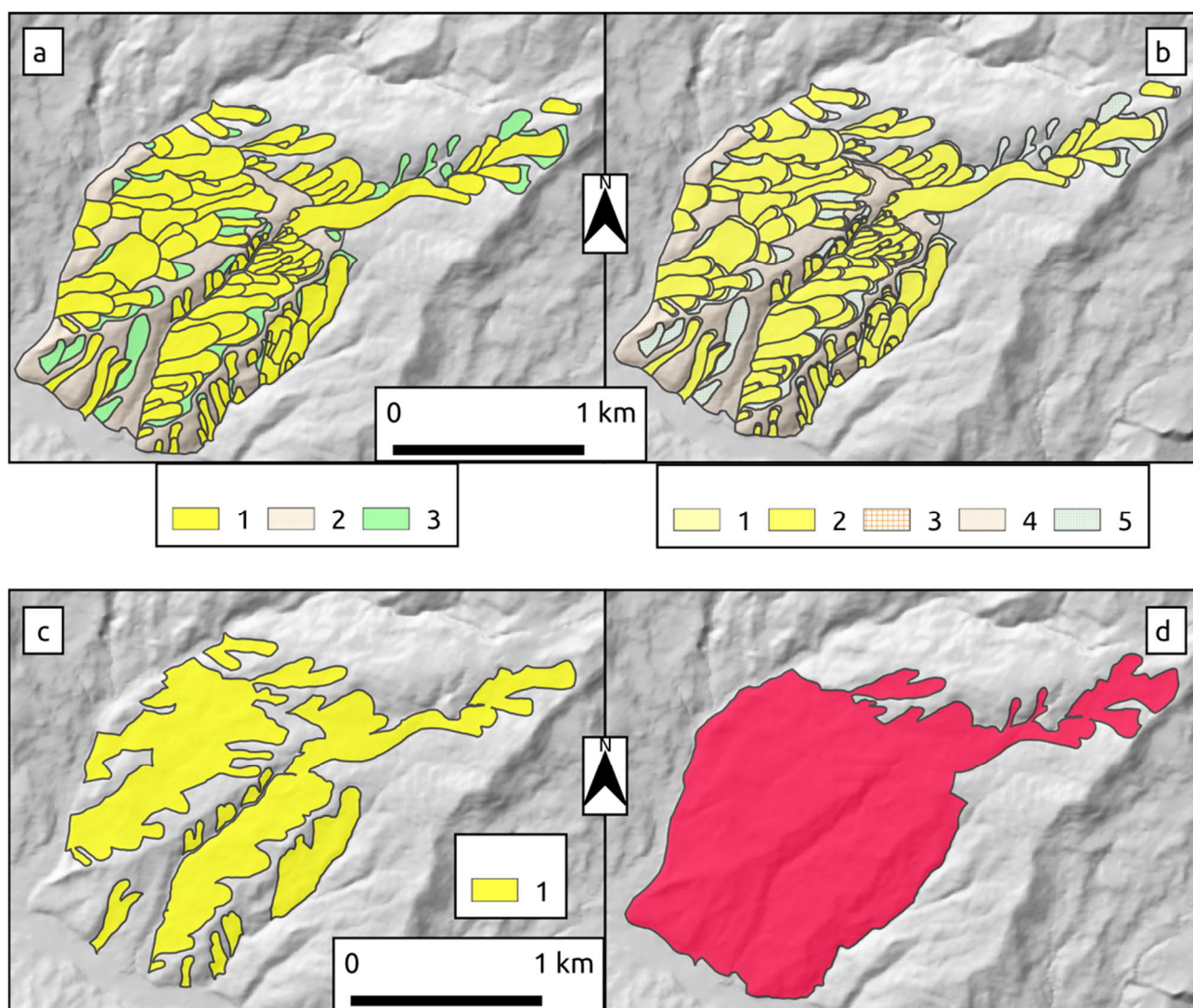
Figure 48 – Landslide maps: a) Focal level, 1) clay rotational slide – earthflow, 2) rock slope deformation, 3) soil creep; b) landslide components, 1) clay rotational slide . earthflow detachment area, 2) clay rotational slide – earthflow body, 3) rock slope deformation trench, 4) rock slope deformation body, 5) soil creep; c) landslide complexes, 1) soil rotational slide complex; d) landslide systems

The oldest recognized event is the basal rock slope deformation, which experienced its last noticeable reactivation around the second half of the 1800 and the first years of 1900. Other movements on top of the deep-seated deformation, may have experienced their first activation even before these dates and then being passively carried down valley by the biggest movement, but for sure they experienced further reactivations through the last century to present days, as testified by several deformations along the local road network (Figure 47a). This is to say that the last reactivation of the deep-seated slope deformation, can be considered as the first event for this landslide system, as we have no information about previous movements. After this event, the slope experienced several shallower phenomena such as rotational slides coupled with surficial soil creep, with various overlapping degree, some of them are responsible for the latest damages to the Old Roscigno village and its final abandonment (Figure 49).
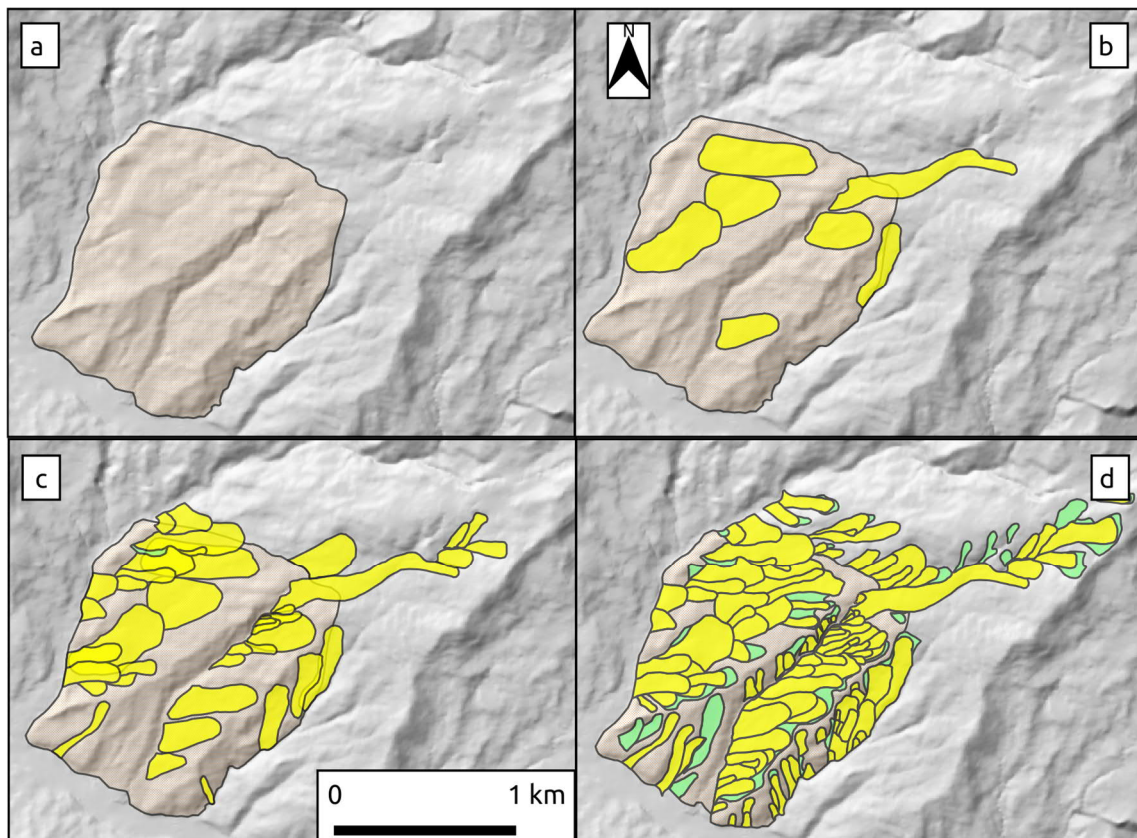
Figure 49 - Temporal succession of the landslides forming the Old Roscigno landslide system, the multitude of events has been grouped into four phases for representation purposes

As for the previous case study, the reference hillslope has been derived both for the initial deep-seated rock slope deformation and then for the entire Old Roscigno landslide system. The two resulting zonation are almost the same size, the reference hillslope of the entire system just adds a portion of upper slope. This could be related to the fact that the deep-seated deformation "embraces" almost all the landslide system, for exception of the highest rotational movements.

rock slope deformation reference hillslope
Old Roscigno landslide system reference hillslope
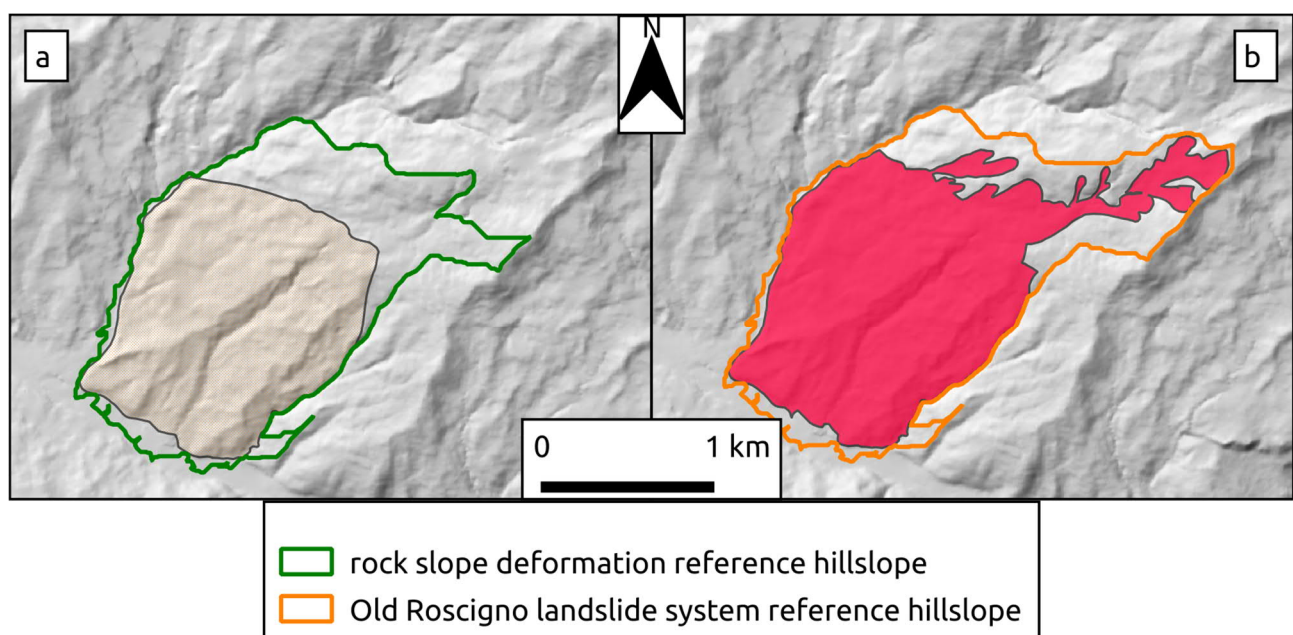
Figure 50 - Reference hillslope for both the Old Roscigno rock slope deformation and its corresponding landslide system

5.2.5   Approaches comparison

Comparing morphometric features with the landslide inventory, using the datasets shown in Figure 51, the following values results computing the confusion matrix:

- Non-filtered values:
    - False Positive Rate = 4,7%
    - True Positive Rate = 27,3%
    - Accuracy = 73,3%
    - Precision = 73,6%
- Filtered values:
    - False Positive Rate = 0,8%
    - True Positive Rate = 23,5%
    - Accuracy = 74,7%
    - Precision = 93,0%
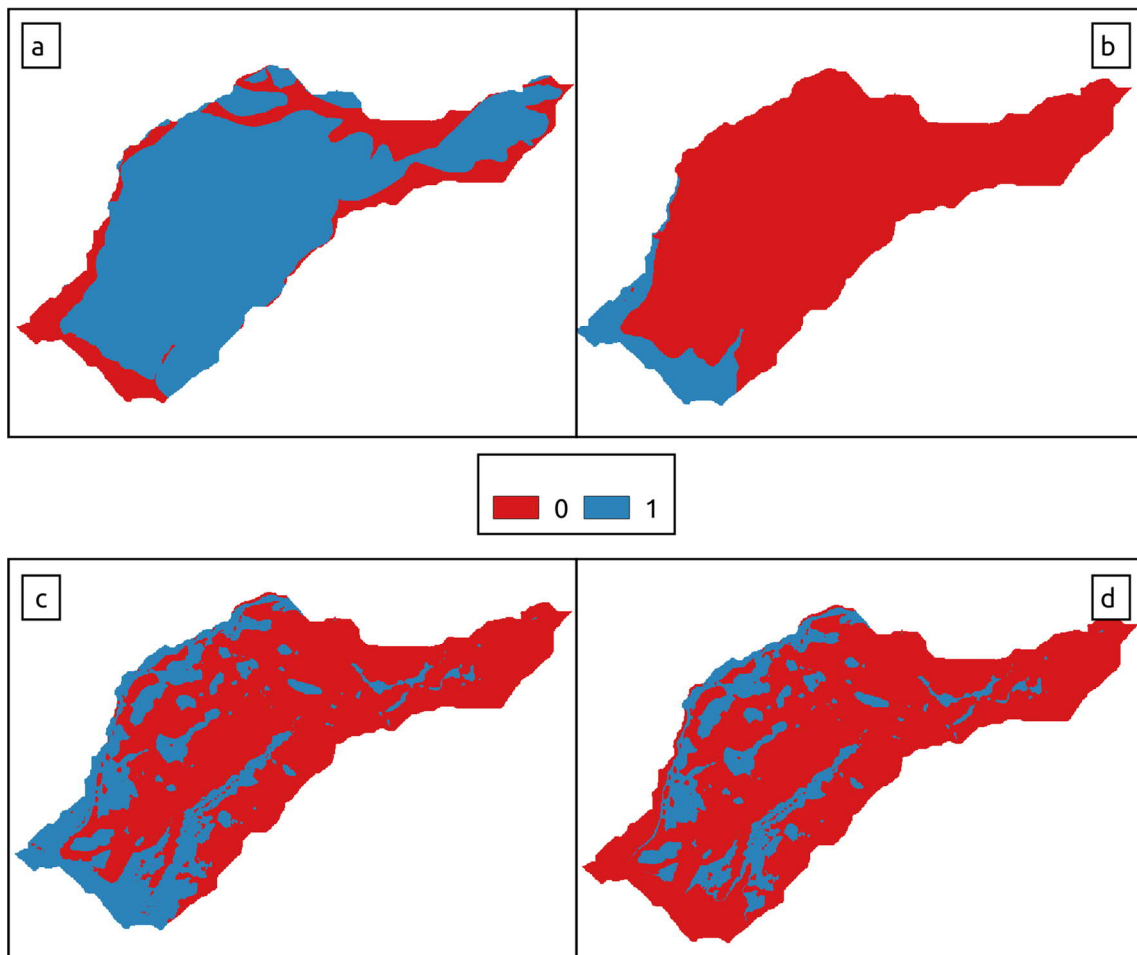
Figure 51 - Input datasets for the confusion matrix: a) actual values, 0 = no landslide, 1 = landslide; b) filter, 0 = non-fluvial domains, 1 = fluvial domain; c, d) predicted values before and after the filtering operation, 0 = other domains, 1 = landslide domain

5.3   Rocca di Sciara

The Rocca di Sciara relief is located in southern Italy (Northern Sicily), along the left slope of the Imera river valley, close to the Caltavuturo village (PA) (Figure 52). Several landslide processes have affected this area and their features are still evident in the area of interest and on the slopes around the Imera basin. The last event, occurred on the north-eastern slope on April 10th, 2015, had a great impact for the transportation network, as it severely damaged an important connection road and a highway.
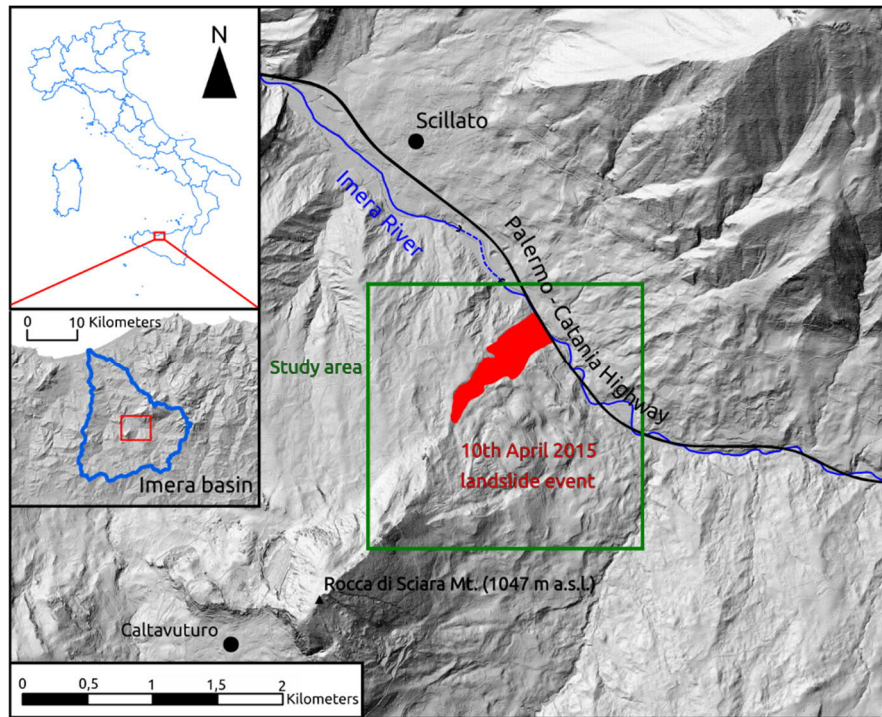
Figure 52 - Case study location

5.3.1   Geological and geomorphological settings

In the study area the outcropping materials mainly belongs to the upper section of the Imerese basin Succession (Catalano et al. 2011) and to the Portella Colla member of the Numidian Flysch (Wezel 1970; Dongarrà and Ferla 1982).

Starting from the oldest, the following formations have been identified along the north-eastern slope of the Rocca di Sciara relief: i) Crisanti Fm. (upper Jurassic – upper Cretaceous), limestone megabreccias and thick-bedded calcarenites; ii) Caltavuturo Fm. (Eocene – lower Oligocene), reddish to greyish thin-bedded or laminated calcilutites, marly limestones and clayey marls; iii) Numidian Flysch – Portella Colla member (upper Oligocene – lower Miocene), laminated brownish claystones with quartz sandstones intercalations; iv) Argille Varicolori Fm. (Cretaceous – Paleocene), varicoloured claystones and marls with chaotic structure, flint nodules and quartz-arenites.

The Crisanti Fm. limestones made up the main structure of the relief and widely outcrop in the upper section of the slope with a dip-slope attitude. Downslope these deposits are covered by the siliciclastic terrains of the Caltavuturo Fm. which outcrops in the middle section of the slope, often presenting folded structures. This formation is covered in some areas by Quaternary deposits made of boulders from the Crisanti Fm. Some of these boulder deposits reach the lower section of the

slope, which is mainly covered by landslide debris. The Numidian Flysch does not crop out directly but its presence in the lower portion of the slope is inferred both from landslide activity and the analysis of boreholes log-stratigraphies, which showed also the interdigitation of landslide debris and alluvial deposits along the Imera riverbed. The Argille Varicolori Fm. crops out in the north-western section of the study area and is not directly involved in the landslide phenomena object of this study (Figure 54).
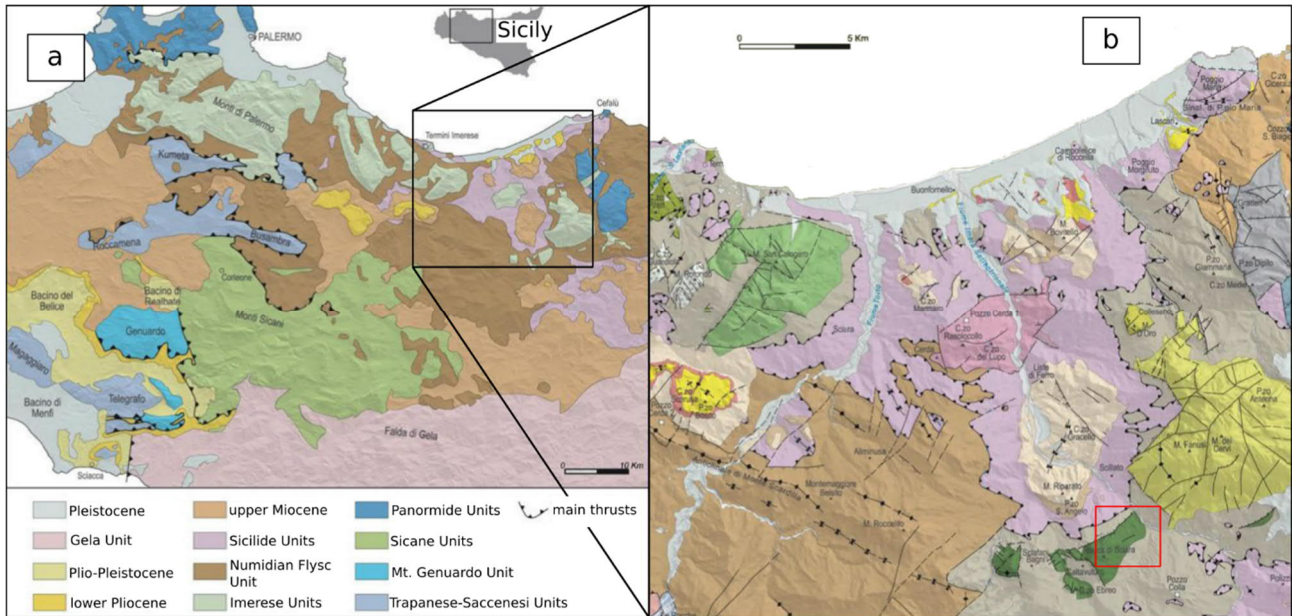
Figure 53 - a) regional geological settings; b) local geological settings, the red box highlights the study area
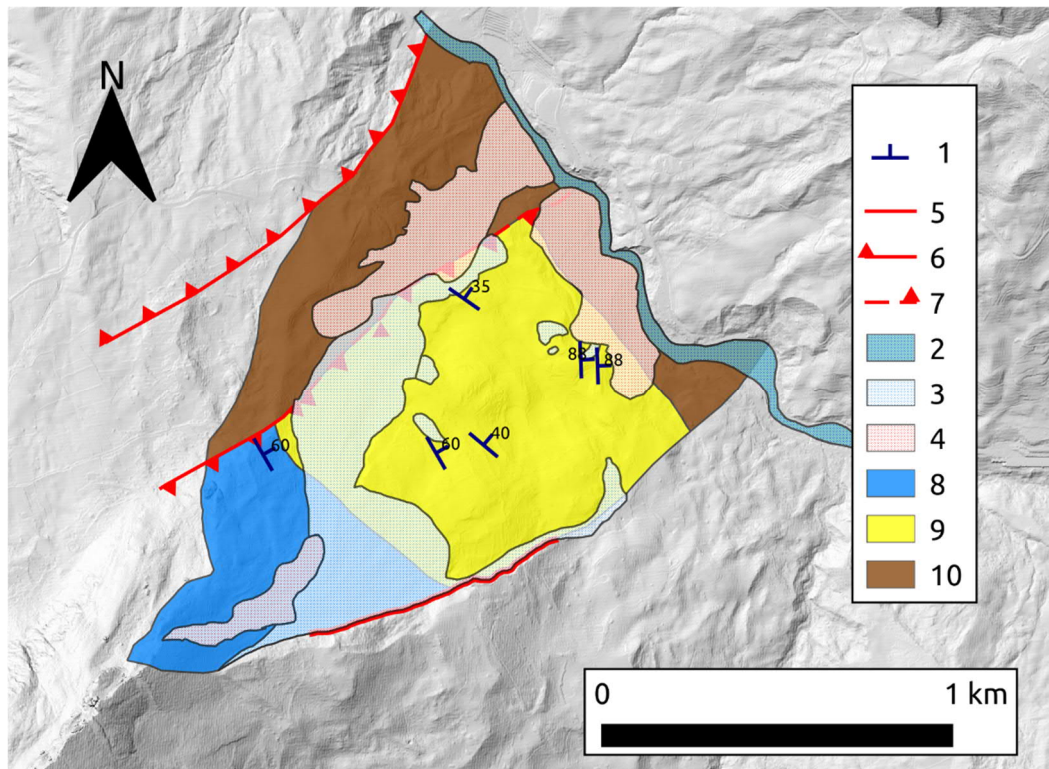
Figure 54 - Geological map of the study area: 1) bedding with dip angle; 2) alluvial deposits; 3) boulder deposits; 4) landslide debris; 5) uncertain fault; 6) thrust fault; 7) transpressive fault; 8) Crisanti Fm.; 9) Caltavuturo Fm.; 10) Numidian Flysch

The present morphology of the north-eastern slope results from the sum of several landslide events. At the bottom of the carbonate slopes, in the highest part of the slope, extensive limestone boulders deposits can be found; these deposits are interpreted as the result of impulsive events (rock avalanches), as in some areas they are found covering old soils. The middle section of the slope shows alternation of flat surfaces or counterslopes, divergent-straight slopes and several meters deep depressions; all these landforms suggest an ancient gravitational activity which produced the sliding of the upper terrigenous formations over the underlying limestones. The lowest section of the slope, along the Imera River, is presently shaped by landslide events, with shallow rotational slides involving the Numidian Flysch terrains (as the 2015 event) which periodically invades the Imera riverbed.

5.3.2 The 2015 Scillato landslide

The 2015 Scillato landslide produced the collapse of about 200 m of the A19 "Palermo-Catania" highway and 250 m of Provincial Route SP24, causing great inconvenience for regional traffic (Figure 55b). Fortunately, no people were injured. The rainfall records collected in the Caltavuturo and Scillato pluviometric stations show that cumulated rainfall reached 603 mm in the period between January and April 2015, thus exceeding two times the average value of the area (Basile 2015). Indeed, the Caltavuturo station recorded a total of 574 mm rains between January and 10th April 2015 while average cumulative value in the reference period is 330 mm, and the Scillato Station recorded 603 mm of rainfall while the cumulative average value is 354 mm (Basile 2015). Substantial rainfall events were recorded between 21st and 28th February, with 130 mm of cumulative rainfall at Caltavuturo station and 140 mm at Scillato station. The next significant episode occurred between 5th and 8th March, when 70 mm of cumulative rainfall were reached at Caltavuturo station and 110 mm at Scillato station. The last event occurred between 27th and 29th March, when cumulative rains of the order of 60 mm for Caltavuturo and 65 mm for Scillato stations were reached (Basile 2015).

According to the report of Caltavuturo Municipality, the first evidence of landslide activation took place on 3rd March 2015 in correspondence of the SP24. Between the 23rd March and 4th April, concurrently with the last significant rainfall event, the slope instability process quickly escalated involving the SP24. Finally, on 10th April the landslide evolved producing the collapse of the Imera Viaduct (Basile 2015).

The total length of the sliding body is about 700 m and the detachment areas are located between 300 m and 380 m a.s.l. with vertical slips ranging from few meters to about 10 meters along the main scarps. The depth of the failure surface, inferred by combining log-stratigraphies data and geometrical constraints, is about 30 m. In the detachment area the movement had rotational features, such as concave crown zones and counterslopes with water stagnations, while the main movement evolved into an earth flow/slide-type downslope. From the field surveys and exploitation of the optical high-resolution image, resulted that the landslide exhibited distinct movements that simultaneously converged down valley. The displaced mass is strongly deformed internally; lateral margins and surfaces of rupture are extensive visible on the landslide flanks and in the upper source areas respectively.

Figure 55 - The Scillato landslide: a) view of the Rocca di Sciara north-eastern slope; b) the damage highway (courtesy of ANAS s.p.a.); c, d) detachment area of some features of the 2015 event

5.3.3   Top-Down approach

The topographic dataset used for this case study is derived from national LIDAR data acquired in the June 2009. The original dataset has 1m resolution and has been resampled using a bilinear interpolation in Grass GIS to a 5m resolution dataset for computational optimization.

The analysis of the Topographic Position Index shows the slope domains of the Rocca di Sciara north-eastern slope, ranging from the high ridge of Rocca di Sciara top to the Imera valley. In this representation, the Rocca di Sciara I well distinguished against the broad valley of the Imera river and a few flat zones are highlighted along the slopes. Instead, values of the standardized TPI shows much greater details about the local morphologies highlighting a complex arrangement of concave and convex feature along the slope, which could be probably related to landslides (Figure 56).
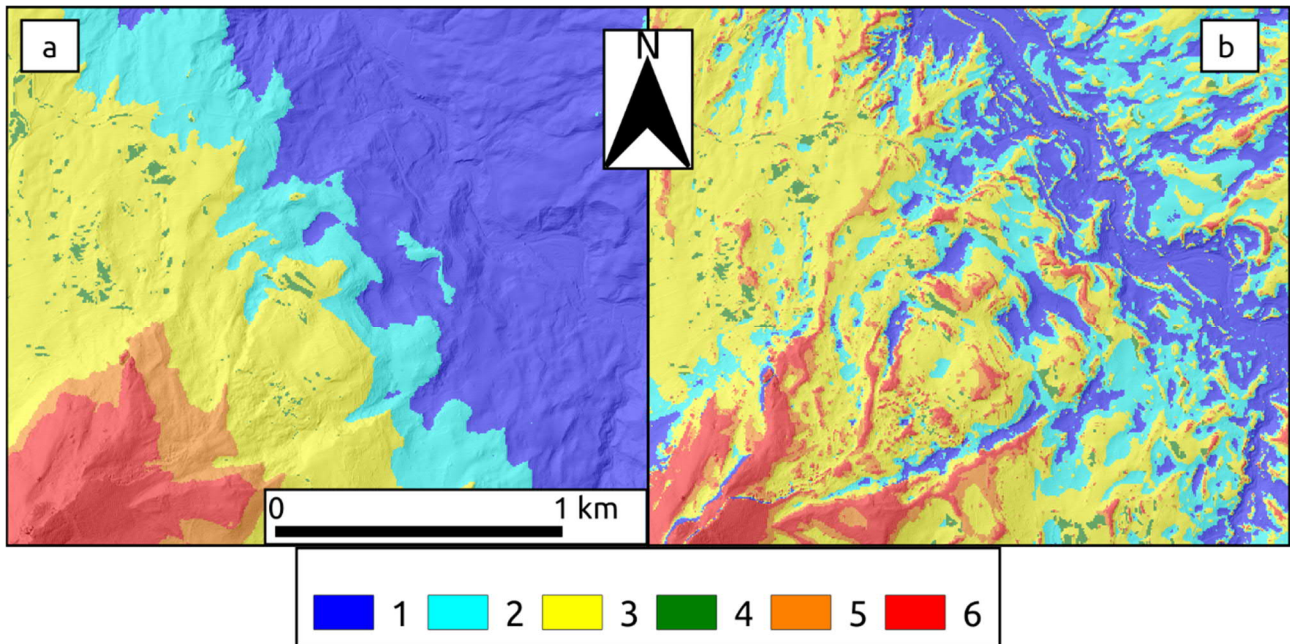
Figure 56 - TPI maps reclassified in slope positions: a) effective values, b) standardized values. 1) valley; 2) lower slope; 3) middle slope; 4) flat slope; 5) upper slope; 6) ridge

From the analysis of the Slope-Area function, thresholds for the contributing area have been derived which define slope processes domains:

- I-II – Hillslope to channel transition: 56 m^2;
- II-III – Channels to landslide dominated channels: 2.371 m^2;
- III-IV – Landslide dominated channels to alluvial channels: 749.894 m^2.
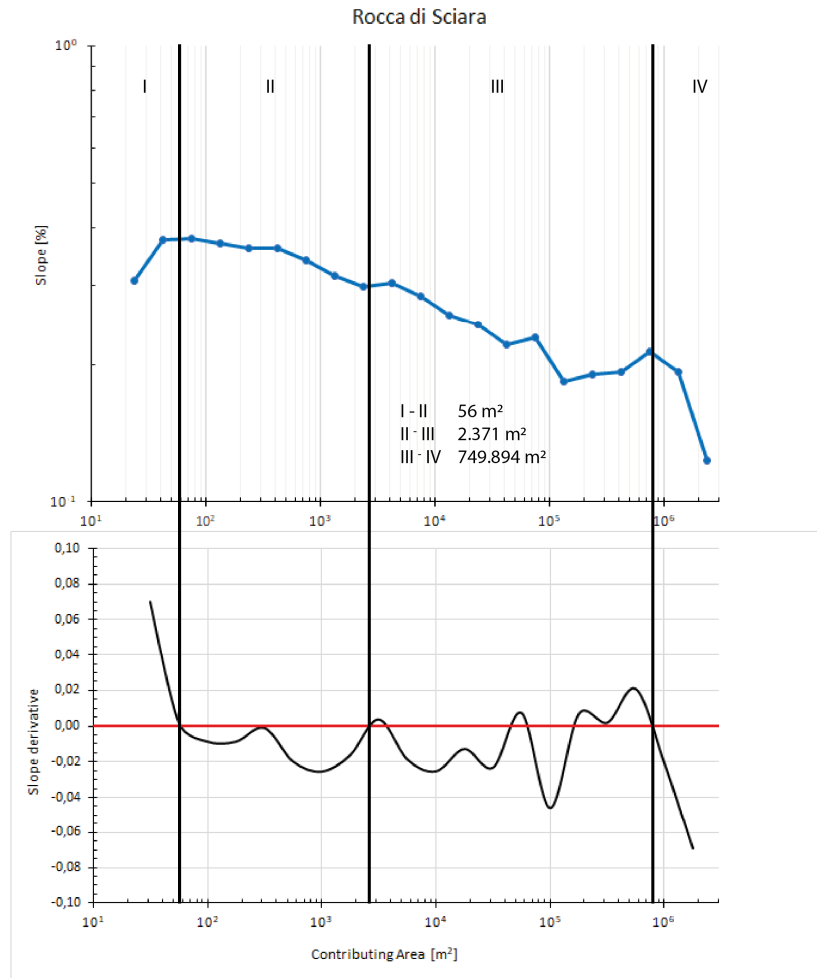
Figure 57 - Slope-area plot for the Rocca di Sciara area

The graphical plots of both TPI and standardized TPI against the contributing area have been also thresholded using the previous derived values for the slope. In detail, the III region of the Slope-Area plot correspond to a standardized TPI range from -35,04 to -146,10, while the IV region correspond to the TPI values less than -40,71 (Figure 58). These ranges have been used to derive candidate landslide related features, reclassifying the mean values of the standardized TPI, and the fluvial domain, reclassifying the mean values of the actual TPI.
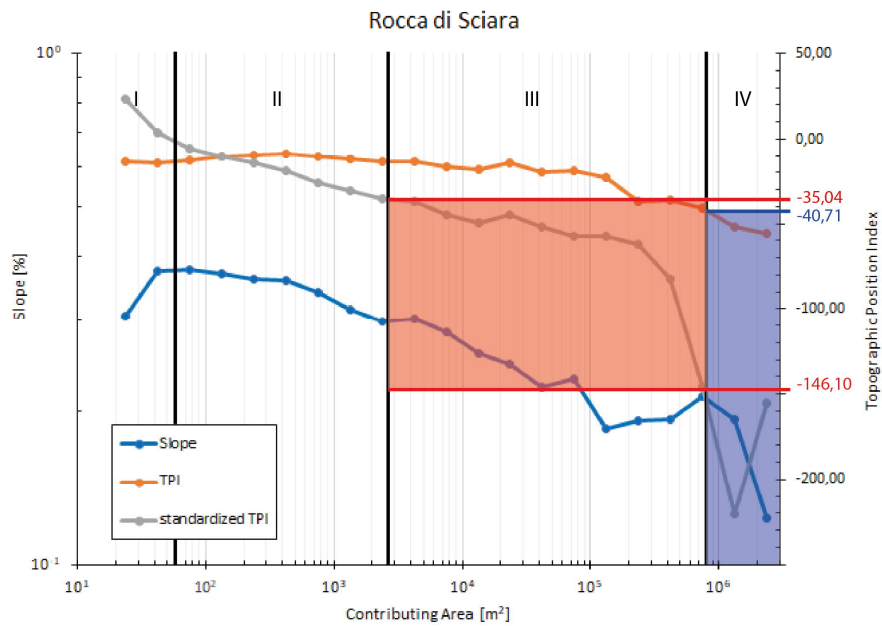
Figure 58 - TPI values in the Slope-Area plot
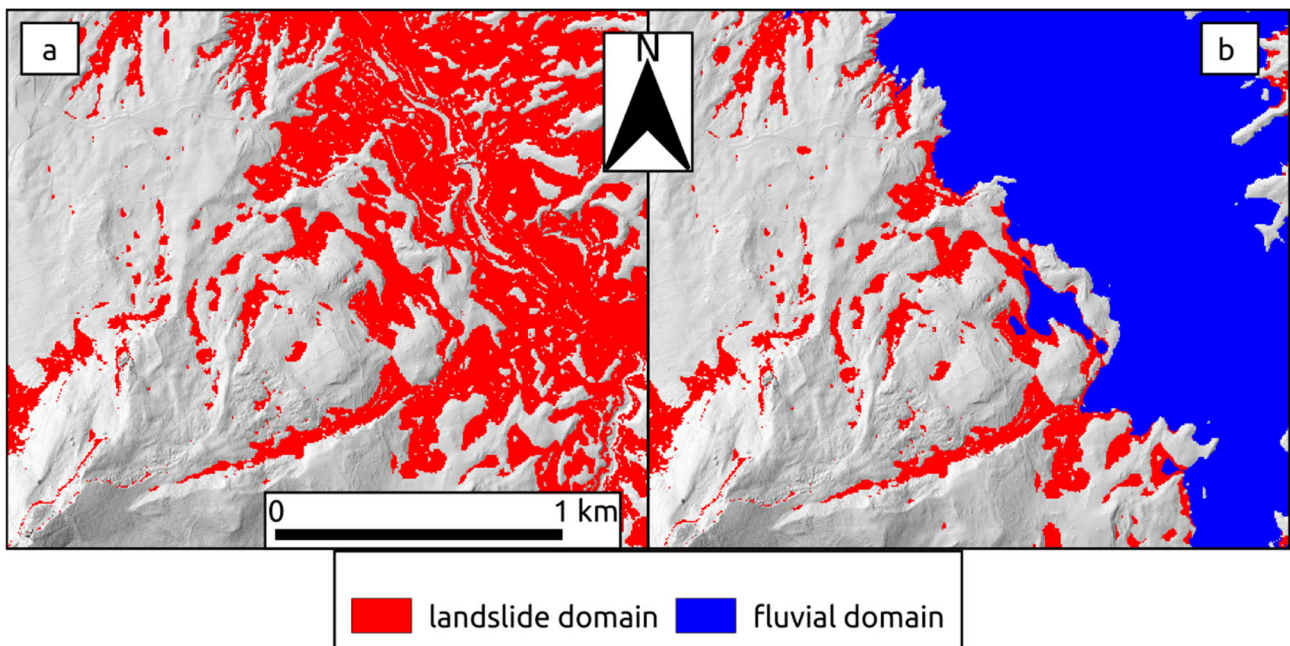
Figure 59 - Landslide domain form the reclassification of the standardized TPI dataset, a) non-filtered values, B) filtered values

5.3.4   Bottom-Up approach

The landslide inventory has been built collecting the available data such as previous inventories, both local (PAI – Northern Imera River Basin Plan) and national (IFFI Project), through the interpretation of a multi-temporal series of aerial photographs and by means of field survey (May 2017). Inventoried landslides have been then stored using the object-oriented model. The focal class contains all the inventoried landslides after the aggregation of the stored components, derived from the evidences collected in the field and by previous data analysis. In the lower portion of the slope there are two clusters of rotational slides which can be aggregated in two rotational slide complexes, the northern one contains the 2005 and 2015 rotational slides and interacts with some peripheral

earth flows also related to the 2015 event. The southern rotational slide complex developed above a spread-like movement. The three rock avalanche deposits in the upper portion of the slope can be also aggregated in a rock avalanche complex and on the scarps left by these phenomena currently occur rock falls. All these objects lay above a rock slope deformation. From the aggregation of all the mentioned objects results the Rocca di Sciara landslide system (Figure 60).
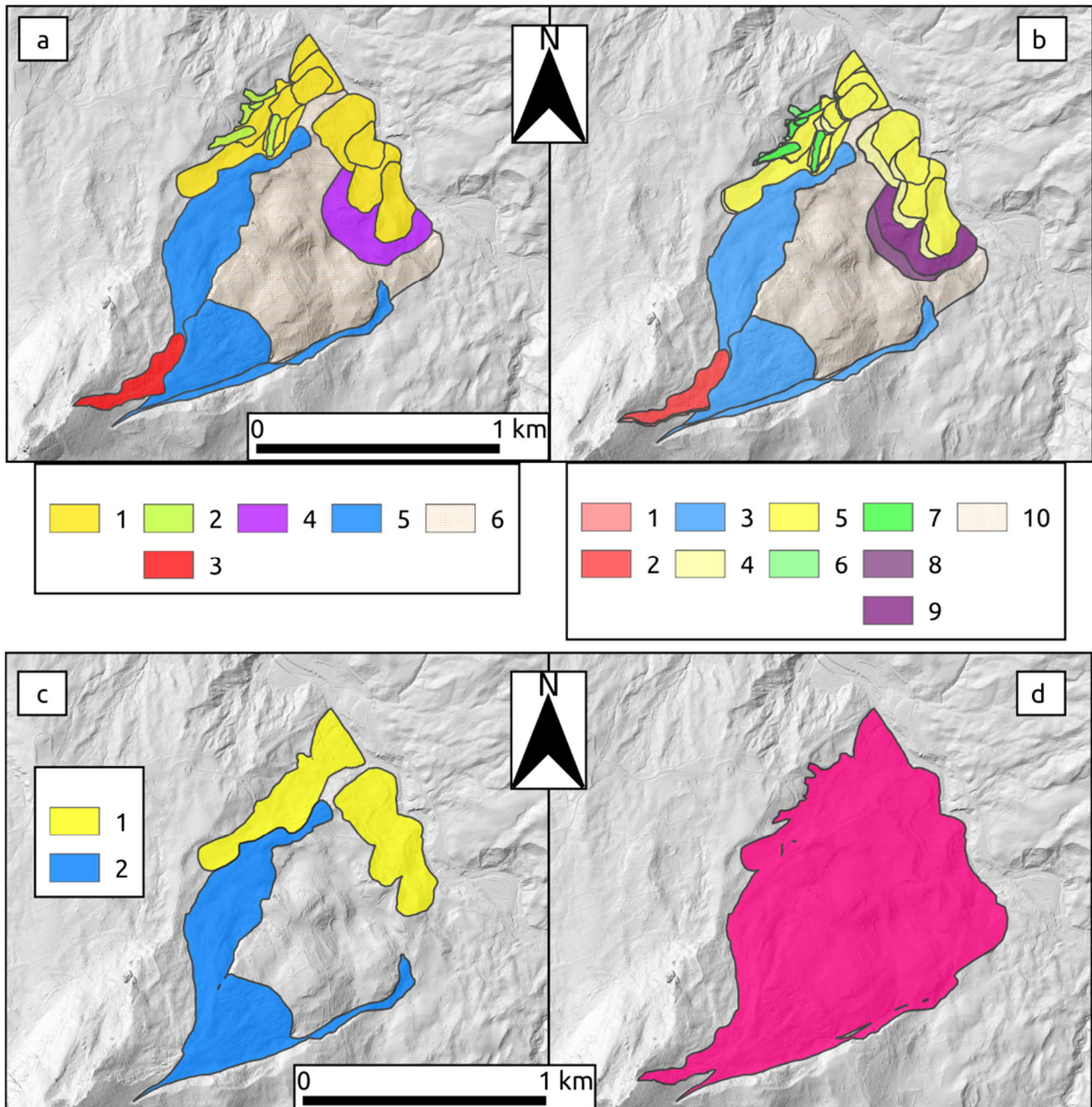
Figure 60 – Landslide maps: a) focal level,1) clay rotational slide, 2) earthflow, 3) rockfall, 4) rock slope spread, 5) rock avalanche, 6) rock slope deformation; b) landslide components, 1) rock fall detachment area, 2) rockfall debris, 3) rock avalanche deposit, 4) clay rotational slide detachment, 5) clay rotational slide body, 6) earthflow source area, 7) earthflow debris, 8) rock slope spread trench, 9) rock slope spread body, 10) rock slope deformation body; c) landslide complexes, 1) soil rotational slide complex, 2) rock avalanche complex; d) landslide systems

Referring to the Rocca di Sciara landslide system the oldest event recognized is the rock slope deformation which presumably caused the sliding of the Caltavuturo Fm. deposits over the limestones of the Crisanti Fm. The upper portion of this movement has been then covered by the occurrence of the three rock avalanches. After these major events the landslide system evolved with shallower phenomena such as rock falls in the upper section and rotational slides – earth flows in the lower portion favoured by the outcropping of the Numidian Flysch with a dip-slope bedding. The southern rotational slide complex can be dated between the beginning of the last century and the 1960, as during the investigation phases for the construction of the highway they were reported as "active landslides" (Graziano 2016). The last two events contains the 2005 rotational slide (Basile 2015) and the march 2015 landslides.
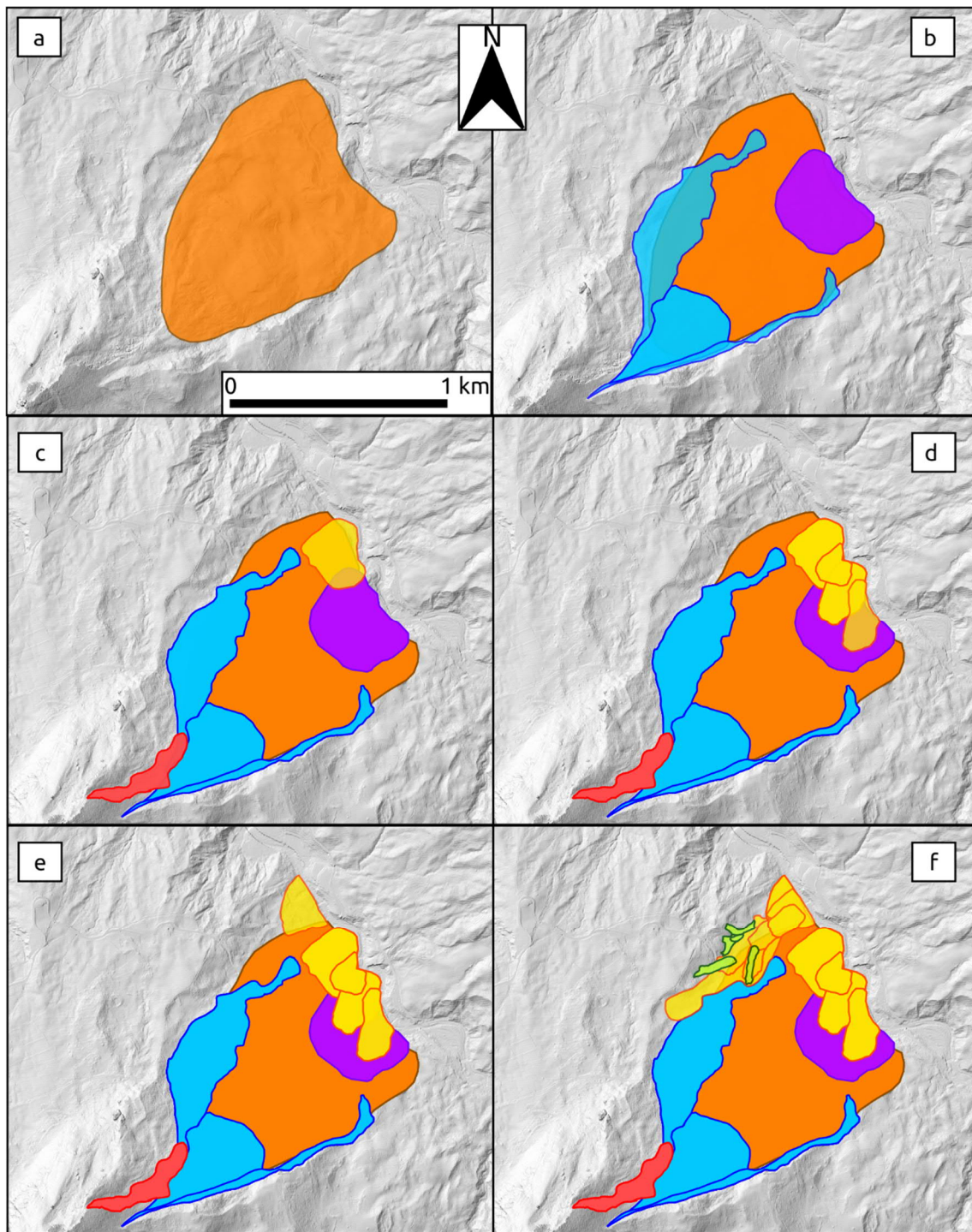
Figure 61 - Event series for the Rocca di Sciara landslide system: note that b, c and d represent cumulative steps and not just three events, while e represent the snapshot of the slope after the 2005 event and 6 is the actual condition of the slope, containing the 2015 effect.

In this case, the reference hillslope has been built iteratively, starting from the objects of interest, i.e. the landslides from the 2015 event, and pretending to not knowing if those landslides were part of a system or not, like a blind test (Figure 62):

1. In the first step, we just define the reference hillslope for the objects of the 2015 event. Within this area we have at least two other objects sharing a functional interaction, the rotational slide from 2005 and a rock avalanche deposit;

2. We compute a new reference hillslope including the last two objects. This time, once again, other two objects share a functional interaction with the initial set, a rock fall and another rock avalanche;

3. Repeating the process with the new set of objects, another rock avalanche falls within the reference hillslope, overlapping the previous rock avalanche. This time there is also a great portion of the basal rock slope deformation within the reference hillslope. In the previous steps it has been willingly ignored for the purpose of the demonstration;

4. Considering also the rock slope deformation, the reference hillslope so obtained, reaches the rock slope spread and the rotational slide complex at the foot of the slope, both in functional interaction with the deep-seated movement;

5. Recomputing again the reference hillslope on this set allow the definition of the reference hillslope for the entire system and to define the system itself in the case where we are not aware of it.
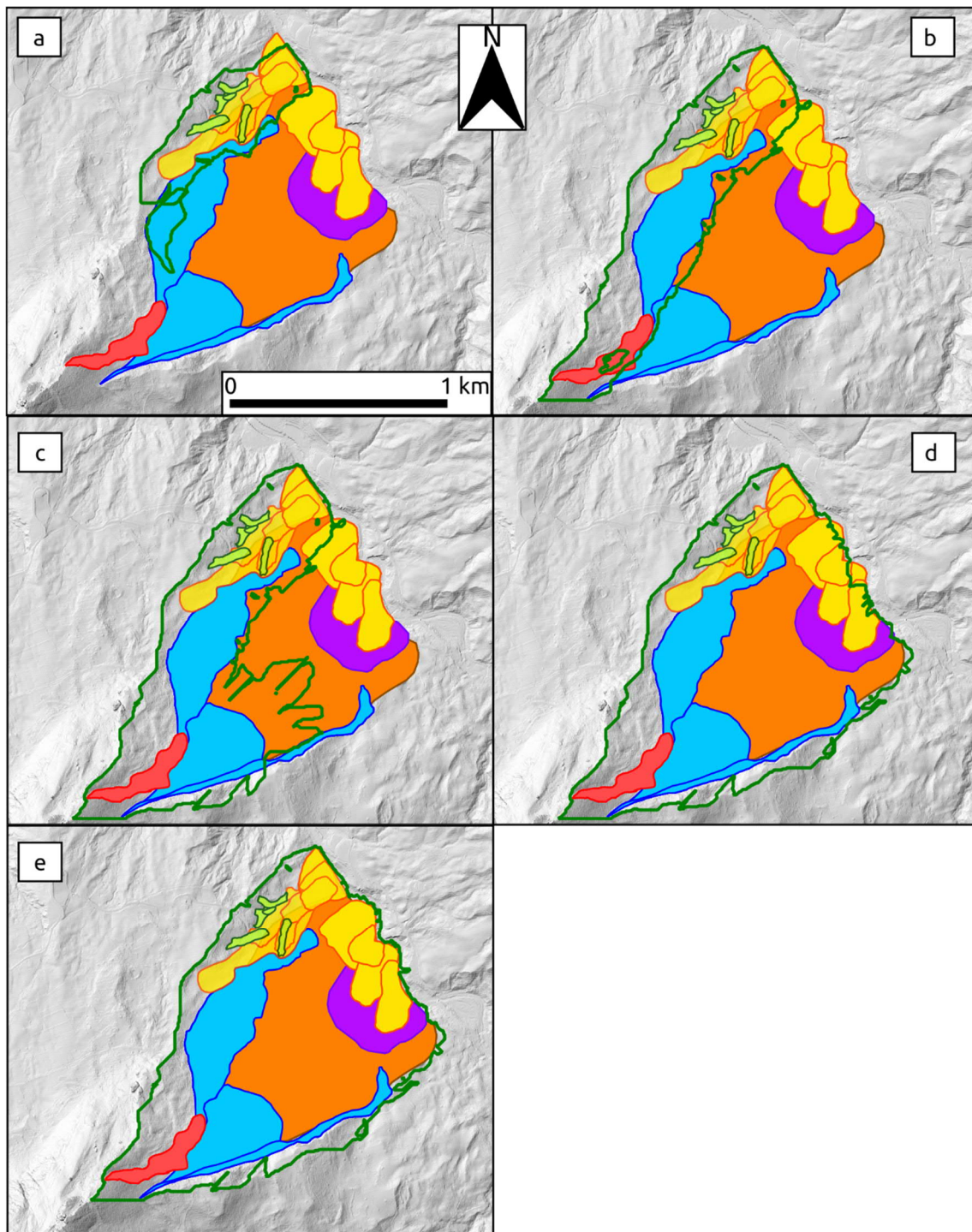
Figure 62 - Landslide system identification using the reference hillslope (green outlined polygon)

5.3.5   Approaches comparison

Comparing morphometric features with the landslide inventory, the following values results computing the confusion matrix:

- Non-filtered values:
    - o   False Positive Rate = 4%
    - o   True Positive Rate = 40,6%
    - o   Accuracy = 73,9%
    - o   Precision = 86,9%

- Filtered values:
    - False Positive Rate = 1,5%
    - True Positive Rate = 17,1%
    - Accuracy = 66,1%
    - Precision = 88,4%
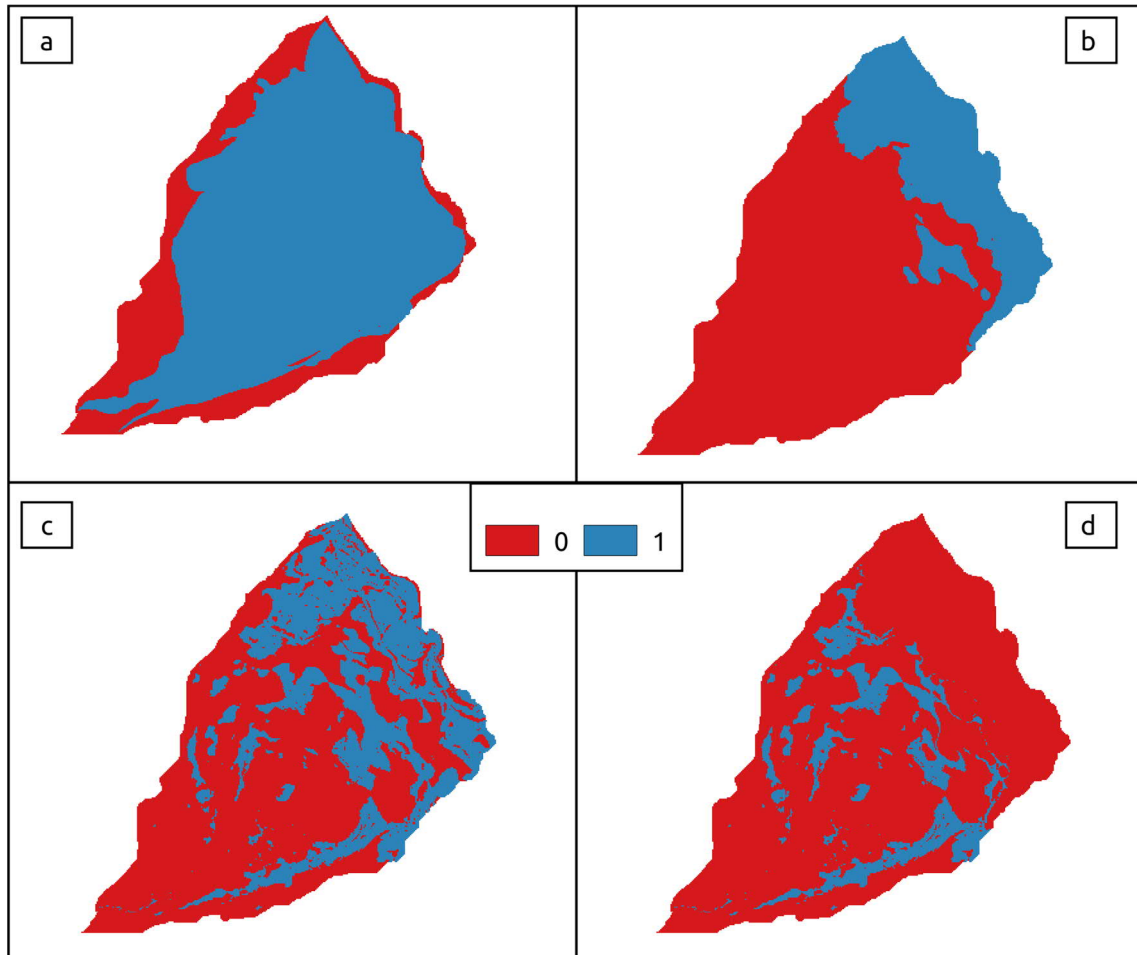
Figure 63 - Input datasets for the confusion matrix: a) actual values, 0 = no landslide, 1 = landslide; b) filter, 0 = non-fluvial domains, 1 = fluvial domain; c, d) predicted values before and after the filtering operation, 0 = other domains, 1 = landslide domain

6   Discussions

6.1   The object-oriented model and its database implementation

The proposed object-oriented model for landslides allows to store and preserve spatial and temporal relations between landslide objects. In this object-oriented approach the landslide inventory is built preserving spatial relations so that every inventoried landslide is stored entirely, and its topological connections can be easily retrieved by queries. Overlapping and nested landslides are then handled with the hierarchical classification, which leads to the simplification of the history of gravity-induced instability on a hillslope into one super-landslide object, a complex or a system, depending on the movement types involved. Moreover, temporal attributes ensure the correct vertical sorting of the mapped objects for the correct visualization of the dataset. Besides, temporal characterization allows to perform temporal queries on the dataset. This, along with the implementation of temporal paradigms, evolve common GIS applications to the level of T-GIS. Within an ideally complete dataset, temporal queries allow to retrieve various useful information, such as snapshots of the slope at any time period, temporal relations between landslides, helpful for investigating cause-effect relationships, or the number, hence the time-series, of events that affected the slope, essential for frequency analysis. However, in order to perform spatial and temporal analysis, the dataset should be as complete as possible. Completeness implies spatial and temporal accuracy: whereas the first can be achieved with a meticulous mapping of present-day features, the second can be quite challenging. Reconstructing the temporal evolution of a slope means to collect features that may not be visible today anymore. This task can only be performed consulting pre-existing material such as previous inventories, optical images both aerial and satellite, previous maps or historical data. All of these operations unfortunately are time-consuming and difficult to perform over large areas, moreover, in some areas there may be lack of previous information (Guzzetti et al. 2012). In such cases, building an inventory using the proposed object-oriented model can be an efficient starting point to store present available data ready to be easily updated with future occurrences. On the other hand, previous multi-temporal inventories, when available, can easily be rearranged following the object-oriented model. Converting snapshot-based datasets into one event-based dataset reduce data redundancy, thus data volume, in fact if the same landslide is part of different snapshots and has not experienced reactivations, can be simplified into one landslide object with the proper temporal collocation.

Referring to the case studies, the implementation of the object-oriented model for landslides within a database structure allowed the automatic reconstruction of the hierarchical levels starting from the input landslide dataset which is the only information needed for the model to work. Landslide components can be also stored as a further level of detail, but are not mandatory for the hierarchical aggregation, as the hierarchical organization starts from the focal level and goes up, firstly generating landslide complex and then landslide systems.

6.2   Top-Down vs Bottom-Up

The analysis of confusion matrices for the three case studies tested the performance of the top-down approach, results are summarized in Figure 64. As stated before, false positive rate and precision values have been chosen as metrics, as the morphometric analyses used in this work do not recognize entire landslides but some of their peculiar features, or rather concave morphologies along

the slopes disconnected from main valleys. In fact, true positive rates are less of 50% for all the case studies and further decrease when the prediction dataset is filtered to remove fluvial domain. Accuracy values float around 70% and slightly decrease after the filtering operation, which means that roughly three times over four the prediction is correct, considering the set of true positive and true negative values. These accuracy values, even with a low true positive rate, are the consequence of a very low false positive rate, which is generally below 5% and further drops after the filtering operation. Low values of false positive rate denote a low rate of occurrence of type II errors. Regarding precision, for two case studies, values reach about 90% on the filtered dataset, which means that about 90% of the values predicted as positive are actually true. The Corniolo case study is quite an exception, in fact precision values are below 50%. Even considering other metrics, this dataset is not so much affected by the filtering operation. This behaviour could be related to the overall morphology of the area and to landslide types affecting the different areas. In the Corniolo area, false positive rate is higher than the other case studies, which means that the analysis detects concave features that are not related to landsliding but maybe to local litho-structural features. Besides, the analysis fails in the detecting of the three large rock compound slides. In the other two case studies, the morphometric approach performs better, but, in these cases, surficial landsliding is much more abundant. In both the cases, the analysis does not detect deep-seated movements directly, but it shows features related to the shallower phenomena developed on top of them. In the Mt. Pruno case study, the only detected feature ascribable to the deep-seated slope deformation is the main trench in the Old Roscigno village area.
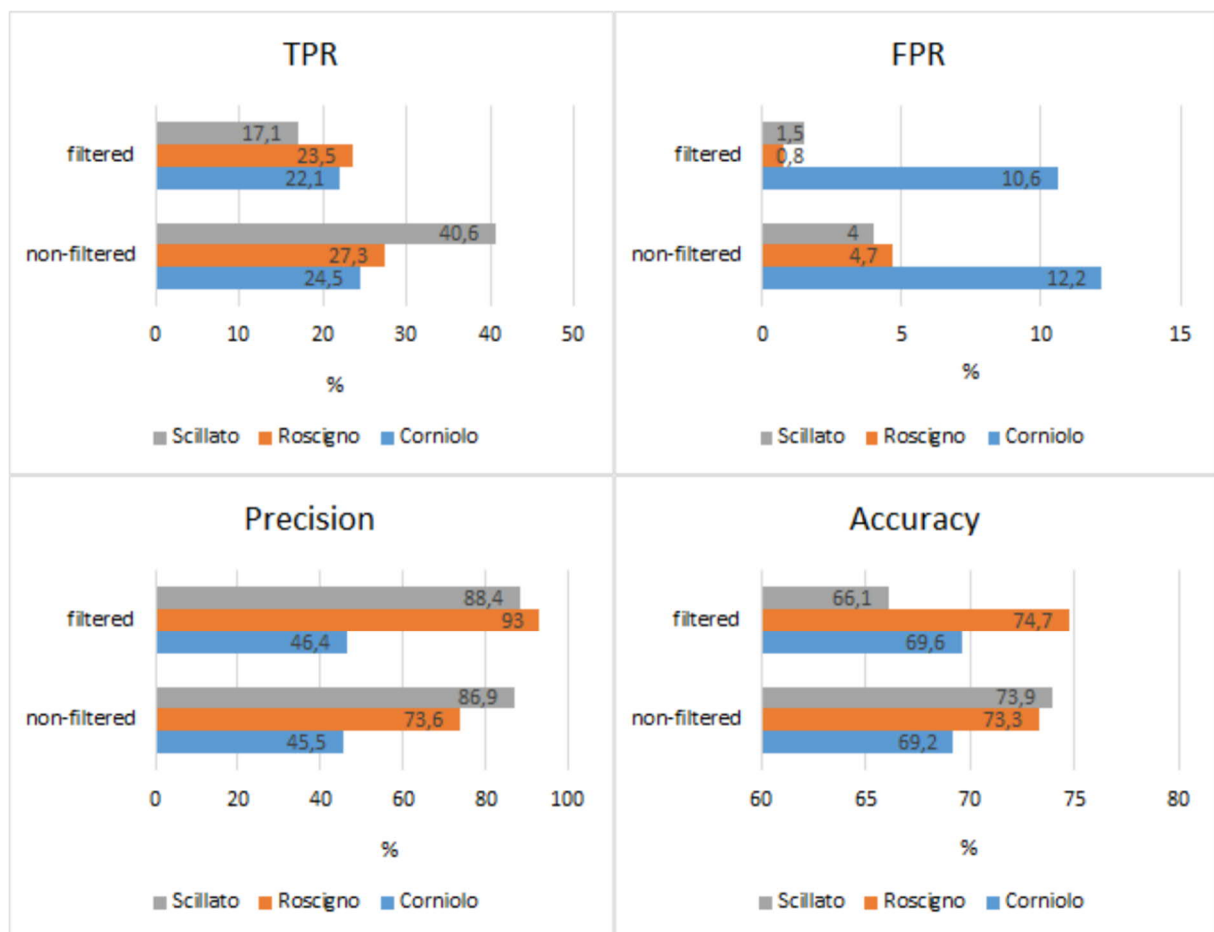
Figure 64 - Confusion results for the three case studies

6.3   The reference hillslope

The reference hillslope, being derived as the closest portion of landscape to a reference landslide object, can be considered the basic terrain unit to be investigated when studying a landslide, as it has the maximum likelihood to be involved in a future reactivation of the movement. Moreover, this area could be the starting point to search whether that specific phenomenon interacts with other landslides or not. If within the reference hillslope there is no evidence of other movements, then the landslide can be considered as an isolated object. On the contrary, if within the reference hillslope boundary there are other landslides, or portion of them, having a functional interaction with the considered object, then those movements will be aggregated into a super-landslide object, being a complex or a system depending on their type of movement. Considering the last event that affected the Rocca di Sciara north-eastern slope, within its reference hillslope other landslide feature are contained sharing a functional interaction with the reference movements, as the objects of the 2005 event and a rock avalanche deposit (Figure 65). Lastly, if within the reference hillslope are contained, or partially contained, other movements not sharing a functional interaction with the reference object, that could be considered as a transient state from an isolated landslide object to a composite super-landslide object, as they share portion of the reference hillslope, hence there is the chance of interaction in any future reactivation. This is the case, for example, of the Poggio Baldi landslide system: within its reference hillslope portion of a rock compound slide is contained but they are disconnected. In this case, indeed, their distance is within a few dozens of meters, thus it is very likely that a future reactivation of one of them can involve the other (Figure 37). A preliminary analysis can be conducted also using the grid-based technique described in the top-down approach. If any candidate landslide feature lies within the reference hillslope, then it should be worth of investigation.
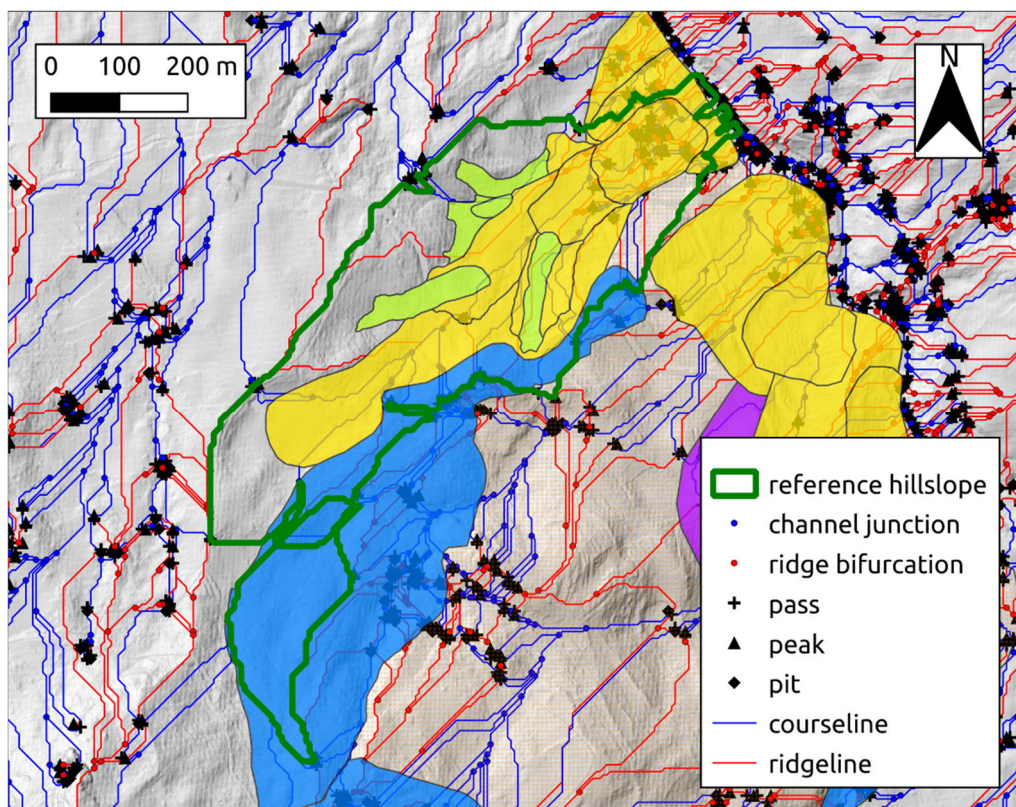
Figure 65 - Reference hillslope for the 2015 Scillato event

7 Future developments

Future developments are planned for the implementation of a fully object-oriented interface for the QGIS software written in Python language in order to fully exploit object-oriented potential. Moreover, this kind of implementation will allow to further specialize defined landslide classes with specific dedicated attributes, enriching various landslide types description within a single dataset, without creating different tables like in a classic relational model. Further work can also be done on the definition of spatio-temporal topological relations. For example, the relation covers – covered by, can be specialized considering if the object A is just covered by the object B, or if the object B completely erase the object A (Figure 66).
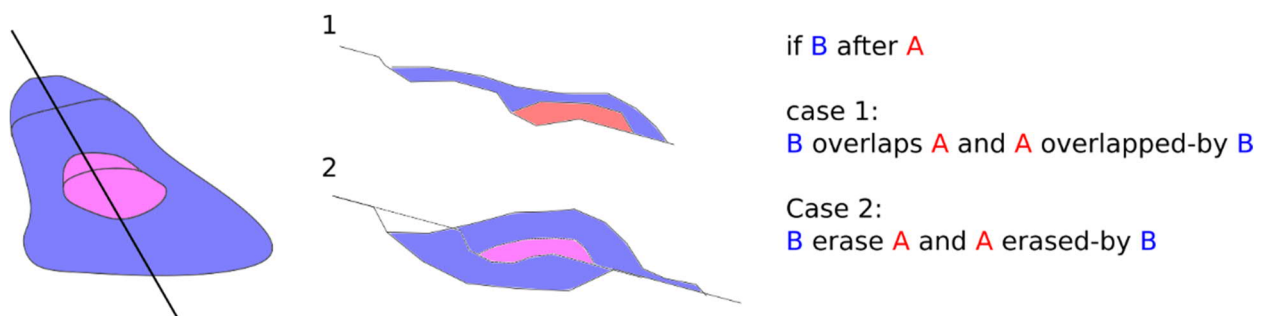
Figure 66 - Specialization of the "overlap" spatio-temporal topological relation

The use of surface networks could also be extended as part of the top-down approach. From preliminary analyses, the recognition of patterns in the surface network structure could highlight geomorphological objects, as peculiar arrangement of nodes and edges can be characteristic of certain landforms. As for example, the pattern represented by an isolated peak with one outcoming ridgeline, reaching a saddle from which depart two courseline that reach a junction surrounding the initial peak, can be representative of rotational slides, instead a series of converging courselines departing from a series of straight ridgelines could be characteristic of hydro-wedge structures (Cascini et al. 2008; Cuomo and Guida 2016) (Figure 67). Besides, giving a hierarchy to both nodes and edges can be useful in order to generalize the whole network and define different hierarchical levels of slope units.
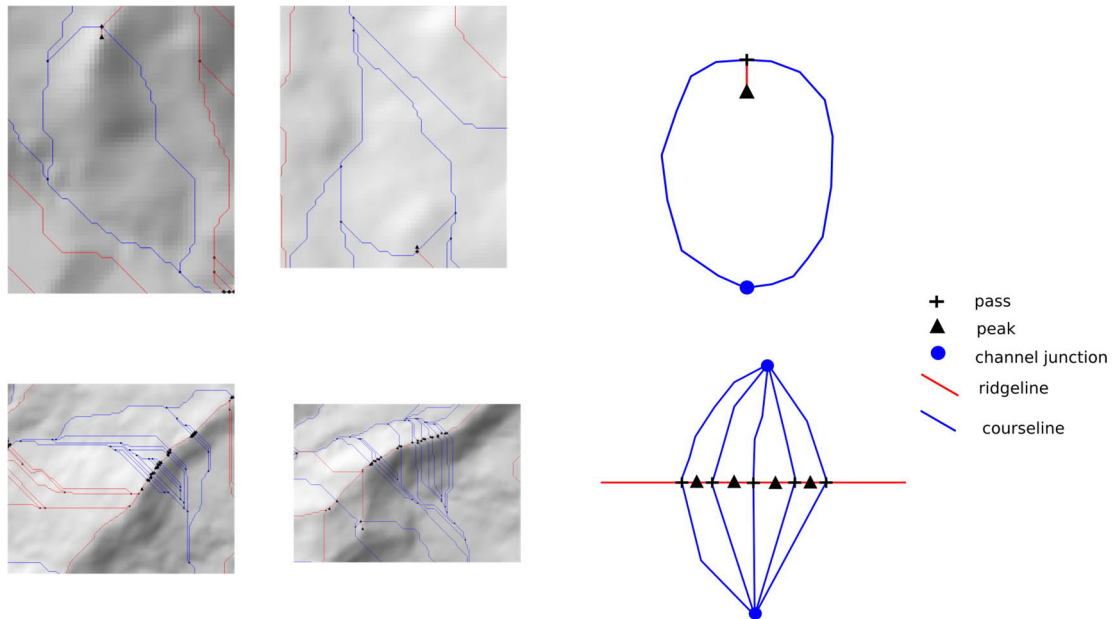
Figure 67 - Surface Network patterns

The object-oriented model, here defined for landslide, can be also extended to any other type of geomorphic processes as useful resource for different kind of problematics, such as to fluvial features for analysing fluvial dynamics or evaluating hydraulic hazard, or to structural geomorphological features as a resource for seismic hazard studies.

8 Conclusions

This research led to the development of an object-oriented model for landslides. Complex spatio-temporal arrangements of landslides are handled through an object-oriented classification and a hierarchical organization of objects based on rigorous topological relations. The focal level of the hierarchy is set containing landslides themselves, classified depending on their movement type, and two orders of super-classes are defined:

- Landslide complexes aggregate landslide member of the same class with functional interaction, i.e. spatial overlap;
- Landslide systems group landslides or landslide complexes members of different classes sharing a functional interaction.

Instead, a level of decomposition stores landslide components, such as detachment areas and bodies. Landslide objects are also characterized with temporal attributes using an event-based approach, essential for the temporal-vertical sorting of phenomena and to perform temporal queries.

In order to test the model, two main strategies have been developed: i) a top-down approach, exploiting morphometric analyses on DEMs to derive landslide-related morphologies and ii) a bottom-up approach, based on the creation of the landslide inventory by means of usual techniques, such as field surveys, remote sensing data analysis and desk studies. Inventoried objects have been stored referring to the proposed object-oriented model and for every object a basic terrain unit has been derived, called the reference hillslope. The reference hillslope is derived from a mathematical abstraction of the topographic surface, the Surface Network. Collecting all the surface network derived regions in which the reference object is contained define the reference hillslope. Both the approaches have been tested on three selected case studies in Italy. Results show how the object-oriented classification can be a powerful model to derive landslide hierarchies and manage complex spatio-temporal superimposition of landslides. Encapsulating all spatial and temporal relations between landslides within the definition of a landslide complex or a landslide system, also avoid physical data fragmentation and logic inconsistency, as topology of data comply with topology of real-world features and vertical relations are preserved.

The defined model has been implemented using the object-relational database management system PostgreSQL, which, even not being fully object-oriented, allow to reproduce some basic functions as aggregation, encapsulation and overriding using views, custom functions and custom data types. Such implementation allowed to automatically organize inventoried phenomena into hierarchies, defining landslide complexes and landslide systems, providing a powerful tool to manage the natural complexity of the spatio-temporal superimposition of several landsliding events.

The comparison of the Top-Down and the Bottom-Up approaches highlighted the limitations of grid-based techniques, such as the Topographic Position Index and the Slope – Area relation, for the automatic recognition of landslides. The methodology returned good results in the recognition surficial landsliding, such as rotational slides or flow-like movements, but failed in the detection of deep-seated phenomena. This outcome suggest that the Top-Down approach should be used as support for the Bottom-Up approach and, as for now, cannot be the main strategy. On the other hand, the Bottom-Up approach has proved to be a good method for the definition of landslide

hierarchies, starting from a usual landslide inventory and then applying the proposed object-oriented model. This model allows the automatic aggregation of landslide objects into super-objects when the required criteria are met, simplifying such situations where an operator has to face with superimpositions of several landsliding events. Spatial relations between landslide objects also contribute to the definition of the number of interacting phenomena and their relative position in space, such information is indeed needed to determine the spatial extent of a deformation area and infer its volume. The obtained set of information consequently affects the concept of landslide hazard. If several landslides interact, their level of hazard should not be defined just for each object but should be related with the other interfering phenomena. Moreover, when a landslide is part of a landslide complex and/or of a landslide system, different levels of hazard could be defined for the different hierarchical levels. As for now, these aspects concerning hierarchical objects and their associated hazard have not been investigated yet and the presented model sets the basis for future works inherent this topic.

The implementation of temporal analyses in a GIS allows the user to retrieve useful information over a landslide dataset, such as the number of events that affected a hillslope, the number of reactivations for a single movement and temporal snapshots of the slope at any recorded time period. The temporal succession of interacting landslides also describes the past evolution of a slope helping the formulation of future reactivation scenarios. Such temporal analysis requires that the landslide inventory is built collecting multi-temporal information from a variety of sources. Sometimes such data are not available; in that case, using an object-oriented model can be both a starting point to best represent actual conditions and a base dataset ready to store future updates.

The coupling of this object-oriented classification with the definition of the reference hillslope, defined as the minimal area to search in order to assess whether a landslide is an isolated phenomenon or interacts with other movements, sets the starting point for the study of engineering problems involving such complex arrangements of landslides. As of now, it is possible to define and effectively store their spatial and temporal relations, moreover, the computation of the reference hillslope allows to objectively define an "area of interest" for every considered object, being it a single landslide or an entire landslide system. However, defining that a landslide is part of a larger landslide system can be not always the final answer at every problem, in fact such a system may be composed of objects evolving on long-term which may not affect considerably, or not at all, the objective of a particular study. In this perspective, further efforts are needed in order to characterize the landslide hierarchical levels in relation to engineering works, to be able to quantify the interactions between landslides and anthropic activities at the different scales and to effectively plan and design intervention strategies.

9 References

Abolmasov B, Milenković S, Marjanović M, et al (2015) A geotechnical model of the Umka landslide with reference to landslides in weathered Neogene marls in Serbia. Landslides 12:689–702. doi: 10.1007/s10346-014-0499-4

Aleotti P, Chowdhury R (1999) Landslide hazard assessment: summary review and new perspectives. Bull Eng Geol Environ 58:21–44. doi: 10.1007/s100640050066

Alexander D (1988) Valtellina Landslide and Flood Emergency, Northern Italy, 1987. Disasters 12:212–222. doi: 10.1111/j.1467-7717.1988.tb00671.x

Allen JF (1983) Maintaining Knowledge about Temporal Intervals. Commun ACM 26:832–843

Aloia A, Guida D (2012) I geositi: la voce della natura del geoparco del Cilento, Vallo di Diano e Alburni

Alvioli M, Marchesini I, Guzzetti F (2018) Nation-wide, general-purpose delineation of geomorphological slope units in Italy. PeerJ Prepr 1–5. doi: 10.7287/peerj.preprints.27066

Alvioli M, Marchesini I, Reichenbach P, et al (2016) Automatic delineation of geomorphological slope units with r.slopeunits v1.0 and their optimization for landslide susceptibility modeling. Geosci Model Dev 9:3975–3991. doi: 10.5194/gmd-9-3975-2016

APAT (2007) Carta Geomorfologica d'Italia - 1:50.000 - Guida alla rappresentazione cartografica. Quad. Ser. III 10:34

Atkinson M, DeWitt D, Maier D, et al (1990) The Object-Oriented Database System Manifesto. In: Deductive Object-Oriented Databases. Proc. First Int. Conf. Deductive Object-Oriented Databases Kyoto Res. Park. Kyoto, Japan, 4–6 December, 1989

Aziz T, Haq E, Muhammad D (2018) Performance based Comparison between RDBMS and OODBMS. Int J Comput Appl 180:42–46. doi: 10.5120/ijca2018916410

Barla G, Paronuzzi P (2013) The 1963 Vajont Landslide: 50th Anniversary. Rock Mech Rock Eng 46:1267–1270. doi: 10.1007/s00603-013-0483-7

Barredo JI, Benavides A, Hervás J, Van Westen CJ (2000) Comparing heuristic landslide hazard assessment techniques using GIS in the Tirajana basin, Gran Canaria Island, Spain. Int J Appl Earth Obs Geoinf 2000:9–23

Barzani MM, Salleh KBO (2016) Automated classification of landform , Z . R . B in Iran. Int J Appl Environ Sci 11:915–926

Basile G (2015) FRANA DELLA S.P. 24 – Viadotto Imera A19 RAPPORTO TECNICO-GEOLOGICO. Regione Siciliana – Presidenza - Dipartimento della Protezione Civile S.17 - CENTRO FUNZIONALE DECENTRATO MULTIRISCHIO INTEGRATO

Berti M, Corsini A, Daehne A (2013) Comparative analysis of surface roughness algorithms for the identification of active landslides. Geomorphology 182:1–18. doi: 10.1016/j.geomorph.2012.10.022

Bittner T, Stell JC (2008) Approximation. Encycl. GIS 21–25

Blanc J, Grime D, Blateyron F (2011) Surface characterization based upon significant topographic features. J Phys Conf Ser 311:6. doi: 10.1088/1742-6596/311/1/012014

Blaschke T, Hay GJ, Kelly M, et al (2014) Geographic Object-Based Image Analysis - Towards a new paradigm. ISPRS J Photogramm Remote Sens 87:180–191. doi: 10.1016/j.isprsjprs.2013.09.014

Booth AM, Roering JJ, Rempel AW (2013) Topographic signatures and a general transport law for deep-seated landslides in a landscape evolution model. J Geophys Res Earth Surf 118:603–624. doi: 10.1002/jgrf.20051

Borgatti L, Corsini A, Barbieri M, et al (2006) Large reactivated landslides in weak rock masses: A case study from the Northern Apennines (Italy). Landslides 3:115–124. doi: 10.1007/s10346-005-0033-9

Borges KA V., Davis Jr. CA, Laender AHF (2001) OMT-G: An object-oriented data model for geographic applications. Geoinformatica 5:221–260. doi: 10.1023/A:1011482030093

Boyer SE, Elliott D (1982) Thrust Systems. Am Assoc Pet Geol Bull 66:1196–1230. doi: 10.1306/03B5A77D-16D1-11D7-8645000102C1865D

Bozzano F, Caporossi P, Esposito C, et al (2017) Mechanism of the Montescaglioso Landslide (Southern Italy) Inferred by Geological Survey and Remote Sensing. In: Mikos M, Tiwari B, Yin Y, Sassa K (eds) Advancing Culture of Living with Landslides. Springer, Cham, pp 97–106

Bozzano F, Della Seta M, Martino S (2016) Time-dependent evolution of rock slopes by a multi-modelling approach. Geomorphology 263:113–131. doi: 10.1016/j.geomorph.2016.03.031

Bremer T, Edelsbrunner H, Hamann B, Pascucci V (2004) A Topological Hierarchy for Functions on Triangulated Surfaces. IEEE Trans Vis Comput Graph 10:385–396

Budimir MEA, Atkinson PM, Lewis HG (2015) A systematic review of landslide probability mapping using logistic regression. Landslides 12:419–436. doi: 10.1007/s10346-014-0550-5

Calcaterra D, Guida D, Budetta P, et al (2014) Moving geosites : how landslides can become focal points in Geoparks 2 From Landslide to Moving Geosite. Latest trends Eng Mech Struct Eng Geol - Proc 7th Int Conf Eng Mec Stru Eng Geol (EMESEG '14)2 2:162–171

Câmara G, Souza RCM, Freitas UM, Garrido J (1996) Spring : Integrating Remote Sensing and GIS by Object-oriented Data Modelling. Comput Graph 20:395–403

Cammarosano A, Cavuoto G, Danna M, et al (2004) Nuovi dati sui flysch del cilento (Appennino meridionale, Italia). Boll. della Soc. Geol. Ital. 123:253–273

Carrara A, Cardinali M, Detti R, et al (1991) GIS techniques and statistical models in evaluating landslide hazard. Earth Surf Process Landforms 16:427–445. doi: 10.1002/esp.3290160505

Cascini L, Cuomo S, Guida D (2008) Typical source areas of May 1998 flow-like mass movements in the Campania region, Southern Italy. Eng Geol 96:107–125. doi: 10.1016/j.enggeo.2007.10.003

Castilla G, Hay GJ (2008) Image objects and geographic objects. In: Blaschke T, Lang S, Hay GJ (eds) Object-Based Image Analysis. Springer, pp 91–110

Catalano R, Avellone G, Basilone L, et al (2011) foglio 609 - 596 TERMINI IMERESE - CAPO PLAIA. NOTE Illus. della Cart. Geol. D'ITALIA alla scala 150.000 224

Catane SG, Veracruz NAS, Flora JRR, et al (2019) Mechanism of a low-angle translational block slide: evidence from the September 2018 Naga landslide, Philippines. Landslides. doi: 10.1007/s10346-019-01212-9

Catenacci V (1996) Il dissesto idrogeologico e geoambientale in Italia dal dopoguerra al 1990

Chaudhri AB (1993) Object Database Management Systems: An Overview. BCS OOPS Newsl 18:1–28

Chen Y, Wang Z, Chen Z (2012) Implementation of object-oriented GIS data model with topological relations between spatial objects. Int J Adv Comput Sci 2:334–338. doi: 10.1117/12.2011995

Chung-Jo F, Fabbri AG (1999) Probabilistic Prediction Models for Landslide Hazard Mapping. Photogramm Eng Remote Sens 65:1389–1399

Clarke KC, Romero BE (2017) On the topology of topography: a review. Cartogr Geogr Inf Sci 44:271–282. doi: 10.1080/15230406.2016.1164625

Clementini E (2004) Modeling Spatial Objects affected by Uncertainty. In: de Caluwe R, de Tré G, Bordogna G (eds) Spatio-Temporal Databases. Springer, pp 211–236

Clementini E, Sharma J, Egenhofer MJ (1994) Modelling topological spatial relations: Strategies for query processing. Comput Graph 18:815–822. doi: 10.1016/0097-8493(94)90007-8

Codd EF (1970) A Relational Model of Data for Large Shared Data Banks. Commun ACM 13:377–387. doi: 10.1145/357980.358007

Cohn AG, Bennett B, Gooday J, Gotts NM (1997) Qualitative Spatial Representation and Reasoning with the Region Connection Calculus. Geoinformatica 1:1–44

Coico P (2010) Analisi a scala regionale dei sistemi ambientali interessati da scenari di multirischio idrogeologico. Università di Napoli Federico II

Coico P, Calcaterra D, De Pippo T, Guida D (2013) A Preliminary Perspective on Landslide Dams of Campania Region, Italy. Landslide Sci Pract 6:83–90. doi: 10.1007/978-3-642-31427-8

Corbi I, De Vita P, Guida D, et al (1999) Mid-term geomorphological evolution of the Covatta valley, Biferno river basin, Molise, Italy. Geogr Fis e Din Quat 22:115–128

Corbi I, Guida M, Tetamo G, Vallario A (1996) Considerazioni sul rischio a franare di aree campione nel bacino del Fiume Biferno (Molise). Mem della Soc Geol Ital 51:1087–1100

Corsini A, Borgatti L, Caputo G, et al (2006) Investigation and monitoring in support of the structural mitigation of large slow moving landslides: An example from Ca' Lita (Northern Apennines, Reggio Emilia, Italy). Nat Hazards Earth Syst Sci 6:55–61. doi: 10.5194/nhess-6-55-2006

Crosta GB, Chen H, Lee CF (2004) Replay of the 1987 Val Pola Landslide, Italian Alps. Geomorphology 60:127–146. doi: 10.1016/j.geomorph.2003.07.015

Crozier MJ (2010a) Deciphering the effect of climate change on landslide activity: A review. Geomorphology 124:260–267. doi: 10.1016/j.geomorph.2010.04.009

Crozier MJ (2010b) Landslide geomorphology: An argument for recognition, with examples from New Zealand. Geomorphology 120:3–15. doi: 10.1016/j.geomorph.2009.09.010

Cruden DM, Varnes DJ (1996) Landslides Types and Processes. In: Landslides: Investigation and Mitigation. p 77

Cuomo A, Guida D (2016) Using hydro-chemograph analyses to reveal runoff generation processes in a Mediterranean catchment. Hydrol Process 30:4462–4476. doi: 10.1002/hyp.10935

Dahl O-J (2002) The Roots of Object-Oriented Programming : Simula 67. In: Broy M, Denert E (eds) Software Pioneers. Springer, pp 78–90

Dahl O-J, Nygaard K (1968) Class and subclass declarations. In: Simulation Programming Languages. Proceeding from the IFIP Working Conference, Oslo, May, 1967. p 17

Dai FC, Lee CF (2002) Landslide characteristics and slope instability modeling using GIS, Lantau Island, Hong Kong. Geomorphology 42:213–228. doi: 10.1016/S0169-555X(01)00087-3

De Felice G, Fogliaroni P, Wallgrün JO (2011) A Hybrid Geometric-Qualitative Spatial Reasoning System and Its Applications in GIS. Lect Notes Comput Sci 6899:188–209

De Reu J, Bourgeois J, Bats M, et al (2013) Application of the topographic position index to heterogeneous landscapes. Geomorphology 186:39–49. doi: 10.1016/j.geomorph.2012.12.015

de Riso R, Santo A (1997) Geologia, evoluzione geomorfologica e frane del bacino del T. Pietra (Campania). Quad di Geol Appl 4:19–33

Del Monte M, D'Orefice M, Luberti GM, et al (2016) Geomorphological classification of urban landscapes: the case study of Rome (Italy). J Maps 12:30. doi: 10.1080/17445647.2016.1187977

Devoto S, Biolchi S, Bruschi VM, et al (2012) Geomorphological map of the NW Coast of the Island of Malta (Mediterranean Sea). J Maps 8:33–40. doi: 10.1080/17445647.2012.668425

Di Luzio E (2019) Geological setting and structural archtecture of the mountain ridges hosting the Poggio Baldi landslide: (Santa Sofia, FC)

Di Martire D, Ramondini M, Calcaterra D (2015) Integrated monitoring network for the hazard assessment of slowmoving landslides at Moio della Civitella (Italy). Rend Online Soc Geol Ital 35:109–112. doi: 10.3301/ROL.2015.76

Dittrich K (1986) Object-Oriented Database Systems: The notation and The Issues. In: International Workshop in Object-Oriented Database Systems, Pacific Grove, CA, Washington D.C. pp 2–4

Dongarrà G, Ferla P (1982) Le argille di Portella Colla e del Flysch Numidico auct. (M. Madonie - Sicilia) - Aspetti deposizionali e diagenetici. Rend della Soc Ital di Mineral e Petrol 38:1119–1133

Dragicévić S (2004) Fuzzy Sets for Representing the Spatial and Temporal Dimension in GIS Databases. In: Spatio-Temporal Databases. pp 11–27

Drăguţ L, Blaschke T (2006) Automated classification of landform elements using object-based image analysis. Geomorphology 81:330–344. doi: 10.1016/j.geomorph.2006.04.013

Dramis F, Guida D, Cestari A (2011) Nature and Aims of Geomorphological Mapping. In: Smith MJ, Paron P, Griffiths JS (eds) Geomorphological Mapping: methods and applications. Elsevier

Dufresne A, Bösmeier A, Prager C (2016) Sedimentology of rock avalanche deposits – Case study and review. Earth-Science Rev 163:234–259. doi: 10.1016/j.earscirev.2016.10.002

Egenhofer MJ, Frank AU (1992) Object-Oriented Modeling for GIS. URISA J 4:3–19. doi: 10.1.1.16.887

Egenhofer MJ, Frank AU (1987) Object-Oriented Databases: Database Requirements for GIS. In: International Geographic Information systems (IGIS) Symposium: The Research Agenda, Arlington, Virginia, USA, 15-18 November, 1987. pp 15–18

Egenhofer MJ, Franzosa RD (1991) Point-set topological spatial relations. Int J Geogr Inf Syst 5:161–174. doi: 10.1080/02693799108927841

Egenhofer MJ, Herring JR (1990a) A mathematical framework for the definition of topological relationship. In: Proceedings of Fourth International Symposium on Spatial Data Handling, Zurich, Switzerland (1990). pp 803–813

Egenhofer MJ, Herring JR (1990b) Categorizing binary topological relations between regions, lines, and points in geographic databases. The 1–28

Eisank C, Drăguţ L, Blaschke T (2011) A generic procedure for semantics-oriented landform classification using object-based image analysis. Geomorphometry 125–128

Esposito G, Salvini R, Matano F, et al (2017) Multitemporal monitoring of a coastal landslide through SFM-derived point cloud comparison. Photogramm Rec 32:459–479. doi: 10.1111/phor.12218

ESRI (2019) Topology in ArcGIS. http://desktop.arcgis.com/en/arcmap/latest/manage-data/topologies/topology-in-arcgis.htm. Accessed 20 Feb 2019

Evans SG, Bent AL (2004) The Las Colinas landslide, Santa Tecla: A highly destructive flowslide triggered by the January 13, 2001, El Salvador earthquake. Spec Pap Geol Soc Am 375:25–37. doi: 10.1130/0-8137-2375-2.25

Evans SG, Guthrie RH, Roberts NJ, Bishop NF (2007) The disastrous 17 February 2006 rockslide-debris avalanche on Leyte Island, Philippines: A catastrophic landslide in tropical mountain terrain. Nat Hazards Earth Syst Sci 7:89–101. doi: 10.5194/nhess-7-89-2007

Feizizadeh B, Blaschke T (2013) A semi-automated object based image analysis approach for landslide delineation. 2013 Eur Sp agency living planet Symp 2013:9–13. doi: 10.1016/j.geomorph.2006.09.023

Fernández T, Jimenéz J, Fernández P, et al (2008) Automatic detection of landslide features with remote sensing techniques in the beltic cordilleras (Granada, southern Spain). Int Arch Photogramm Remote Sens Spat Inf Sci XXXVII:351–356

Fiorillo F, Guadagno FM, Aquino S, De Blasio A (2001) The December 1999 Cervinara landslides: further debris flows in the pyroclastic deposits of Campania (southern Italy). Bull Eng Geol Environ 60:171–184. doi: 10.1007/s100640000093

Fonseca FT, Egenhofer MJ (1999) Ontology-Driven Geographic Information Systems. In: 7th ACM Symposium on Advances in Geographic Information System. p 7

Froude MJ, Petley DN (2018) Global fatal landslide occurrence from 2004 to 2016. Nat Hazards Earth Syst Sci 18:2161–2181. doi: 10.5194/nhess-18-2161-2018

Gattinoni P, Scesi L, Arieni L, Canavesi M (2012) The February 2010 large landslide at Maierato, Vibo Valentia, Southern Italy. Landslides 9:255–261. doi: 10.1007/s10346-011-0296-2

Genevois R, Tecca PR (2013) The Vajont Landslide: State-of-the-Art. Ital J Eng Geol Environ 15–40. doi: 10.4408/IJEGE.2013-06.B-02

Ghongade RS, Pursani PJ (2014) Comparison of Relational Database and Object Oriented Database. Int J Mod Trends Eng Res 1:27–33

Glover E, Pennock DM, Lawrence S, Krovetz R (2002) Inferring hierarchical descriptions. Int Conf Inf Knowl Manag Proc 507–514

Graziano G vito (2016) Studio geologico – geomorfologico e idrogeologico del versante in frana al km 57+500 della A19 Palermo – Catania

Greco G (2016) Roscigno: tra la città rudere e i ruderi del Parco Archeologico del Monte Pruno. Territ della Cult 23:24–39

Gröger G, Reuter M, Plümer L (2004) Representation of a 3-D City Model in Spatial Object-Relational Databases. In: Proceedings of the 20th Congress of International Society for Photogrammetry and Remote Sensing, Istanbul, Turkey. 2004. p 6

Gruber FE, Baruck J, Geitner C (2017) Algorithms vs. surveyors: A comparison of automated landform delineations and surveyed topographic positions from soil mapping in an Alpine environment. Geoderma 308:9–25. doi: 10.1016/j.geoderma.2017.08.017

Guerricchio A, Fortunato G, Guglielmo EA, et al (2010) Condizionamenti idrogeologici e da DGPV nell'attivazione della grande frana di Maierato (VV) del 2010. Tec per la Dif dall'inquinamento 31:1–58

Guerricchio A, Melicoro G, Panaro V (2000) Deformazioni gravitative dei versanti nel territorio comunale di Torve (Basilicata). Boll della Soc Geol Ital 119:613–622

Guida D, Cestari A, Cuomo A, et al (2015) The Salerno University Geomorphological Informative Mapping System: the Licosa polygenetic case study (Cilento European geopark, southern Italy). Geomorphometry 53–56

Guida D, Guida M, Perriello Zampelli S, et al (1987) Deformazioni gravitative al margine di morfostrutture carbonatiche: un esempio nel Monte Bulgheria (Campania). Mem della Soc Geol Ital 37:363–373

Guida D, Iaccarino G, Lanzara R, Peduto F (1995) Proposta di classificazione tassonomica dei fenomeni franosi. In: Giornate poster sulle ricerche del Gruppo Geomineralogico, V Conferenza Scientifica Annuale del Dipartimento di Scienze della Terra, Univ. "Federico II", Napoli

Guida D, Iaccarino G, Perrone V (1988) Nuovi dati sulla successione del flysch del cilento nell'area di Monte Centaurino: relazioni tra unità litostratigrafiche, unità litotecniche e principali sistemi franosi. Mem della Soc Geol Ital 41:299–310

Guida D, Nocera N, Siervo V (2006) Analisi morfoevolutiva sulla riattivazione di sistemi franosi a cinematismo intermittente in Appennino campano-lucano (Italia meridionale). G Di Geol Appl 3:114–122. doi: 10.1474/GGA.2006-03.0-15.0108

Guida D, Siervo V, Cestari A, Palmieri V (2012) Application of " GmIS _ Unisa " geomorphological mapping system to regional planning . Rend Online Soc Geol Ital 21:1155–1157

Guilbert E, Moulin B (2017) Towards a Common Framework for the Identification of Landforms on

Terrain Models. ISPRS Int J Geo-Information 6:12. doi: 10.3390/ijgi6010012

Guilbert E, Moulin B, Cortés Murcia A (2016) a Conceptual Model for the Representation of Landforms Using Ontology Design Patterns. ISPRS Ann Photogramm Remote Sens Spat Inf Sci III–2:15–22. doi: 10.5194/isprsannals-III-2-15-2016

Gustavsson M, Kolstrup E (2009) New geomorphological mapping system used at different scales in a Swedish glaciated area. Geomorphology 110:37–44. doi: 10.1016/j.geomorph.2008.12.022

Gustavsson M, Kolstrup E, Seijmonsbergen AC (Harry) (2006) A new symbol-and-GIS based detailed geomorphological mapping system: Renewal of a scientific discipline for understanding landscape development. Geomorphology 77:90–111. doi: 10.1016/j.geomorph.2006.01.026

Gustavsson M, Seijmonsbergen AC (Harry), Kolstrup E (2008) Structure and contents of a new geomorphological GIS database linked to a geomorphological map - With an example from Liden, central Sweden. Geomorphology 95:335–349. doi: 10.1016/j.geomorph.2007.06.014

Gutierrez C, Hurtado CA, Vaisman A (2007) Introducing time into RDF. IEEE Trans Knowl Data Eng 19:207–218. doi: 10.1109/TKDE.2007.34

Guzzetti F (2006) Landslide hazard and risk assessment

Guzzetti F, Carrara A, Cardinali M, Reichenbach P (1999) Landslide hazard evaluation: a review of current techniques and their application in a multi-scale study, Central Italy. Geomorphology 31:181–216. doi: 10.1016/S0169-555X(99)00078-1

Guzzetti F, Mondini AC, Cardinali M, et al (2012) Landslide inventory maps: New tools for an old problem. Earth-Science Rev 112:42–66. doi: 10.1016/j.earscirev.2012.02.001

Haigh MJ, Rawat JS, Bartarya SK, Rawat MS (1993) Environmental influences on landslide activity: Almora Bypass, Kumaun Lesser Himalaya. Nat Hazards 8:153–170. doi: 10.1007/BF00605439

Hay GJ, Castilla G (2008) Geographic Object-Based Image Analysis (GEOBIA): A new name for a new discipline. In: Blaschke T, Lang S, Hay GJ (eds) Object-Based Image Analysis. Springer, pp 75–89

Heywood I, Cornelius S, Carver S (2006) An introduction to geographical information systems, 3rd edn. Pearson

Holmevik JR (1994) Compiling SIMULA: A Historical Study of Technological Genesis. IEEE Ann Hist Comput 16:25–37

Holt P (2007) Development of an Object-Oriented GIS for Maritime Archaeology - Motivation, Implementation and Results. www.3HConsulting.com 8

Hu Y, Miller HJ, Li X (2014) Detecting and Analyzing Mobility Hotspots using Surface Networks. Trans GIS 18:911–935. doi: 10.1111/tgis.12076

Hungr O, Leroueil S, Picarelli L (2014) The Varnes classification of landslide types, an update. Landslides 11:167–194. doi: 10.1007/s10346-013-0436-y

ISPRA (2018) Aggiornamento ed integrazioni delle linee guida della Carta Geomorfologica d'Italia alla scala 1:50.000. Quad. Ser. III 13:95

Jenness J (2006) Topographic Position Index (tpi_jen.avx) Extension for ArcView 3.x, v. 1.3a

Khaddaj S, Adamu A, Morad M (2005) Construction of an Integrated Object Oriented System for Temporal GIS. Am J Appl Sci 2:1584–1594

Kindler E, Krivy I (2011) Object-oriented simulation of systems with sophisticated control. Int J Gen Syst 40:313–343. doi: 10.1080/03081079.2010.539975

Kiran Kumar BVSSD, Sinha P, Bhatt PCP (1996) DO-GIS - a distributed and object oriented GIS. Proc 7th Int Symp Spat data Handl Adv GIS Res II, 12-16 august 1996, Delft, Netherlands Vol 1 SDH '96 37–49

Klose M (2015) Landslide Databases as Tool for Integreted Assessment of Landslide Risk

Kösters G, Pagel B-U, Six H-W (1996) GeoOOA: Object-Oriented Analysis for Geographic Information Systems. IEEE Int Conf Requir Eng 245–253

Kösters G, Pagel BU, Six H-W (1997) GIS-application development with GEOOOA. Int J Geogr Inf Sci 11:307–335. doi: 10.1080/136588197242293

Kriticos T, Robinson TR, Davies TRH (2015) Regional coseismic landslide hazard assessment without historical landslide inventories: A new approach. J Geophys Res Earth Surf 120:711–729

Lee EM, Hall JM, Meadowcroft IC (2001) Coastal cliff recession : the use of probabilistic prediction methods. Geomorphology 40:239–269

Lewis J, Loftus W (2015) Java Software Solutions - Foundations of Program Design. Pearson

Li X, Myint SW, Zhang Y, et al (2014) Object-based land-cover classification for metropolitan Phoenix, Arizona, using aerial photography. Int J Appl Earth Obs Geoinf 33:321–330. doi: 10.1016/j.jag.2014.04.018

Louw G, van Niekerk A (2019) Object-based land surface segmentation scale optimisation: An ill-structured problem. Geomorphology 327:377–384. doi: 10.1016/j.geomorph.2018.11.021

Löwner MO (2013) 3D topological relationships of landforms and their spatial schema-based representation. Geo-Spatial Inf Sci 16:238–246. doi: 10.1080/10095020.2013.866616

Luo W, Liu C-C (2018) Innovative landslide susceptibility mapping supported by geomorphon and geographical detector methods. Landslides 15:465–474. doi: 10.1007/s10346-017-0893-9

Lupiano V, Rago V, Terranova OG, Iovine G (2019) Landslide inventory and main geomorphological features affecting slope stability in the Picentino river basin (Campania, southern Italy). J Maps 5647:. doi: 10.1080/17445647.2018.1563836

Maiorano RMS, Russo G, Viggiani C (2014) A landslide in stiff, intact clay. Acta Geotech 9:817–829. doi: 10.1007/s11440-013-0249-0

Malinowski E, Zimányi E (2004) OLAP Hierarchies: A conceptual perspective. Lect Notes Comput Sci 3084:477–491

Marinos V, Stoumpos G, Papazachos C (2019) Landslide Hazard and Risk Assessment for a Natural Gas Pipeline Project: The Case of the Trans Adriatic Pipeline, Albania Section. Geosciences 9:61. doi: 10.3390/geosciences9020061

Martelli L (2002) foglio 265 - BAGNO DI ROMAGNA. NOTE Illus. della Cart. Geol. D'ITALIA alla scala 150.000 108

Martino S (2017) Earthquake-induced landslides in Italy: from the distribution of effects to the hazard mapping. Ital J Eng Geol Environ 1:53–67. doi: 10.4408/IJEGE.2017-01.O-04

Mazzanti P, Bozzano F, Brunetti A, et al (2017) Experimental Landslide Monitoring Site of Poggio Baldi Landslide (Santa Sofia, N-Appennine, Italy). In: Mikoš M, Arbanas Ž, Yin Y, Sassa K (eds) Advancing Culture of Living with Landslides. Springer, pp 259–266

Mezaal MR, Pradhan B (2018) An improved algorithm for identifying shallow and deep-seated landslides in dense tropical forest from airborne laser scanning data. Catena 167:147–159. doi: 10.1016/j.catena.2018.04.038

Miccadei E, Orrù P, Piacentini T, et al (2012) Geomorphological map of the Tremiti Islands (Puglia, Southern Adriatic Sea, Italy), scale 1:15,000. J Maps 8:74–87. doi: 10.1080/17445647.2012.668765

Montgomery DR, Foufoula-Georgiou E (1993) Channel Network Source Representation Using Digital Elevation Models. Water Resour Res 29:3925–3934. doi: 10.1029/93WR02463

Moosavi V, Talebi A, Shirmohammadi B (2014) Producing a landslide inventory map using pixel-based and object-oriented approaches optimized by Taguchi method. Geomorphology 204:646–656. doi: 10.1016/j.geomorph.2013.09.012

Morelli S, Pazzi V, Frodella W, Fanti R (2018) Kinematic Reconstruction of a Deep-Seated Gravitational Slope Deformation by Geomorphic Analyses. Geosciences 8:26. doi: 10.3390/geosciences8010026

Mostardini F, Merlini S (1986) Appennino Centro-Meridionale - Sezioni Geologiche e Proposta di Modello Strutturale. Mem. della Soc. Geol. Ital. 35:177–202

Murillo-García FG, Alcántara-Ayala I, Ardizzone F, et al (2015) Satellite stereoscopic pair images of very high resolution: a step forward for the development of landslide inventories. Landslides 12:277–291. doi: 10.1007/s10346-014-0473-1

Napolitano E, Marchesini I, Salvati P, et al (2018) LAND-deFeND – An innovative database structure for landslides and floods and their consequences. J Environ Manage 207:203–218. doi: 10.1016/j.jenvman.2017.11.022

Nebel B, Bürckert HJ (1995) Reasoning About Temporal Relations: A Maximal Tractable Subclass of Allen's Interval Algebra. J ACM 42:43–66. doi: 10.1145/200836.200848

Niethammer U, James MR, Rothmund S, et al (2012) UAV-based remote sensing of the Super-Sauze landslide : Evaluation and results. Eng Geol 128:2–11

Odum EP, Barrett GW (2005) Fundamentals of Ecology, Fifth

Oracle® (2019) Oracle Database 19c Documentation. Manuals

Pankow KL, Moore JR, Mark Hale J, et al (2014) Massive landslide at Utah copper mine generates wealth of geophysical data. GSA Today 24:4–9. doi: 10.1130/GSATG191A.1

Parise M (1994) Il Rilevamento Geomorfologico a Grande Scala Nell'Interpretazione Della Cinematica Dei Movimenti Gravitativi. Geol Rom 30:273–282

Parise M (2003) Observation of surface features on an active landslide , and implications for understanding its history of movement. Nat Hazards Earth Syst Sci 3:569–580

Paron P, Vargas R (2007) Landform of selected study areas in Somaliland and Southern Somalia. Integrated Landform Mapping Approach at semi-detailed scale using Remote Sensing and GIS techniques

Petley DN (2012) Global patterns of loss of life from landslides. Geology 40:927–930. doi: 10.1130/G33217.1

Peuquet DJ, Duan N (1995) An event-based spatiotemporal data model (ESTDM) for temporal analysis of geographical data. Int J Geogr Inf Syst 9:7–24. doi: 10.1080/02693799508902022

Pfaltz JL (1976) Surface Networks. Geogr Anal 8:77–93. doi: 10.1111/j.1538-4632.1976.tb00530.x

Phillips D (2018) Python 3 Object-Oriented Programming, 3rd edn. Packt

Piacentini D, Troiani F, Soldati M, et al (2012) Statistical analysis for assessing shallow-landslide susceptibility in South Tyrol (south-eastern Alps, Italy). Geomorphology 151–152:196–206. doi: 10.1016/j.geomorph.2012.02.003

Posada N, Sol D (2000) Object oriented database for a GIS. In: Brebbia CA, Pascolo P (eds) Management Information System. WIT Press

Powers DMW (2007) Evaluation: From Precision, Recall and F-Factor to ROC, Informedness, Markedness & Correlation. Tech Rep SIE

Putignano ML, Schiattarella M (2008) Struttura , esumazione ed evoluzione morfologica del nucleo mesozoico del Monte Motola (Cilento , Italia meridionale). Boll della Soc Geol Ital 127:477–493

Rana SS (2004) Surface Networks : New techniques for their automated extraction , generalisation and application

Rana SS (2000) Experiments on generalization and visualization of surface metworks. UCL Cent Adv Spat Anal - Work Pap Ser

Randell DA, Cui Z, Cohn AG (1992) A Spatial Logic based on Regions and Connection. In: 3rd Int. conf. on Knowledge Representation and Reasoning, Morgan Kaufmann, 1992. p 12

Reichenbach P, Rossi M, Malamud BD, et al (2018) A review of statistically-based landslide susceptibility models. Earth-Science Rev 180:60–91. doi: 10.1016/j.earscirev.2018.03.001

Ricci Lucchi F (1981) The Miocene Marnoso-Arenacea turbidites, Romagna and Umbria Apennines. In: Excursion guidebook, 2nd European regional meeting. International association of sedimentology, Bologna. pp 229–303

Roback K, Clark MK, West AJ, et al (2018) The size, distribution, and mobility of landslides caused by the 2015 M w 7.8 Gorkha earthquake, Nepal. Geomorphology 301:121–138. doi: 10.1016/j.geomorph.2017.01.030

Rocca L, Jenny B, Puppo E (2017) A continuous scale-space method for the automated placement of spot heights on maps. Comput Geosci 109:216–227. doi: 10.1016/j.cageo.2017.09.003

Romeo S, Kieffer DS, Di Matteo L (2014) The ingelsberg landslide (Bad Hofgastein, Austria): Description and first results of monitoring system (GBInSAR technique). Rend Online Soc Geol

Ital 32:24–27. doi: 10.3301/ROL.2014.144

Sahner J, Weber B, Prohaska S, Lamecker H (2008) Extraction of feature lines on surface meshes based on discrete morse theory. Comput Graph Forum 27:735–742. doi: 10.1111/j.1467-8659.2008.01202.x

Samia J, Temme A, Bregt A, et al (2017a) Do landslides follow landslides? Insights in path dependency from a multi-temporal landslide inventory. Landslides 14:547–558. doi: 10.1007/s10346-016-0739-x

Samia J, Temme A, Bregt A, et al (2017b) Characterization and quantification of path dependency in landslide susceptibility. Geomorphology 292:16–24. doi: 10.1016/j.geomorph.2017.04.039

Schädler W, Borgatti L, Corsini A, et al (2015) Geomechanical assessment of the Corvara earthflow through numerical modelling and inverse analysis. Landslides 12:495–510. doi: 10.1007/s10346-014-0498-5

Schneider B (2003) Surface Networks: Extension of the Topology and Extraction from Bilinear Surface Patches. In: Proceedings of the 7th International Conference on Geocomputation

Senin N, Blunt LA, Leach RK, Pini S (2013) Morphologic segmentation algorithms for extracting individual surface features from areal surface topography maps. Surf Topogr Metrol Prop 1:1–11. doi: 10.1088/2051-672X/1/1/015005

SGN (1994) Carta Geomorfologica d'Italia - 1:50.000 - Guida al rilevamento. Quad. Ser. III 4:42

Shahrabi BA, Kainz W (1993) An Implantation Approach for Object-oriented Topographic Databases using Standard Tools. In: Auto-Carto 11 Proceedings. Eleventh International Symposium on Computer-Assisted Cartography. Oct 30 to Nov 1, 1993, Minneapolis, Minnesota. pp 103–112

Simon HA (1962) The Architecture of Complexity. Proc Am Philos Soc 106:467–482. doi: 10.1080/02841850903061437

Singh L, Scheuermann P, Chen B (1997) Generationg Association Rules from Semi-Structured Documents Using an Extended Concept Hierarchy. In: Conference on Information and Knowledge Management. pp 193–200

Sinistra Sele River Basin Authority (2012) Sinistra Sele River Basin Plan. PAI

Smaavik TF, Heyerdahl H (2016) The Refne landslide , Halden , Norway : case history and use of risk assessment. Proc 17th Nord Geotech Meet Challenges Nord Geotech 25th-28th May

Stefanini MC (2004) Spatio-temporal analysis of a complex landslide in the Northern Apennines (Italy) by means of dendrochronology. Geomorphology 63:191–202. doi: 10.1016/j.geomorph.2004.04.003

Tagil S, Jenness J (2008) GIS-based automated landform classification and topographic, landcover and geologic attributes of landforms around the Yazoren Polje, Turkey. J. Appl. Sci. 8:910–921

The PostgreSQL GDG (2019) PostgreSQL 11 Documentation. Manuals 3509

Torreggiani PL (2009) Studio geologico-geotecnico della frana di Corniolo, Comune di S.Sofia (FC). Geol dell' EMILIA ROMAGNA 36:39–47

Tschan AP (1999) An Introduction to Object-Oriented GIS in Archaeology. CAA1998 New Tech Old

Times Comput Appl Quant Methods Archaeol Proc 26th Conf Barcelona, March 1998 (BAR Int Ser 757) 303–316

Tseng CM, Lin CW, Dalla Fontana G, Tarolli P (2015) The topographic signature of a major typhoon. Earth Surf Process Landforms 40:1129–1136. doi: 10.1002/esp.3708

Tsichritzis DC, Lochovsky FH (1976) Hierarchical Data-Base Management: A Survey. ACM Comput Surv 8:105–123. doi: 10.1145/356662.356667

Uzielli M, Catani F, Tofani V, Casagli N (2015a) Risk analysis for the Ancona landslide II: estimation of risk to buildings. Landslides 12:83–100. doi: 10.1007/s10346-014-0477-x

Uzielli M, Catani F, Tofani V, Casagli N (2015b) Risk analysis for the Ancona landslide I: characterization of landslide kinematics. Landslides 12:69–82. doi: 10.1007/s10346-014-0474-0

Valiante M, Bozzano F, Guida D (2016) The Sant'Andrea-Molinello landslide system (Mt. Pruno, Roscigno, Italy). Rend Online Soc Geol Ital 41:214–217. doi: 10.3301/ROL.2016.132

Van Beek P, Manchak DW (1996) The design and experimental analysis of algorithms for temporal reasoning. J Artif Intell Res 4:1–18

Van Den Eeckhaut M, Kerle N, Poesen J, Hervás J (2012) Object-oriented identification of forested landslides with derivatives of single pulse LiDAR data. Geomorphology 173–174:30–42. doi: 10.1016/j.geomorph.2012.05.024

Van Westen CJ, Rengers N, Soeters R (2003) Use of Geomorphological Information in Indirect Landslide Susceptibility Assessment. Nat Hazards 30:399–419. doi: 10.1023/B

Varnes DJ (1978) Slope Movement Types and Processes. In: Landslides Analysis and Control - Special Report 176. pp 11–33

Vergari F, Troiani F, Faulkner H, et al (2019) The use of the slope–area function to analyse process domains in complex badland landscapes. Earth Surf Process Landforms 44:273–286. doi: 10.1002/esp.4496

Vitale S, Ciarcia S (2018) Tectono-stratigraphic setting of the Campania region (Southern Italy). J Maps 14:9–21. doi: 10.1080/17445647.2018.1424655

Vitale S, Ciarcia S, Mazzoli S, et al (2010) Structural analysis of the "Internal" Units of Cilento, Italy: New constraints on the Miocene tectonic evolution of the southern Apennine accretionary wedge. Comptes Rendus - Geosci 342:475–482. doi: 10.1016/j.crte.2010.03.005

Vitale S, Ciarcia S, Mazzoli S, Zaghloul MN (2011) Tectonic evolution of the "Liguride" accretionary wedge in the Cilento area, southern Italy: A record of early Apennine geodynamics. J Geodyn 51:25–36. doi: 10.1016/j.jog.2010.06.002

Vitale S, Ciarcia S, Tramparulo FDA (2013) Deformation and stratigraphic evolution of the Ligurian Accretionary Complex in the southern Apennines (Italy). J Geodyn 66:120–133. doi: 10.1016/j.jog.2013.02.008

Wang W, Li W, Zhang C, Zhang W (2018a) Improving Object-Based Land Use/Cover Classification from Medium Resolution Imagery by Markov Chain Geostatistical Post-Classification. Land 7:31. doi: 10.3390/land7010031

Wang YF, Cheng QG, Lin QW, et al (2018b) Insights into the kinematics and dynamics of the Luanshibao rock avalanche (Tibetan Plateau, China) based on its complex surface landforms. Geomorphology 317:170–183. doi: 10.1016/j.geomorph.2018.05.025

Weiss AD (2001) Topographic position and landforms analysis. In: ESRI User Conference, San Diego, CA

Wezel FC (1970) Geologia del Flysch Numidico della Sicilia nord-orientale. Mem della Soc Geol Ital 9:225–280

Wolf GW (1991) Characterization of functions representing topographic surfaces. Proc Autocarto 10 186–204

Wolf GW (2017) Scale independent surface characterisation: Geography meets precision surface metrology. Precis Eng 49:456–480. doi: 10.1016/j.precisioneng.2016.12.005

Worboys MF (1994) Object-oriented approaches to geo-referenced information. Int J Geogr Inf Syst 8:385–399. doi: 10.1080/02693799408902008

Worboys MF, Hearnshaw HM, Maguire DJ (1990) Object-oriented data modelling for spatial databases. Int J Geogr Inf Syst 4:369–383. doi: 10.1080/02693799008941553

Worboys MF, Hornsby K (2004) From Objects to Events: GEM, the Geospatial Event Model. In: Egenhofer MJ, Freksa C, Miller HJ (eds) Geographic Information Science - Third International conference, GIScience 2004 - Adelphi, MD, USA, October 2004 - Prooceedings. Springer, pp 327–343

Wu J (2013) Hierarchy Theory : An Overview. In: Rozzi R, Pickett S, Palmer C, et al. (eds) Linking Ecology and Ethics for a Changing World: Values, Philosohpy, and Actions, Ecology and Ethics

Wu J (1999) Hierarchy and Scaling: Extrapolating Information Along a Scaling Ladder. Can J Remote Sens 5:367–380

Yesilnacar E, Topal T (2005) Landslide susceptibility mapping: A comparison of logistic regression and neural networks methods in a medium scale study, Hendek region (Turkey). Eng Geol 79:251–266. doi: 10.1016/j.enggeo.2005.02.002

Yuan M (2008) Temporal GIS and Applications. Encycl. GIS 1307

Zhou W, Huang G, Troy A, Cadenasso ML (2009) Object-based land cover classification of shaded areas in high spatial resolution imagery of urban areas: A comparison study. Remote Sens Environ 113:1769–1777. doi: 10.1016/j.rse.2009.04.007

Zuosheng Y, Weimin C, Zhangrong C, et al (1994) Subaqueous landslide system in the Huanghe river (Yellow river) delta. Oceanol. Limnol. Sin. 6:573

Appendix

This appendix contains all the codes I developed through my research. First, a custom plugin for Grass GIS written in python, for the computation of Topographic Position Index, then, the SQL code used to structure the PostgreSQL DB used for this work will be presented.

Topographic Position Index (TPI) plugin for Grass GIS
Input parameters:

- Elevation raster, required;
- Neighbourhood size, expressed in cell, it's the size of the moving window, required;

Flags:

- -r: if checked, automatically aligns the Grass computational region to the input elevation raster;
- -d: if checked, the plugin will compute also the Deviation from Mean Elevation;
- -s: if checked, the plugin will compute also the standardized TPI;
- -l: if checked, the plugin automatically reclassifies the Topographic Position Index raster into Slope Positions

```
#!/usr/bin/env python
# -*- coding: utf-8 -*-

#%module
#% description: Topographic Position Index
#% label: TPI
#% keyword: raster
#% keyword: elevation
#%end

#%option G_OPT_R_ELEV
#% key: dtm
#% key_desc: elevation
#% label: elevation
#% description: Elevation data (!!!remove @mapset!!!)
#% required: yes
#%end

#%option
#% key: neighborhood
#% key_desc: neighborhood
#% label: neighborhood
#% description: Size of the moving window
#% type: integer
#% required: yes
#%end

#%flag
#% key: r
#% description: Set the current region to match input raster size and resolution
#% label: Align region to inpur raster
#%end

#%flag
#% key: d
```

```
#% description: Compute also Deviation from Mean Elevation
#% label: Compute DEV
#%end

#%flag
#% key: s
#% description: Compute also standardized Topographic Position Index
#% label: Compute standardized TPI
#%end

#%flag
#% key: l
#% description: Compute also slope position classification
#% label: Compute slope position raster
#%end


import sys
import os
import grass.script as grass

# check if you are using this script in Grass GIS
if 'GISBASE' not in os.environ:
    grass.message('You must be in GRASS GIS to run this program.')
    sys.exit(1)


def main():
    dtm = options['dtm']
    neigh = int(options['neighborhood'])
    radius = int((neigh-1)/2)
    region = flags['r']
    dev = flags['d']
    stand = flags['s']
    land = flags['l']
    if region:
        grass.use_temp_region()
        grass.run_command(
            'g.region',
            flags='a',
            raster=dtm,
            align=dtm)
        grass.message('region aligned')
    grass.message('neighbourhood radius: %s cells' % radius)
    grass.message('computing neighbors average...')
    grass.run_command(
        'r.neighbors',
        flags='c',
        overwrite=True,
        input=dtm,
        output='__temp__%s_avg_%05dc' % (dtm, radius),
        method='average',
        size=neigh)
    grass.message('tping...')
    grass.mapcalc(
        '{a} = int((("{b}" - {c}) + 0.5)'.format(
            a='%s_tpi_%05dc' % (dtm, radius),
            b=dtm,
            c='__temp__%s_avg_%05dc' % (dtm, radius)),
        overwrite=True)
    stat = grass.parse_command(
        'r.univar',
```

```python
        flags='g',
        map='%s_tpi_%05dc' % (dtm, radius))
    mean = float(stat['mean'])
    std = float(stat['stddev'])
    colorscale_tpi = open(os.environ['TMPDIR']+'/colorscale_tpi.txt', 'w+r')
    colorscale_tpi.write('%(min)s 0:0:255\n0 255:255:128\n%(max)s 255:0:0\nnv
255:255:255\ndefault 255:255:255' % stat)
    colorscale_tpi.close()
    grass.run_command(
        'r.colors',
        quiet=True,
        map='%s_tpi_%05dc' % (dtm, radius),
        rules=os.environ['TMPDIR']+'/colorscale_tpi.txt')
    if dev:
        grass.message('computing neighbors standard deviation...')
        grass.run_command(
            'r.neighbors',
            flags='c',
            overwrite=True,
            input=dtm,
            output='__temp__%s_std_%05dc' % (dtm, radius),
            method='stddev',
            size=neigh)
        grass.message('deving...')
        grass.mapcalc(
            '{a} = ({b} - {c}) / {d}'.format(
                a='%s_dev_%05dc' % (dtm, radius),
                b=dtm,
                c='__temp__%s_avg_%05dc' % (dtm, radius),
                d='__temp__%s_std_%05dc' % (dtm, radius)),
            overwrite=True)
    if land:
        stand = True
    if stand:
        grass.message('computing standardized tpi...')
        grass.mapcalc(
            '{a} = int((((({b} - {c}) / {d}) * 100) + 0.5)'.format(
                a='%s_std_tpi_%05dc' % (dtm, radius),
                b='%s_tpi_%05dc' % (dtm, radius),
                c=mean,
                d=std),
            overwrite=True)


def cleanup():
    grass.message('cleaning temp files...')
    grass.run_command(
        'g.remove',
        flags='fb',
        quiet=True,
        type='raster',
        pattern='__temp__*')
    grass.message('done')


if __name__ == "__main__":
    options, flags = grass.parser()
    main()
    cleanup()
```

Database SQL code

This is the SQL code need to reproduce the PostgreSQL database used for this research.

```
CREATE DATABASE loom
    WITH
    OWNER = postgres
;

CREATE EXTENSION postgis;

CREATE SCHEMA dictionaries;

CREATE TABLE dictionaries.material_types (
  material_type TEXT PRIMARY KEY
);

/*
+-----------------+
| material_type   |
|-----------------|
| rock            |
| ice             |
| soil            |
+-----------------+
*/

CREATE TABLE dictionaries.materials (
  material_type TEXT REFERENCES dictionaries.material_types(material_type),
  material TEXT PRIMARY KEY
);

/*
+-----------------+------------+
| material_type   | material   |
|-----------------+------------|
| rock            | rock       |
| ice             | ice        |
| soil            | clay       |
| soil            | silt       |
| soil            | sand       |
| soil            | gravel     |
| soil            | debris     |
| soil            | boulders   |
| soil            | soil       |
| soil            | peat       |
+-----------------+------------+
*/


CREATE TABLE dictionaries.movement_types (
  movement_type TEXT PRIMARY KEY
);

/*
+-------------------+
| movement_type     |
|-------------------|
| fall              |
| topple            |
| slide             |
| spread            |
| flow              |
| slope deformation |
+-------------------+
*/

CREATE TABLE dictionaries.landslide_types (
```

```
  material_type TEXT REFERENCES dictionaries.material_types(material_type),
  material TEXT REFERENCES dictionaries.materials(material),
  movement_type TEXT REFERENCES dictionaries.movement_types(movement_type),
  landslide_type TEXT PRIMARY KEY
);

/*
+-----------------+-----------+------------------+---------------------------+
| material_type   | material  | movement_type    | landslide_type            |
|-----------------+-----------+------------------+---------------------------|     | rock
| rock      | fall             | rock fall          |
| ice             | ice       | fall             | ice fall                  |
| soil            | boulders  | fall             | boulder fall              |
| soil            | debris    | fall             | debris fall               |
| soil            | silt      | fall             | silt fall                 |
| rock            | rock      | topple           | rock block topple         |
| rock            | rock      | topple           | rock flexural topple      |
| soil            | gravel    | topple           | gravel topple             |
| soil            | sand      | topple           | sand topple               |
| soil            | silt      | topple           | silt topple               |
| rock            | rock      | slide            | rock rotational slide     |
| rock            | rock      | slide            | rock planar slide         |
| rock            | rock      | slide            | rock wedge slide          |
| rock            | rock      | slide            | rock compound slide       |
| rock            | rock      | slide            | rock irregular slide      |
| soil            | clay      | slide            | clay rotational slide     |
| soil            | silt      | slide            | silt rotational slide     |
| soil            | clay      | slide            | clay planar slide         |
| soil            | silt      | slide            | silt planar slide         |
| soil            | gravel    | slide            | gravel slide              |
| soil            | sand      | slide            | sand slide                |
| soil            | debris    | slide            | debris slide              |
| soil            | clay      | slide            | clay compound slide       |
| soil            | silt      | slide            | silt compound slide       |
| rock            | rock      | spread           | rock slope spread         |
| soil            | sand      | spread           | sand liquefaction spread  |
| soil            | silt      | spread           | silt liquefaction spread  |
| soil            | clay      | spread           | sensitive clay spread     |
| rock            | rock      | flow             | rock avalanche            |
| ice             | ice       | flow             | ice avalanche             |
| soil            | sand      | flow             | sand dry flow             |
| soil            | silt      | flow             | silt dry flow             |
| soil            | debris    | flow             | debris dry flow           |
| soil            | sand      | flow             | sand flowslide            |
| soil            | silt      | flow             | silt flowslide            |
| soil            | debris    | flow             | debris flowslide          |
| soil            | clay      | flow             | sensitive clay flowslide  |
| soil            | debris    | flow             | debris flow               |
| soil            | clay      | flow             | mud flow                  |
| soil            | debris    | flow             | debris flood              |
| soil            | debris    | flow             | debris avalanche          |
| soil            | soil      | flow             | earthflow                 |
| soil            | peat      | flow             | peat flow                 |
| rock            | rock      | slope deformation | mountain slope deformation |
| rock            | rock      | slope deformation | rock slope deformation    |
| soil            | soil      | slope deformation | soil slope deformation    |
| soil            | soil      | slope deformation | soil creep                |
| soil            | soil      | slope deformation | solifluction              |
+-----------------+-----------+------------------+---------------------------+
*/

CREATE TABLE dictionaries.regions_topologies (
  de9im_name TEXT NOT NULL,
  de9im_matrix TEXT NOT NULL,
  rcc8_name TEXT NOT NULL,
  rcc8_code TEXT NOT NULL
);

/*
+---------------------+---------------+------------------------------------+-------------+
| de9im_name          | de9im_matrix  | rcc8_name                          | rcc8_code   |
|---------------------+---------------+------------------------------------+-------------|
| intersect - equals  | 2FFF1FFF2     | equal                              | EQ          |
```

```
| disjoint             | FF2FF1212      | disconnected                     | DC       |
| intersect - touches  | FF2F01212      | externally connected             | EC       |
| intersect - touches  | FF2F11212      | externally connected             | EC       |
| intersect - contains | 212FF1FF2      | non-tangential proper part       | NTPP     |
| intersect - contains | 212F01FF2      | tangential proper part           | TPP      |
| intersect - contains | 212F11FF2      | tangential proper part           | TPP      |
| intersect - within   | 2FF1FF212      | non-tangential proper part inverse | iNTPP  |
| intersect - within   | 2FF10F212      | tangential proper part inverse   | iTPP     |
| intersect - within   | 2FF11F212      | tangential proper part inverse   | iTPP     |
| intersect - overlaps | 212101212      | partially overlapping            | PO       |
| intersect - overlaps | 212111212      | partially overlapping            | PO       |
+----------------------+----------------+----------------------------------+----------+
*/

CREATE TABLE dictionaries.temporal_predicates (
  predicate TEXT PRIMARY KEY
);


/*
+---------------+
| predicate     |
|---------------|
| before        |
| after         |
| meets         |
| met-by        |
| overlaps      |
| overlapped-by |
| during        |
| includes      |
| starts        |
| started-by    |
| finishes      |
| finished-by   |
| equals        |
+---------------+
*/

CREATE TABLE dictionaries.regions_st_topologies (
  rcc8_name TEXT NOT NULL,
  A_age TEXT REFERENCES dictionaries.temporal_predicates(predicate),
  B_age TEXT REFERENCES dictionaries.temporal_predicates(predicate),
  A_vs_B TEXT NOT NULL,
  B_vs_A TEXT NOT NULL
);


/*
+------------------------------------+--------+--------+----------------+----------------+
| rcc8_name                          | a_age  | b_age  | a_vs_b         | b_vs_a         |
|------------------------------------+--------+--------+----------------+----------------|
| partially overlapping              | before | after  | overlapped by  | overlaps       |
| partially overlapping              | after  | before | overlaps       | overlapped by  |
| tangential proper part             | before | after  | covered by     | covers         |
| tangential proper part             | after  | before | superimposed on | contains      |
| non-tangential proper part         | before | after  | covered by     | covers         |
| non-tangential proper part         | after  | before | superimposed on | contains      |
| tangential proper part inverse     | before | after  | contains       | superimposed on |
| tangential proper part inverse     | after  | before | covers         | covered by     |
| non-tangential proper part inverse | before | after  | contains       | superimposed on |
| non-tangential proper part inverse | after  | before | covers         | covered by     |
+------------------------------------+--------+--------+----------------+----------------+
*/

CREATE TABLE f0_landslide_objs (
  landslide_obj_id CHAR(7) NOT NULL CONSTRAINT lnsobjid_format CHECK
(landslide_obj_id SIMILAR TO 'LNS'||'_'||'[0-9]{3}'),
  event_id CHAR(3) NOT NULL CONSTRAINT evid_format CHECK (event_id SIMILAR TO
'[0-9]{3}'),
  landslide_event_id CHAR(11) PRIMARY KEY CONSTRAINT lnsevid_format CHECK
(landslide_event_id SIMILAR TO (landslide_obj_id)||'_'||(event_id)),
```

```sql
  overlap_index INT NOT NULL,
  mov_type_1 TEXT NOT NULL REFERENCES
dictionaries.landslide_types(landslide_type),
  mov_type_2 TEXT REFERENCES dictionaries.landslide_types(landslide_type),
  insert_time TIMESTAMPTZ DEFAULT now(),
  date DATE DEFAULT '1000-01-01',
  date_range_start DATE DEFAULT '1000-01-01',
  date_range_end DATE DEFAULT '1000-01-01',
  geom GEOMETRY(POLYGON, 4326)
);

-- objs sequences

CREATE SEQUENCE rf_id
AS INT;
CREATE SEQUENCE sf_id
AS INT;
CREATE SEQUENCE rt_id
AS INT;
CREATE SEQUENCE st_id
AS INT;
CREATE SEQUENCE rrs_id
AS INT;
CREATE SEQUENCE rps_id
AS INT;
CREATE SEQUENCE rws_id
AS INT;
CREATE SEQUENCE rcs_id
AS INT;
CREATE SEQUENCE ris_id
AS INT;
CREATE SEQUENCE srs_id
AS INT;
CREATE SEQUENCE sps_id
AS INT;
CREATE SEQUENCE scs_id
AS INT;
CREATE SEQUENCE rss_id
AS INT;
CREATE SEQUENCE gss_id
AS INT;
CREATE SEQUENCE css_id
AS INT;
CREATE SEQUENCE ra_id
AS INT;
CREATE SEQUENCE sdf_id
AS INT;
CREATE SEQUENCE gswf_id
AS INT;
CREATE SEQUENCE cswf_id
AS INT;
CREATE SEQUENCE dsd_id
AS INT;
CREATE SEQUENCE ssd_id
AS INT;

CREATE TABLE schema.f0_rf_objs (
  class TEXT DEFAULT 'rock fall',
  rf_oid TEXT PRIMARY KEY DEFAULT
'RF_'||to_char(nextval('schema.rf_id'::regclass), '000'),
  ) INHERITS (schema.f0_landslide_objs);
CREATE TABLE schema.f0_sf_objs (
```

```sql
  class TEXT DEFAULT 'soil fall',
  sf_oid TEXT PRIMARY KEY DEFAULT
'SF_'||to_char(nextval('schema.sf_id'::regclass), '000'),
  ) INHERITS (schema.f0_landslide_objs);
CREATE TABLE schema.f0_rt_objs (
  class TEXT DEFAULT 'rock topple',
  rt_oid TEXT PRIMARY KEY DEFAULT
'RT_'||to_char(nextval('schema.rt_id'::regclass), '000'),
  ) INHERITS (schema.f0_landslide_objs);
CREATE TABLE schema.f0_st_objs (
  class TEXT DEFAULT 'soil topple',
  st_oid TEXT PRIMARY KEY DEFAULT
'ST_'||to_char(nextval('schema.st_id'::regclass), '000'),
  ) INHERITS (schema.f0_landslide_objs);
CREATE TABLE schema.f0_rrs_objs (
  class TEXT DEFAULT 'rock rotational slide',
  rrs_oid TEXT PRIMARY KEY DEFAULT
'RRS_'||to_char(nextval('schema.rrs_id'::regclass), '000'),
  ) INHERITS (schema.f0_landslide_objs);
CREATE TABLE schema.f0_rps_objs (
  class TEXT DEFAULT 'rock planar slide',
  rps_oid TEXT PRIMARY KEY DEFAULT
'RPS_'||to_char(nextval('schema.rps_id'::regclass), '000'),
  ) INHERITS (schema.f0_landslide_objs);
CREATE TABLE schema.f0_rws_objs (
  class TEXT DEFAULT 'rock wedge slide',
  rws_oid TEXT PRIMARY KEY DEFAULT
'RWS_'||to_char(nextval('schema.rws_id'::regclass), '000'),
  ) INHERITS (schema.f0_landslide_objs);
CREATE TABLE schema.f0_rcs_objs (
  class TEXT DEFAULT 'rock compound slide',
  rcs_oid TEXT PRIMARY KEY DEFAULT
'RCS_'||to_char(nextval('schema.rcs_id'::regclass), '000'),
  ) INHERITS (schema.f0_landslide_objs);
CREATE TABLE schema.f0_ris_objs (
  class TEXT DEFAULT 'rock irregular slide',
  ris_oid TEXT PRIMARY KEY DEFAULT
'RIS_'||to_char(nextval('schema.ris_id'::regclass), '000'),
  ) INHERITS (schema.f0_landslide_objs);
CREATE TABLE schema.f0_srs_objs (
  class TEXT DEFAULT 'soil rotational slide',
  srs_oid TEXT PRIMARY KEY DEFAULT
'SRS_'||to_char(nextval('schema.srs_id'::regclass), '000'),
  ) INHERITS (schema.f0_landslide_objs);
CREATE TABLE schema.f0_sps_objs (
  class TEXT DEFAULT 'soil planar slide',
  sps_oid TEXT PRIMARY KEY DEFAULT
'SPS_'||to_char(nextval('schema.sps_id'::regclass), '000'),
  ) INHERITS (schema.f0_landslide_objs);
CREATE TABLE schema.f0_scs_objs (
  class TEXT DEFAULT 'soil compound slide',
  scs_oid TEXT PRIMARY KEY DEFAULT
'SCS_'||to_char(nextval('schema.scs_id'::regclass), '000'),
  ) INHERITS (schema.f0_landslide_objs);
CREATE TABLE schema.f0_rss_objs (
  class TEXT DEFAULT 'rock slope spread',
  rss_oid TEXT PRIMARY KEY DEFAULT
'RSS_'||to_char(nextval('schema.rss_id'::regclass), '000'),
  ) INHERITS (schema.f0_landslide_objs);
CREATE TABLE schema.f0_gss_objs (
  class TEXT DEFAULT 'granular soil spread',
```

```
  gss_oid TEXT PRIMARY KEY DEFAULT
'GSS_'||to_char(nextval('schema.gss_id'::regclass), '000'),
  ) INHERITS (schema.f0_landslide_objs);
CREATE TABLE schema.f0_css_objs (
  class TEXT DEFAULT 'cohesive soil spread',
  css_oid TEXT PRIMARY KEY DEFAULT
'CSS_'||to_char(nextval('schema.css_id'::regclass), '000'),
  ) INHERITS (schema.f0_landslide_objs);
CREATE TABLE schema.f0_ra_objs (
  class TEXT DEFAULT 'rock avalanche',
  ra_oid TEXT PRIMARY KEY DEFAULT
'RA_'||to_char(nextval('schema.ra_id'::regclass), '000'),
  ) INHERITS (schema.f0_landslide_objs);
CREATE TABLE schema.f0_sdf_objs (
  class TEXT DEFAULT 'soil dry flow',
  sdf_oid TEXT PRIMARY KEY DEFAULT
'SDF_'||to_char(nextval('schema.sdf_id'::regclass), '000'),
  ) INHERITS (schema.f0_landslide_objs);
CREATE TABLE schema.f0_gswf_objs (
  class TEXT DEFAULT 'granular soil wet flow',
  gswf_oid TEXT PRIMARY KEY DEFAULT
'GSWF_'||to_char(nextval('schema.gswf_id'::regclass), '000'),
  ) INHERITS (schema.f0_landslide_objs);
CREATE TABLE schema.f0_cswf_objs (
  class TEXT DEFAULT 'cohesive soil wet flow',
  cswf_oid TEXT PRIMARY KEY DEFAULT
'CSWF_'||to_char(nextval('schema.cswf_id'::regclass), '000'),
  ) INHERITS (schema.f0_landslide_objs);
CREATE TABLE schema.f0_dsd_objs (
  class TEXT DEFAULT 'deep-seated slope deformation',
  dsd_oid TEXT PRIMARY KEY DEFAULT
'DSD_'||to_char(nextval('schema.dsd_id'::regclass), '000'),
  ) INHERITS (schema.f0_landslide_objs);
CREATE TABLE schema.f0_ssd_objs (
  class TEXT DEFAULT 'soil slope deformation',
  ssd_oid TEXT PRIMARY KEY DEFAULT
'SSD_'||to_char(nextval('schema.ssd_id'::regclass), '000'),
  ) INHERITS (schema.f0_landslide_objs);

-- isolated landslides

CREATE OR REPLACE VIEW isolated_rf_objs AS
WITH
p1 AS (
        SELECT landslide_event_id AS lid
        FROM f0_rf_objs),
p2 AS (
        SELECT
                p1.lid,
                (SELECT ST_Union(geom) FROM f0_rf_objs WHERE landslide_event_id
!= p1.lid) AS n_geom
        FROM p1),
p3 AS (
        SELECT f0_rf_objs.*,
                (ST_Relate(geom, p2.n_geom, '2********')) AS cfi
        FROM f0_rf_objs, p2
        WHERE f0_rf_objs.landslide_event_id = p2.lid)
SELECT *
FROM p3
WHERE cfi IS FALSE OR cfi IS NULL
;
CREATE OR REPLACE VIEW isolated_sf_objs AS
```

```
WITH
p1 AS (
        SELECT landslide_event_id AS lid
        FROM f0_sf_objs),
p2 AS (
        SELECT
                p1.lid,
                (SELECT ST_Union(geom) FROM f0_sf_objs WHERE landslide_event_id
!= p1.lid) AS n_geom
        FROM p1),
p3 AS (
        SELECT f0_sf_objs.*,
                (ST_Relate(geom, p2.n_geom, '2********')) AS cfi
        FROM f0_sf_objs, p2
        WHERE f0_sf_objs.landslide_event_id = p2.lid)
SELECT *
FROM p3
WHERE cfi IS FALSE OR cfi IS NULL
;
CREATE OR REPLACE VIEW isolated_rt_objs AS
WITH
p1 AS (
        SELECT landslide_event_id AS lid
        FROM f0_rt_objs),
p2 AS (
        SELECT
                p1.lid,
                (SELECT ST_Union(geom) FROM f0_rt_objs WHERE landslide_event_id
!= p1.lid) AS n_geom
        FROM p1),
p3 AS (
        SELECT f0_rt_objs.*,
                (ST_Relate(geom, p2.n_geom, '2********')) AS cfi
        FROM f0_rt_objs, p2
        WHERE f0_rt_objs.landslide_event_id = p2.lid)
SELECT *
FROM p3
WHERE cfi IS FALSE OR cfi IS NULL
;
CREATE OR REPLACE VIEW isolated_st_objs AS
WITH
p1 AS (
        SELECT landslide_event_id AS lid
        FROM f0_st_objs),
p2 AS (
        SELECT
                p1.lid,
                (SELECT ST_Union(geom) FROM f0_st_objs WHERE landslide_event_id
!= p1.lid) AS n_geom
        FROM p1),
p3 AS (
        SELECT f0_st_objs.*,
                (ST_Relate(geom, p2.n_geom, '2********')) AS cfi
        FROM f0_st_objs, p2
        WHERE f0_st_objs.landslide_event_id = p2.lid)
SELECT *
FROM p3
WHERE cfi IS FALSE OR cfi IS NULL
;
CREATE OR REPLACE VIEW isolated_rrs_objs AS
WITH
p1 AS (
```

```
        SELECT landslide_event_id AS lid
        FROM f0_rrs_objs),
p2 AS (
        SELECT
                p1.lid,
                (SELECT ST_Union(geom) FROM f0_rrs_objs WHERE landslide_event_id
!= p1.lid) AS n_geom
        FROM p1),
p3 AS (
        SELECT f0_rrs_objs.*,
                (ST_Relate(geom, p2.n_geom, '2********')) AS cfi
        FROM f0_rrs_objs, p2
        WHERE f0_rrs_objs.landslide_event_id = p2.lid)
SELECT *
FROM p3
WHERE cfi IS FALSE OR cfi IS NULL
;
CREATE OR REPLACE VIEW isolated_rps_objs AS
WITH
p1 AS (
        SELECT landslide_event_id AS lid
        FROM f0_rps_objs),
p2 AS (
        SELECT
                p1.lid,
                (SELECT ST_Union(geom) FROM f0_rps_objs WHERE landslide_event_id
!= p1.lid) AS n_geom
        FROM p1),
p3 AS (
        SELECT f0_rps_objs.*,
                (ST_Relate(geom, p2.n_geom, '2********')) AS cfi
        FROM f0_rps_objs, p2
        WHERE f0_rps_objs.landslide_event_id = p2.lid)
SELECT *
FROM p3
WHERE cfi IS FALSE OR cfi IS NULL
;
CREATE OR REPLACE VIEW isolated_rws_objs AS
WITH
p1 AS (
        SELECT landslide_event_id AS lid
        FROM f0_rws_objs),
p2 AS (
        SELECT
                p1.lid,
                (SELECT ST_Union(geom) FROM f0_rws_objs WHERE landslide_event_id
!= p1.lid) AS n_geom
        FROM p1),
p3 AS (
        SELECT f0_rws_objs.*,
                (ST_Relate(geom, p2.n_geom, '2********')) AS cfi
        FROM f0_rws_objs, p2
        WHERE f0_rws_objs.landslide_event_id = p2.lid)
SELECT *
FROM p3
WHERE cfi IS FALSE OR cfi IS NULL
;
CREATE OR REPLACE VIEW isolated_rcs_objs AS
WITH
p1 AS (
        SELECT landslide_event_id AS lid
        FROM f0_rcs_objs),
```

```
p2 AS (
        SELECT
                p1.lid,
                (SELECT ST_Union(geom) FROM f0_rcs_objs WHERE landslide_event_id
!= p1.lid) AS n_geom
        FROM p1),
p3 AS (
        SELECT f0_rcs_objs.*,
                (ST_Relate(geom, p2.n_geom, '2********')) AS cfi
        FROM f0_rcs_objs, p2
        WHERE f0_rcs_objs.landslide_event_id = p2.lid)
SELECT *
FROM p3
WHERE cfi IS FALSE OR cfi IS NULL
;
CREATE OR REPLACE VIEW isolated_ris_objs AS
WITH
p1 AS (
        SELECT landslide_event_id AS lid
        FROM f0_ris_objs),
p2 AS (
        SELECT
                p1.lid,
                (SELECT ST_Union(geom) FROM f0_ris_objs WHERE landslide_event_id
!= p1.lid) AS n_geom
        FROM p1),
p3 AS (
        SELECT f0_ris_objs.*,
                (ST_Relate(geom, p2.n_geom, '2********')) AS cfi
        FROM f0_ris_objs, p2
        WHERE f0_ris_objs.landslide_event_id = p2.lid)
SELECT *
FROM p3
WHERE cfi IS FALSE OR cfi IS NULL
;
CREATE OR REPLACE VIEW isolated_srs_objs AS
WITH
p1 AS (
        SELECT landslide_event_id AS lid
        FROM f0_srs_objs),
p2 AS (
        SELECT
                p1.lid,
                (SELECT ST_Union(geom) FROM f0_srs_objs WHERE landslide_event_id
!= p1.lid) AS n_geom
        FROM p1),
p3 AS (
        SELECT f0_srs_objs.*,
                (ST_Relate(geom, p2.n_geom, '2********')) AS cfi
        FROM f0_srs_objs, p2
        WHERE f0_srs_objs.landslide_event_id = p2.lid)
SELECT *
FROM p3
WHERE cfi IS FALSE OR cfi IS NULL
;
CREATE OR REPLACE VIEW isolated_sps_objs AS
WITH
p1 AS (
        SELECT landslide_event_id AS lid
        FROM f0_sps_objs),
p2 AS (
        SELECT
```

```
                p1.lid,
                (SELECT ST_Union(geom) FROM f0_sps_objs WHERE landslide_event_id
!= p1.lid) AS n_geom
        FROM p1),
p3 AS (
        SELECT f0_sps_objs.*,
                (ST_Relate(geom, p2.n_geom, '2*******')) AS cfi
        FROM f0_sps_objs, p2
        WHERE f0_sps_objs.landslide_event_id = p2.lid)
SELECT *
FROM p3
WHERE cfi IS FALSE OR cfi IS NULL
;
CREATE OR REPLACE VIEW isolated_scs_objs AS
WITH
p1 AS (
        SELECT landslide_event_id AS lid
        FROM f0_scs_objs),
p2 AS (
        SELECT
                p1.lid,
                (SELECT ST_Union(geom) FROM f0_scs_objs WHERE landslide_event_id
!= p1.lid) AS n_geom
        FROM p1),
p3 AS (
        SELECT f0_scs_objs.*,
                (ST_Relate(geom, p2.n_geom, '2*******')) AS cfi
        FROM f0_scs_objs, p2
        WHERE f0_scs_objs.landslide_event_id = p2.lid)
SELECT *
FROM p3
WHERE cfi IS FALSE OR cfi IS NULL
;
CREATE OR REPLACE VIEW isolated_rss_objs AS
WITH
p1 AS (
        SELECT landslide_event_id AS lid
        FROM f0_rss_objs),
p2 AS (
        SELECT
                p1.lid,
                (SELECT ST_Union(geom) FROM f0_rss_objs WHERE landslide_event_id
!= p1.lid) AS n_geom
        FROM p1),
p3 AS (
        SELECT f0_rss_objs.*,
                (ST_Relate(geom, p2.n_geom, '2*******')) AS cfi
        FROM f0_rss_objs, p2
        WHERE f0_rss_objs.landslide_event_id = p2.lid)
SELECT *
FROM p3
WHERE cfi IS FALSE OR cfi IS NULL
;
CREATE OR REPLACE VIEW isolated_gss_objs AS
WITH
p1 AS (
        SELECT landslide_event_id AS lid
        FROM f0_gss_objs),
p2 AS (
        SELECT
                p1.lid,
```

```
                (SELECT ST_Union(geom) FROM f0_gss_objs WHERE landslide_event_id
!= p1.lid) AS n_geom
        FROM p1),
p3 AS (
        SELECT f0_gss_objs.*,
                (ST_Relate(geom, p2.n_geom, '2********')) AS cfi
        FROM f0_gss_objs, p2
        WHERE f0_gss_objs.landslide_event_id = p2.lid)
SELECT *
FROM p3
WHERE cfi IS FALSE OR cfi IS NULL
;
CREATE OR REPLACE VIEW isolated_css_objs AS
WITH
p1 AS (
        SELECT landslide_event_id AS lid
        FROM f0_css_objs),
p2 AS (
        SELECT
                p1.lid,
                (SELECT ST_Union(geom) FROM f0_css_objs WHERE landslide_event_id
!= p1.lid) AS n_geom
        FROM p1),
p3 AS (
        SELECT f0_css_objs.*,
                (ST_Relate(geom, p2.n_geom, '2********')) AS cfi
        FROM f0_css_objs, p2
        WHERE f0_css_objs.landslide_event_id = p2.lid)
SELECT *
FROM p3
WHERE cfi IS FALSE OR cfi IS NULL
;
CREATE OR REPLACE VIEW isolated_ra_objs AS
WITH
p1 AS (
        SELECT landslide_event_id AS lid
        FROM f0_ra_objs),
p2 AS (
        SELECT
                p1.lid,
                (SELECT ST_Union(geom) FROM f0_ra_objs WHERE landslide_event_id
!= p1.lid) AS n_geom
        FROM p1),
p3 AS (
        SELECT f0_ra_objs.*,
                (ST_Relate(geom, p2.n_geom, '2********')) AS cfi
        FROM f0_ra_objs, p2
        WHERE f0_ra_objs.landslide_event_id = p2.lid)
SELECT *
FROM p3
WHERE cfi IS FALSE OR cfi IS NULL
;
CREATE OR REPLACE VIEW isolated_sdf_objs AS
WITH
p1 AS (
        SELECT landslide_event_id AS lid
        FROM f0_sdf_objs),
p2 AS (
        SELECT
                p1.lid,
                (SELECT ST_Union(geom) FROM f0_sdf_objs WHERE landslide_event_id
!= p1.lid) AS n_geom
```

```sql
        FROM p1),
p3 AS (
        SELECT f0_sdf_objs.*,
                (ST_Relate(geom, p2.n_geom, '2********')) AS cfi
        FROM f0_sdf_objs, p2
        WHERE f0_sdf_objs.landslide_event_id = p2.lid)
SELECT *
FROM p3
WHERE cfi IS FALSE OR cfi IS NULL
;
CREATE OR REPLACE VIEW isolated_gswf_objs AS
WITH
p1 AS (
        SELECT landslide_event_id AS lid
        FROM f0_gswf_objs),
p2 AS (
        SELECT
                p1.lid,
                (SELECT ST_Union(geom) FROM f0_gswf_objs WHERE landslide_event_id
!= p1.lid) AS n_geom
        FROM p1),
p3 AS (
        SELECT f0_gswf_objs.*,
                (ST_Relate(geom, p2.n_geom, '2********')) AS cfi
        FROM f0_gswf_objs, p2
        WHERE f0_gswf_objs.landslide_event_id = p2.lid)
SELECT *
FROM p3
WHERE cfi IS FALSE OR cfi IS NULL
;
CREATE OR REPLACE VIEW isolated_cswf_objs AS
WITH
p1 AS (
        SELECT landslide_event_id AS lid
        FROM f0_cswf_objs),
p2 AS (
        SELECT
                p1.lid,
                (SELECT ST_Union(geom) FROM f0_cswf_objs WHERE landslide_event_id
!= p1.lid) AS n_geom
        FROM p1),
p3 AS (
        SELECT f0_cswf_objs.*,
                (ST_Relate(geom, p2.n_geom, '2********')) AS cfi
        FROM f0_cswf_objs, p2
        WHERE f0_cswf_objs.landslide_event_id = p2.lid)
SELECT *
FROM p3
WHERE cfi IS FALSE OR cfi IS NULL
;
CREATE OR REPLACE VIEW isolated_dsd_objs AS
WITH
p1 AS (
        SELECT landslide_event_id AS lid
        FROM f0_dsd_objs),
p2 AS (
        SELECT
                p1.lid,
                (SELECT ST_Union(geom) FROM f0_dsd_objs WHERE landslide_event_id
!= p1.lid) AS n_geom
        FROM p1),
p3 AS (
```

```sql
        SELECT f0_dsd_objs.*,
                (ST_Relate(geom, p2.n_geom, '2********')) AS cfi
        FROM f0_dsd_objs, p2
        WHERE f0_dsd_objs.landslide_event_id = p2.lid)
SELECT *
FROM p3
WHERE cfi IS FALSE OR cfi IS NULL
;
CREATE OR REPLACE VIEW isolated_ssd_objs AS
WITH
p1 AS (
        SELECT landslide_event_id AS lid
        FROM f0_ssd_objs),
p2 AS (
        SELECT
                p1.lid,
                (SELECT ST_Union(geom) FROM f0_ssd_objs WHERE landslide_event_id
!= p1.lid) AS n_geom
        FROM p1),
p3 AS (
        SELECT f0_ssd_objs.*,
                (ST_Relate(geom, p2.n_geom, '2********')) AS cfi
        FROM f0_ssd_objs, p2
        WHERE f0_ssd_objs.landslide_event_id = p2.lid)
SELECT *
FROM p3
WHERE cfi IS FALSE OR cfi IS NULL
;

-- isolated landslide view

CREATE VIEW isolated_landslide_objs AS
SELECT *
FROM isolated_rf_objs
UNION
SELECT *
FROM isolated_sf_objs
UNION
SELECT *
FROM isolated_rt_objs
UNION
SELECT *
FROM isolated_st_objs
UNION
SELECT *
FROM isolated_rrs_objs
UNION
SELECT *
FROM isolated_rps_objs
UNION
SELECT *
FROM isolated_rws_objs
UNION
SELECT *
FROM isolated_rcs_objs
UNION
SELECT *
FROM isolated_ris_objs
UNION
SELECT *
FROM isolated_srs_objs
UNION
```

```
SELECT *
FROM isolated_sps_objs
UNION
SELECT *
FROM isolated_scs_objs
UNION
SELECT *
FROM isolated_rss_objs
UNION
SELECT *
FROM isolated_gss_objs
UNION
SELECT *
FROM isolated_css_objs
UNION
SELECT *
FROM isolated_ra_objs
UNION
SELECT *
FROM isolated_sdf_objs
UNION
SELECT *
FROM isolated_gswf_objs
UNION
SELECT *
FROM isolated_cswf_objs
UNION
SELECT *
FROM isolated_dsd_objs
UNION
SELECT *
FROM isolated_ssd_objs
ORDER BY event_id, overlap_index;

-- landslide complexes id sequence

CREATE SEQUENCE complexes_id
AS INT;

-- landslide complexes aggregation

CREATE OR REPLACE VIEW p1_rf_complex_objs AS
WITH
p1 AS (
        SELECT landslide_event_id AS lid
        FROM f0_rf_objs),
p2 AS (
        SELECT
                p1.lid,
                (SELECT ST_Union(geom) FROM f0_rf_objs WHERE landslide_event_id
!= p1.lid) AS n_geom
        FROM p1),
p3 AS (
        SELECT f0_rf_objs.*,
                (ST_Relate(geom, p2.n_geom, '2********')) AS cfi
        FROM f0_rf_objs, p2
        WHERE f0_rf_objs.landslide_event_id = p2.lid),
p4 AS (
        SELECT *
        FROM p3
        WHERE cfi IS TRUE),
p5 AS (
```

```
                SELECT (ST_Dump(ST_Union(geom))).*
                FROM p4),
p6 AS (
                SELECT
                        p5.path,
                        p4.event_id::REAL,
                        p4.geom
                FROM p4, p5
                WHERE ST_Relate(p4.geom, p5.geom, '2********')),
p7 AS (
                SELECT
                        p6.path,
                        avg(p6.event_id) AS avg_event
                FROM p6
                GROUP BY p6.path)
SELECT
        'CPX_'||to_char(nextval('complexes_id'::regclass), '000') AS
complex_oid,
        'rock fall complex' AS class,
        p7.avg_event,
        p5.geom
FROM p5, p7
WHERE p5.path = p7.path
;
CREATE OR REPLACE VIEW p1_sf_complex_objs AS
WITH
p1 AS (
        SELECT landslide_event_id AS lid
        FROM f0_sf_objs),
p2 AS (
        SELECT
                p1.lid,
                (SELECT ST_Union(geom) FROM f0_sf_objs WHERE landslide_event_id
!= p1.lid) AS n_geom
        FROM p1),
p3 AS (
        SELECT f0_sf_objs.*,
                (ST_Relate(geom, p2.n_geom, '2********')) AS cfi
        FROM f0_sf_objs, p2
        WHERE f0_sf_objs.landslide_event_id = p2.lid),
p4 AS (
        SELECT *
        FROM p3
        WHERE cfi IS TRUE),
p5 AS (
        SELECT (ST_Dump(ST_Union(geom))).*
        FROM p4),
p6 AS (
        SELECT
                p5.path,
                p4.event_id::REAL,
                p4.geom
        FROM p4, p5
        WHERE ST_Relate(p4.geom, p5.geom, '2********')),
p7 AS (
        SELECT
                p6.path,
                avg(p6.event_id) AS avg_event
        FROM p6
        GROUP BY p6.path)
SELECT
```

```sql
        'CPX_'||to_char(nextval('complexes_id'::regclass), '000') AS
complex_oid,
        'soil fall complex' AS class,
        p7.avg_event,
        p5.geom
FROM p5, p7
WHERE p5.path = p7.path
;
CREATE OR REPLACE VIEW p1_rt_complex_objs AS
WITH
p1 AS (
        SELECT landslide_event_id AS lid
        FROM f0_rt_objs),
p2 AS (
        SELECT
                p1.lid,
                (SELECT ST_Union(geom) FROM f0_rt_objs WHERE landslide_event_id
!= p1.lid) AS n_geom
        FROM p1),
p3 AS (
        SELECT f0_rt_objs.*,
                (ST_Relate(geom, p2.n_geom, '2********')) AS cfi
        FROM f0_rt_objs, p2
        WHERE f0_rt_objs.landslide_event_id = p2.lid),
p4 AS (
        SELECT *
        FROM p3
        WHERE cfi IS TRUE),
p5 AS (
        SELECT (ST_Dump(ST_Union(geom))).*
        FROM p4),
p6 AS (
        SELECT
                p5.path,
                p4.event_id::REAL,
                p4.geom
        FROM p4, p5
        WHERE ST_Relate(p4.geom, p5.geom, '2********')),
p7 AS (
        SELECT
                p6.path,
                avg(p6.event_id) AS avg_event
        FROM p6
        GROUP BY p6.path)
SELECT
        'CPX_'||to_char(nextval('complexes_id'::regclass), '000') AS
complex_oid,
        'rock topple complex' AS class,
        p7.avg_event,
        p5.geom
FROM p5, p7
WHERE p5.path = p7.path
;
CREATE OR REPLACE VIEW p1_st_complex_objs AS
WITH
p1 AS (
        SELECT landslide_event_id AS lid
        FROM f0_st_objs),
p2 AS (
        SELECT
                p1.lid,
```

```sql
                (SELECT ST_Union(geom) FROM f0_st_objs WHERE landslide_event_id
!= p1.lid) AS n_geom
        FROM p1),
p3 AS (
        SELECT f0_st_objs.*,
                (ST_Relate(geom, p2.n_geom, '2********')) AS cfi
        FROM f0_st_objs, p2
        WHERE f0_st_objs.landslide_event_id = p2.lid),
p4 AS (
        SELECT *
        FROM p3
        WHERE cfi IS TRUE),
p5 AS (
        SELECT (ST_Dump(ST_Union(geom))).*
        FROM p4),
p6 AS (
        SELECT
                p5.path,
                p4.event_id::REAL,
                p4.geom
        FROM p4, p5
        WHERE ST_Relate(p4.geom, p5.geom, '2********')),
p7 AS (
        SELECT
                p6.path,
                avg(p6.event_id) AS avg_event
        FROM p6
        GROUP BY p6.path)
SELECT
        'CPX_'||to_char(nextval('complexes_id'::regclass), '000') AS
complex_oid,
        'soil topple complex' AS class,
        p7.avg_event,
        p5.geom
FROM p5, p7
WHERE p5.path = p7.path
;
CREATE OR REPLACE VIEW p1_rrs_complex_objs AS
WITH
p1 AS (
        SELECT landslide_event_id AS lid
        FROM f0_rrs_objs),
p2 AS (
        SELECT
                p1.lid,
                (SELECT ST_Union(geom) FROM f0_rrs_objs WHERE landslide_event_id
!= p1.lid) AS n_geom
        FROM p1),
p3 AS (
        SELECT f0_rrs_objs.*,
                (ST_Relate(geom, p2.n_geom, '2********')) AS cfi
        FROM f0_rrs_objs, p2
        WHERE f0_rrs_objs.landslide_event_id = p2.lid),
p4 AS (
        SELECT *
        FROM p3
        WHERE cfi IS TRUE),
p5 AS (
        SELECT (ST_Dump(ST_Union(geom))).*
        FROM p4),
p6 AS (
        SELECT
```

```sql
                p5.path,
                p4.event_id::REAL,
                p4.geom
        FROM p4, p5
        WHERE ST_Relate(p4.geom, p5.geom, '2********')),
p7 AS (
        SELECT
                p6.path,
                avg(p6.event_id) AS avg_event
        FROM p6
        GROUP BY p6.path)
SELECT
        'CPX_'||to_char(nextval('complexes_id'::regclass), '000') AS
complex_oid,
        'rock rotational slide complex' AS class,
        p7.avg_event,
        p5.geom
FROM p5, p7
WHERE p5.path = p7.path
;
CREATE OR REPLACE VIEW p1_rps_complex_objs AS
WITH
p1 AS (
        SELECT landslide_event_id AS lid
        FROM f0_rps_objs),
p2 AS (
        SELECT
                p1.lid,
                (SELECT ST_Union(geom) FROM f0_rps_objs WHERE landslide_event_id
!= p1.lid) AS n_geom
        FROM p1),
p3 AS (
        SELECT f0_rps_objs.*,
                (ST_Relate(geom, p2.n_geom, '2********')) AS cfi
        FROM f0_rps_objs, p2
        WHERE f0_rps_objs.landslide_event_id = p2.lid),
p4 AS (
        SELECT *
        FROM p3
        WHERE cfi IS TRUE),
p5 AS (
        SELECT (ST_Dump(ST_Union(geom))).*
        FROM p4),
p6 AS (
        SELECT
                p5.path,
                p4.event_id::REAL,
                p4.geom
        FROM p4, p5
        WHERE ST_Relate(p4.geom, p5.geom, '2********')),
p7 AS (
        SELECT
                p6.path,
                avg(p6.event_id) AS avg_event
        FROM p6
        GROUP BY p6.path)
SELECT
        'CPX_'||to_char(nextval('complexes_id'::regclass), '000') AS
complex_oid,
        'rock planar slide complex' AS class,
        p7.avg_event,
        p5.geom
```

```sql
FROM p5, p7
WHERE p5.path = p7.path
;
CREATE OR REPLACE VIEW p1_rws_complex_objs AS
WITH
p1 AS (
        SELECT landslide_event_id AS lid
        FROM f0_rws_objs),
p2 AS (
        SELECT
                p1.lid,
                (SELECT ST_Union(geom) FROM f0_rws_objs WHERE landslide_event_id
!= p1.lid) AS n_geom
        FROM p1),
p3 AS (
        SELECT f0_rws_objs.*,
                (ST_Relate(geom, p2.n_geom, '2********')) AS cfi
        FROM f0_rws_objs, p2
        WHERE f0_rws_objs.landslide_event_id = p2.lid),
p4 AS (
        SELECT *
        FROM p3
        WHERE cfi IS TRUE),
p5 AS (
        SELECT (ST_Dump(ST_Union(geom))).*
        FROM p4),
p6 AS (
        SELECT
                p5.path,
                p4.event_id::REAL,
                p4.geom
        FROM p4, p5
        WHERE ST_Relate(p4.geom, p5.geom, '2********')),
p7 AS (
        SELECT
                p6.path,
                avg(p6.event_id) AS avg_event
        FROM p6
        GROUP BY p6.path)
SELECT
        'CPX_'||to_char(nextval('complexes_id'::regclass), '000') AS
complex_oid,
        'rock wedge slide complex' AS class,
        p7.avg_event,
        p5.geom
FROM p5, p7
WHERE p5.path = p7.path
;
CREATE OR REPLACE VIEW p1_rcs_complex_objs AS
WITH
p1 AS (
        SELECT landslide_event_id AS lid
        FROM f0_rcs_objs),
p2 AS (
        SELECT
                p1.lid,
                (SELECT ST_Union(geom) FROM f0_rcs_objs WHERE landslide_event_id
!= p1.lid) AS n_geom
        FROM p1),
p3 AS (
        SELECT f0_rcs_objs.*,
                (ST_Relate(geom, p2.n_geom, '2********')) AS cfi
```

```sql
        FROM f0_rcs_objs, p2
        WHERE f0_rcs_objs.landslide_event_id = p2.lid),
p4 AS (
        SELECT *
        FROM p3
        WHERE cfi IS TRUE),
p5 AS (
        SELECT (ST_Dump(ST_Union(geom))).*
        FROM p4),
p6 AS (
        SELECT
                p5.path,
                p4.event_id::REAL,
                p4.geom
        FROM p4, p5
        WHERE ST_Relate(p4.geom, p5.geom, '2********')),
p7 AS (
        SELECT
                p6.path,
                avg(p6.event_id) AS avg_event
        FROM p6
        GROUP BY p6.path)
SELECT
        'CPX_'||to_char(nextval('complexes_id'::regclass), '000') AS
complex_oid,
        'rock compound slide complex' AS class,
        p7.avg_event,
        p5.geom
FROM p5, p7
WHERE p5.path = p7.path
;
CREATE OR REPLACE VIEW p1_ris_complex_objs AS
WITH
p1 AS (
        SELECT landslide_event_id AS lid
        FROM f0_ris_objs),
p2 AS (
        SELECT
                p1.lid,
                (SELECT ST_Union(geom) FROM f0_ris_objs WHERE landslide_event_id
!= p1.lid) AS n_geom
        FROM p1),
p3 AS (
        SELECT f0_ris_objs.*,
                (ST_Relate(geom, p2.n_geom, '2********')) AS cfi
        FROM f0_ris_objs, p2
        WHERE f0_ris_objs.landslide_event_id = p2.lid),
p4 AS (
        SELECT *
        FROM p3
        WHERE cfi IS TRUE),
p5 AS (
        SELECT (ST_Dump(ST_Union(geom))).*
        FROM p4),
p6 AS (
        SELECT
                p5.path,
                p4.event_id::REAL,
                p4.geom
        FROM p4, p5
        WHERE ST_Relate(p4.geom, p5.geom, '2********')),
p7 AS (
```

```sql
        SELECT
                p6.path,
                avg(p6.event_id) AS avg_event
        FROM p6
        GROUP BY p6.path)
SELECT
        'CPX_'||to_char(nextval('complexes_id'::regclass), '000') AS
complex_oid,
        'rock irregular slide complex' AS class,
        p7.avg_event,
        p5.geom
FROM p5, p7
WHERE p5.path = p7.path
;
CREATE OR REPLACE VIEW p1_srs_complex_objs AS
WITH
p1 AS (
        SELECT landslide_event_id AS lid
        FROM f0_srs_objs),
p2 AS (
        SELECT
                p1.lid,
                (SELECT ST_Union(geom) FROM f0_srs_objs WHERE landslide_event_id
!= p1.lid) AS n_geom
        FROM p1),
p3 AS (
        SELECT f0_srs_objs.*,
                (ST_Relate(geom, p2.n_geom, '2********')) AS cfi
        FROM f0_srs_objs, p2
        WHERE f0_srs_objs.landslide_event_id = p2.lid),
p4 AS (
        SELECT *
        FROM p3
        WHERE cfi IS TRUE),
p5 AS (
        SELECT (ST_Dump(ST_Union(geom))).*
        FROM p4),
p6 AS (
        SELECT
                p5.path,
                p4.event_id::REAL,
                p4.geom
        FROM p4, p5
        WHERE ST_Relate(p4.geom, p5.geom, '2********')),
p7 AS (
        SELECT
                p6.path,
                avg(p6.event_id) AS avg_event
        FROM p6
        GROUP BY p6.path)
SELECT
        'CPX_'||to_char(nextval('complexes_id'::regclass), '000') AS
complex_oid,
        'soil rotational slide complex' AS class,
        p7.avg_event,
        p5.geom
FROM p5, p7
WHERE p5.path = p7.path
;
CREATE OR REPLACE VIEW p1_sps_complex_objs AS
WITH
p1 AS (
```

```
        SELECT landslide_event_id AS lid
        FROM f0_sps_objs),
p2 AS (
        SELECT
                p1.lid,
                (SELECT ST_Union(geom) FROM f0_sps_objs WHERE landslide_event_id
!= p1.lid) AS n_geom
        FROM p1),
p3 AS (
        SELECT f0_sps_objs.*,
                (ST_Relate(geom, p2.n_geom, '2********')) AS cfi
        FROM f0_sps_objs, p2
        WHERE f0_sps_objs.landslide_event_id = p2.lid),
p4 AS (
        SELECT *
        FROM p3
        WHERE cfi IS TRUE),
p5 AS (
        SELECT (ST_Dump(ST_Union(geom))).*
        FROM p4),
p6 AS (
        SELECT
                p5.path,
                p4.event_id::REAL,
                p4.geom
        FROM p4, p5
        WHERE ST_Relate(p4.geom, p5.geom, '2********')),
p7 AS (
        SELECT
                p6.path,
                avg(p6.event_id) AS avg_event
        FROM p6
        GROUP BY p6.path)
SELECT
        'CPX_'||to_char(nextval('complexes_id'::regclass), '000') AS
complex_oid,
        'soil planar slide complex' AS class,
        p7.avg_event,
        p5.geom
FROM p5, p7
WHERE p5.path = p7.path
;
CREATE OR REPLACE VIEW p1_scs_complex_objs AS
WITH
p1 AS (
        SELECT landslide_event_id AS lid
        FROM f0_scs_objs),
p2 AS (
        SELECT
                p1.lid,
                (SELECT ST_Union(geom) FROM f0_scs_objs WHERE landslide_event_id
!= p1.lid) AS n_geom
        FROM p1),
p3 AS (
        SELECT f0_scs_objs.*,
                (ST_Relate(geom, p2.n_geom, '2********')) AS cfi
        FROM f0_scs_objs, p2
        WHERE f0_scs_objs.landslide_event_id = p2.lid),
p4 AS (
        SELECT *
        FROM p3
        WHERE cfi IS TRUE),
```

```
p5 AS (
        SELECT (ST_Dump(ST_Union(geom))).*
        FROM p4),
p6 AS (
        SELECT
                p5.path,
                p4.event_id::REAL,
                p4.geom
        FROM p4, p5
        WHERE ST_Relate(p4.geom, p5.geom, '2********')),
p7 AS (
        SELECT
                p6.path,
                avg(p6.event_id) AS avg_event
        FROM p6
        GROUP BY p6.path)
SELECT
        'CPX_'||to_char(nextval('complexes_id'::regclass), '000') AS
complex_oid,
        'soil compound slide complex' AS class,
        p7.avg_event,
        p5.geom
FROM p5, p7
WHERE p5.path = p7.path
;
CREATE OR REPLACE VIEW p1_rss_complex_objs AS
WITH
p1 AS (
        SELECT landslide_event_id AS lid
        FROM f0_rss_objs),
p2 AS (
        SELECT
                p1.lid,
                (SELECT ST_Union(geom) FROM f0_rss_objs WHERE landslide_event_id
!= p1.lid) AS n_geom
        FROM p1),
p3 AS (
        SELECT f0_rss_objs.*,
                (ST_Relate(geom, p2.n_geom, '2********')) AS cfi
        FROM f0_rss_objs, p2
        WHERE f0_rss_objs.landslide_event_id = p2.lid),
p4 AS (
        SELECT *
        FROM p3
        WHERE cfi IS TRUE),
p5 AS (
        SELECT (ST_Dump(ST_Union(geom))).*
        FROM p4),
p6 AS (
        SELECT
                p5.path,
                p4.event_id::REAL,
                p4.geom
        FROM p4, p5
        WHERE ST_Relate(p4.geom, p5.geom, '2********')),
p7 AS (
        SELECT
                p6.path,
                avg(p6.event_id) AS avg_event
        FROM p6
        GROUP BY p6.path)
SELECT
```

```sql
        'CPX_'||to_char(nextval('complexes_id'::regclass), '000') AS
complex_oid,
        'rock slope spread complex' AS class,
        p7.avg_event,
        p5.geom
FROM p5, p7
WHERE p5.path = p7.path
;
CREATE OR REPLACE VIEW p1_gss_complex_objs AS
WITH
p1 AS (
        SELECT landslide_event_id AS lid
        FROM f0_gss_objs),
p2 AS (
        SELECT
                p1.lid,
                (SELECT ST_Union(geom) FROM f0_gss_objs WHERE landslide_event_id
!= p1.lid) AS n_geom
        FROM p1),
p3 AS (
        SELECT f0_gss_objs.*,
                (ST_Relate(geom, p2.n_geom, '2********')) AS cfi
        FROM f0_gss_objs, p2
        WHERE f0_gss_objs.landslide_event_id = p2.lid),
p4 AS (
        SELECT *
        FROM p3
        WHERE cfi IS TRUE),
p5 AS (
        SELECT (ST_Dump(ST_Union(geom))).*
        FROM p4),
p6 AS (
        SELECT
                p5.path,
                p4.event_id::REAL,
                p4.geom
        FROM p4, p5
        WHERE ST_Relate(p4.geom, p5.geom, '2********')),
p7 AS (
        SELECT
                p6.path,
                avg(p6.event_id) AS avg_event
        FROM p6
        GROUP BY p6.path)
SELECT
        'CPX_'||to_char(nextval('complexes_id'::regclass), '000') AS
complex_oid,
        'granular soil spread complex' AS class,
        p7.avg_event,
        p5.geom
FROM p5, p7
WHERE p5.path = p7.path
;
CREATE OR REPLACE VIEW p1_css_complex_objs AS
WITH
p1 AS (
        SELECT landslide_event_id AS lid
        FROM f0_css_objs),
p2 AS (
        SELECT
                p1.lid,
```

```sql
                (SELECT ST_Union(geom) FROM f0_css_objs WHERE landslide_event_id
!= p1.lid) AS n_geom
        FROM p1),
p3 AS (
        SELECT f0_css_objs.*,
                (ST_Relate(geom, p2.n_geom, '2********')) AS cfi
        FROM f0_css_objs, p2
        WHERE f0_css_objs.landslide_event_id = p2.lid),
p4 AS (
        SELECT *
        FROM p3
        WHERE cfi IS TRUE),
p5 AS (
        SELECT (ST_Dump(ST_Union(geom))).*
        FROM p4),
p6 AS (
        SELECT
                p5.path,
                p4.event_id::REAL,
                p4.geom
        FROM p4, p5
        WHERE ST_Relate(p4.geom, p5.geom, '2********')),
p7 AS (
        SELECT
                p6.path,
                avg(p6.event_id) AS avg_event
        FROM p6
        GROUP BY p6.path)
SELECT
        'CPX_'||to_char(nextval('complexes_id'::regclass), '000') AS
complex_oid,
        'cohesive soil spread complex' AS class,
        p7.avg_event,
        p5.geom
FROM p5, p7
WHERE p5.path = p7.path
;
CREATE OR REPLACE VIEW p1_ra_complex_objs AS
WITH
p1 AS (
        SELECT landslide_event_id AS lid
        FROM f0_ra_objs),
p2 AS (
        SELECT
                p1.lid,
                (SELECT ST_Union(geom) FROM f0_ra_objs WHERE landslide_event_id
!= p1.lid) AS n_geom
        FROM p1),
p3 AS (
        SELECT f0_ra_objs.*,
                (ST_Relate(geom, p2.n_geom, '2********')) AS cfi
        FROM f0_ra_objs, p2
        WHERE f0_ra_objs.landslide_event_id = p2.lid),
p4 AS (
        SELECT *
        FROM p3
        WHERE cfi IS TRUE),
p5 AS (
        SELECT (ST_Dump(ST_Union(geom))).*
        FROM p4),
p6 AS (
        SELECT
```

```
                p5.path,
                p4.event_id::REAL,
                p4.geom
        FROM p4, p5
        WHERE ST_Relate(p4.geom, p5.geom, '2********')),
p7 AS (
        SELECT
                p6.path,
                avg(p6.event_id) AS avg_event
        FROM p6
        GROUP BY p6.path)
SELECT
        'CPX_'||to_char(nextval('complexes_id'::regclass), '000') AS
complex_oid,
        'rock avalanche complex' AS class,
        p7.avg_event,
        p5.geom
FROM p5, p7
WHERE p5.path = p7.path
;
CREATE OR REPLACE VIEW p1_sdf_complex_objs AS
WITH
p1 AS (
        SELECT landslide_event_id AS lid
        FROM f0_sdf_objs),
p2 AS (
        SELECT
                p1.lid,
                (SELECT ST_Union(geom) FROM f0_sdf_objs WHERE landslide_event_id
!= p1.lid) AS n_geom
        FROM p1),
p3 AS (
        SELECT f0_sdf_objs.*,
                (ST_Relate(geom, p2.n_geom, '2********')) AS cfi
        FROM f0_sdf_objs, p2
        WHERE f0_sdf_objs.landslide_event_id = p2.lid),
p4 AS (
        SELECT *
        FROM p3
        WHERE cfi IS TRUE),
p5 AS (
        SELECT (ST_Dump(ST_Union(geom))).*
        FROM p4),
p6 AS (
        SELECT
                p5.path,
                p4.event_id::REAL,
                p4.geom
        FROM p4, p5
        WHERE ST_Relate(p4.geom, p5.geom, '2********')),
p7 AS (
        SELECT
                p6.path,
                avg(p6.event_id) AS avg_event
        FROM p6
        GROUP BY p6.path)
SELECT
        'CPX_'||to_char(nextval('complexes_id'::regclass), '000') AS
complex_oid,
        'soil dry flow complex' AS class,
        p7.avg_event,
        p5.geom
```

```sql
FROM p5, p7
WHERE p5.path = p7.path
;
CREATE OR REPLACE VIEW p1_gswf_complex_objs AS
WITH
p1 AS (
        SELECT landslide_event_id AS lid
        FROM f0_gswf_objs),
p2 AS (
        SELECT
                p1.lid,
                (SELECT ST_Union(geom) FROM f0_gswf_objs WHERE landslide_event_id
!= p1.lid) AS n_geom
        FROM p1),
p3 AS (
        SELECT f0_gswf_objs.*,
                (ST_Relate(geom, p2.n_geom, '2********')) AS cfi
        FROM f0_gswf_objs, p2
        WHERE f0_gswf_objs.landslide_event_id = p2.lid),
p4 AS (
        SELECT *
        FROM p3
        WHERE cfi IS TRUE),
p5 AS (
        SELECT (ST_Dump(ST_Union(geom))).*
        FROM p4),
p6 AS (
        SELECT
                p5.path,
                p4.event_id::REAL,
                p4.geom
        FROM p4, p5
        WHERE ST_Relate(p4.geom, p5.geom, '2********')),
p7 AS (
        SELECT
                p6.path,
                avg(p6.event_id) AS avg_event
        FROM p6
        GROUP BY p6.path)
SELECT
        'CPX_'||to_char(nextval('complexes_id'::regclass), '000') AS
complex_oid,
        'granular soil wet flow complex' AS class,
        p7.avg_event,
        p5.geom
FROM p5, p7
WHERE p5.path = p7.path
;
CREATE OR REPLACE VIEW p1_cswf_complex_objs AS
WITH
p1 AS (
        SELECT landslide_event_id AS lid
        FROM f0_cswf_objs),
p2 AS (
        SELECT
                p1.lid,
                (SELECT ST_Union(geom) FROM f0_cswf_objs WHERE landslide_event_id
!= p1.lid) AS n_geom
        FROM p1),
p3 AS (
        SELECT f0_cswf_objs.*,
                (ST_Relate(geom, p2.n_geom, '2********')) AS cfi
```

```sql
        FROM f0_cswf_objs, p2
        WHERE f0_cswf_objs.landslide_event_id = p2.lid),
p4 AS (
        SELECT *
        FROM p3
        WHERE cfi IS TRUE),
p5 AS (
        SELECT (ST_Dump(ST_Union(geom))).*
        FROM p4),
p6 AS (
        SELECT
                p5.path,
                p4.event_id::REAL,
                p4.geom
        FROM p4, p5
        WHERE ST_Relate(p4.geom, p5.geom, '2********')),
p7 AS (
        SELECT
                p6.path,
                avg(p6.event_id) AS avg_event
        FROM p6
        GROUP BY p6.path)
SELECT
        'CPX_'||to_char(nextval('complexes_id'::regclass), '000') AS
complex_oid,
        'cohesive soil wet flow complex' AS class,
        p7.avg_event,
        p5.geom
FROM p5, p7
WHERE p5.path = p7.path
;
CREATE OR REPLACE VIEW p1_dsd_complex_objs AS
WITH
p1 AS (
        SELECT landslide_event_id AS lid
        FROM f0_dsd_objs),
p2 AS (
        SELECT
                p1.lid,
                (SELECT ST_Union(geom) FROM f0_dsd_objs WHERE landslide_event_id
!= p1.lid) AS n_geom
        FROM p1),
p3 AS (
        SELECT f0_dsd_objs.*,
                (ST_Relate(geom, p2.n_geom, '2********')) AS cfi
        FROM f0_dsd_objs, p2
        WHERE f0_dsd_objs.landslide_event_id = p2.lid),
p4 AS (
        SELECT *
        FROM p3
        WHERE cfi IS TRUE),
p5 AS (
        SELECT (ST_Dump(ST_Union(geom))).*
        FROM p4),
p6 AS (
        SELECT
                p5.path,
                p4.event_id::REAL,
                p4.geom
        FROM p4, p5
        WHERE ST_Relate(p4.geom, p5.geom, '2********')),
p7 AS (
```

```sql
        SELECT
                p6.path,
                avg(p6.event_id) AS avg_event
        FROM p6
        GROUP BY p6.path)
SELECT
        'CPX_'||to_char(nextval('complexes_id'::regclass), '000') AS
complex_oid,
        'deep-seated slope deformation complex' AS class,
        p7.avg_event,
        p5.geom
FROM p5, p7
WHERE p5.path = p7.path
;
CREATE OR REPLACE VIEW p1_ssd_complex_objs AS
WITH
p1 AS (
        SELECT landslide_event_id AS lid
        FROM f0_ssd_objs),
p2 AS (
        SELECT
                p1.lid,
                (SELECT ST_Union(geom) FROM f0_ssd_objs WHERE landslide_event_id
!= p1.lid) AS n_geom
        FROM p1),
p3 AS (
        SELECT f0_ssd_objs.*,
                (ST_Relate(geom, p2.n_geom, '2********')) AS cfi
        FROM f0_ssd_objs, p2
        WHERE f0_ssd_objs.landslide_event_id = p2.lid),
p4 AS (
        SELECT *
        FROM p3
        WHERE cfi IS TRUE),
p5 AS (
        SELECT (ST_Dump(ST_Union(geom))).*
        FROM p4),
p6 AS (
        SELECT
                p5.path,
                p4.event_id::REAL,
                p4.geom
        FROM p4, p5
        WHERE ST_Relate(p4.geom, p5.geom, '2********')),
p7 AS (
        SELECT
                p6.path,
                avg(p6.event_id) AS avg_event
        FROM p6
        GROUP BY p6.path)
SELECT
        'CPX_'||to_char(nextval('complexes_id'::regclass), '000') AS
complex_oid,
        'soil slope deformation complex' AS class,
        p7.avg_event,
        p5.geom
FROM p5, p7
WHERE p5.path = p7.path
;

-- landslide complex view
```

119

```
CREATE VIEW p1_landslide_complex_objs AS
SELECT *
FROM p1_rf_complex_objs
UNION
SELECT *
FROM p1_sf_complex_objs
UNION
SELECT *
FROM p1_rt_complex_objs
UNION
SELECT *
FROM p1_st_complex_objs
UNION
SELECT *
FROM p1_rrs_complex_objs
UNION
SELECT *
FROM p1_rps_complex_objs
UNION
SELECT *
FROM p1_rws_complex_objs
UNION
SELECT *
FROM p1_rcs_complex_objs
UNION
SELECT *
FROM p1_ris_complex_objs
UNION
SELECT *
FROM p1_srs_complex_objs
UNION
SELECT *
FROM p1_sps_complex_objs
UNION
SELECT *
FROM p1_scs_complex_objs
UNION
SELECT *
FROM p1_rss_complex_objs
UNION
SELECT *
FROM p1_gss_complex_objs
UNION
SELECT *
FROM p1_css_complex_objs
UNION
SELECT *
FROM p1_ra_complex_objs
UNION
SELECT *
FROM p1_sdf_complex_objs
UNION
SELECT *
FROM p1_gswf_complex_objs
UNION
SELECT *
FROM p1_cswf_complex_objs
UNION
SELECT *
FROM p1_dsd_complex_objs
UNION
SELECT *
```

```sql
FROM p1_ssd_complex_objs
ORDER BY avg_event;

-- landslide systems id sequence

CREATE SEQUENCE systems_id
AS INT;

-- landslide system aggregation

CREATE VIEW p2_landslide_system_objs AS
WITH
p1 AS (
  SELECT geom FROM p1_landslide_complex_objs
  UNION
  SELECT geom FROM isolated_landslide_objs),
p2 AS (
  SELECT (ST_Dump(ST_Union(geom))).*
  FROM p1)
SELECT
  'SYS_'||to_char(nextval('systems_id'::regclass), '000') AS system_oid,
  p2.geom
FROM p2
;
```